

Molecular and Functional Characterization of the *Arabidopsis*

ESCRT-I complex

Inaugural-Dissertation

zur

Erlangung des Doktorgrades

der Mathematisch-Naturwissenschaftlichen Fakultät

der Universität zu Köln



vorgelegt von

Channakeshavaiah Kolagondanahally Chikkaputtaiah

aus Bengaluru, Indien

2008

Berichterstatter: **Prof. Dr. Martin Hülskamp**
 Prof. Dr. Ute Höcker

Tag der mündlichen Prüfung: 19 January 2009

Acknowledgements

First and foremost I convey my sincere and heartfelt gratitude to **Dr. Swen Schellmann** for his esteemed supervision. I would really like him know how much I owe and respect him for providing valuable guidance, creative suggestions and constructive criticisms (and his very polite way of doing that). His immense support, guidance, encouragement, optimism and promptness are highly acknowledged.

I convey my deepest gratitude to my major advisor **Prof. Dr. Martin Hülskamp** for his guidance and scientific interactions. I am very grateful for all the encouragement and support I received.

I would then like to acknowledge **Prof. Dr. Ute Höcker** and **Prof. Dr. Jürgen Dohmen** my defence committee members and **PD. Dr. Joachim Uhrig** for thesis committee discussions and attendance of my progress reports.

My sincere thanks to **Mojgan Shahriari**, my PhD colleague with whom I had daily discussions (both scientific and general) and for sharing the constructs and research material.

I am very thankful to **Aneta Saboljevic**, another PhD colleague who actually standardized the protoplast isolation and transfection, the technique which our lab uses extensively and for sharing some of her constructs.

I would like to acknowledge our other ELCH members; **Florian Heßner** who helped me in genetic analysis and regular discussions, **Stefanie Herberth** for her help with biochemical experiments, and for solving computer problems in the lab and **Britta Müller** for her technical support and for sharing the constructs and research material.

My sincere thanks to **Dr. Swen Schellmann, Dr. Martina Pesch, Dr. Simona Diguini, Sudheer Gara and Jinu Leo** for critically reading my thesis and their comments.

Many thanks to members of Patterning group; **Rachappa Balkunde, Dr. Simona Diguini, Katja Wester, Burcu Dartan, Dr. Martina Pesch, Dr. Marc Jacoby and Yang Bai** for their direct and indirect help during my PhD.

My thankful wishes to members of the actin group and other group members; **Cordula Jörgens, Philipp Thomas, Valerie Mach, Andrea Shrader, Cho-chun Huang, Christina Selbach, Karstin and Diego Yepes** for their help and support during my PhD.

I am thankful to **Irene Klinkhammer, Birgitt Kernebeck, Bastian Welter and Uschi Claßen** for their technical help and support and thanks to **Elisabeth Rochaz** for her help in administration stuff.

Thanks to former lab members, Dr. Christoph Spitzer, Dr. Daniel Bouyer, Dr. Ullrich Hermann, Dr. Elena Jaime etc... for their help and to all the members of AG Hülskamp.

Special thanks to **Dr. Takashi Tatsuta**, AG Langer for his help in performing BN-PAGE experiments. **Alexander Mayer**, AG Höcker for his help in performing In vitro pulldown experiments and **Dr. Peter Pimpl** for gifting VPS28 antibody.

I owe my sincere thanks to **International Graduate School for Genetics and Functional Genomics**, University of Cologne for offering me the fellowship for my PhD studies. Special note of thanks to **Brigitte Wilcken Bergmann** for administrative and general help.

I pay special thanks to my dear friends **Leo Kurian** and **Rajesh Kooventavida** for scientific discussions, criticism, encouragement and for their kind confidence boosting words when I am down.

Sincere thanks to my batch mates of graduate school **Luis, Rodrigo, Yenyen, Daniela, Joanna, Nelli, Katya** and **Anke** for the fun and partying. Thanks to long list of gradschool friends and cricket mates Sudheer, Bhagi, Raja, Sabari, Sam, Palani, Jayan, Madhu, Vel, Veena, Fiona etc...

I would then like to acknowledge my friends Shiva, Renu, Vivek, Subhanjan, Sharada, Kayal, Vinod, Venki, Viji, Kitty, Asoka, Vani, King, Seena M, Siddu, Yathish, Shivanand, etc....

My heartfelt special thanks to **Jinu Leo, Charles Peter, Ashish Ranjan and Shashi Chitti** for.....you know why right?

My special note of thanks to **Nagaraj** (whom I call my godfather). What I am now is just because of you. Thank you very much for everything.

A very special thanks to my **Amma** and **Appa** for being the best parents. I deeply acknowledge your love, care, practical advices etc...I love you both.

I deeply acknowledge my sisters **Manjula** and **Channalakshmi** and my brother-in-laws **Shankar** and **Venkatesh** for their advice and suggestions.

Finally my deepest gratitude to my one and only brother **Manjunath** for being a friend, philosopher, teacher, advisor, reviewer and what not...thanks for giving me a practical outlook towards life.

Last but not the least, I would like to acknowledge my sweetest one and only sister-in-law **MUTHU** for being my best friend, mother, sister, teacher, mentor.....I think you are the only person with whom I shared all my joys and sorrows.....Thank you very much for being such a wonderful human being.

Channakeshavaiah K. Chikkaputtaiah

**Affectionately dedicated to my beloved
Parents, Brother and Sister in law**

Table of contents

Figure/ Table index

Abbreviation list

Abstract

A. Introduction	1
A 1. The endomembrane system	1
A 2. The ESCRT pathway	1
A 3. The endosomal system in plants	4
A 4. Cytokinesis in plants and animals	5
A 5. ESCRT machinery in cytokinesis	7
A 6. The ESCRT-I complex	9
A 7. A novel fourth component of ESCRT-I complex	11
Aim	13
B. Results	14
B 1. Genetic characterization of the ESCRT-I components	14
B 1.1. Genetic analysis of <i>VPS28</i> and <i>VPS37</i>	14
B 1.2. <i>vps28-1 vps28-2</i> and <i>vps37-1 vps37-2</i> are lethal	16
B 1.3. Double knock-outs <i>elch vps28-1</i> and <i>elch vps28-2</i> and <i>elch vps37-1</i> show synergistic phenotype	17
B 1.4. ESCRT-I members are involved in cytokinesis regulation	18
B 2. Functional analysis of <i>VPS23-2</i>	21
B 2.1 Dominant-negative <i>VPS23-2</i> (<i>VPS23-2-t</i>) phenocopies the <i>elch</i> mutant	21
B 2.2 <i>VPS23-2</i> expressed under the <i>ELCH</i> promoter rescue the <i>elch</i> mutant	23
B 3. Functional characterization of the <i>Arabidopsis</i> ELCH homolog <i>VPS23-3</i>	24
B 3.1 The <i>Arabidopsis</i> ELCH homolog <i>VPS23-3</i> is a component of the plant ESCRT system	24

B 3.1.1 VPS23-3 is expressed ubiquitously	24
B 3.1.2 VPS23-3 is localized on endosomes	26
B 3.1.3 YFP:VPS23-3 binds to ubiquitin <i>in vitro</i>	28
B 3.1.4 N-terminal UEV domain is necessary for ubiquitin binding	29
B 3.1.5 YFP:VPS23-3 protein is part of a high molecular weight complex	30
B 3.2 VPS23-3 is functionally different from ELCH	31
B 3.2.1 The truncated VPS23-3 does not phenocopy the <i>elch</i> mutant	31
B 3.2.2 VPS23-3 expressed under the <i>ELCH</i> promoter did not rescue the <i>elch</i> mutant	32
B 3.3 VPS23-3 might serve as a fourth subunit of the <i>Arabidopsis</i> ESCRT-I complex	33
B 3.3.1 VPS23-3 show differential interaction pattern	33
B 3.3.2 <i>In vivo</i> interactions between VPS23-3 and VPS28 homologs occur on endosomes	34
B 3.3.3 VPS23-3 interacts with VPS37 and ELCH interacts with VPS37 in <i>in vitro</i> co-IPs	35
B 3.3.4 <i>vps23-3</i> knock-out show a shift in the molecular weight of the complex on blue native-PAGE	40
C. Discussion	42
C 1. ESCRT components function together in regulating cytokinesis in plants	42
C 2. VPS23-3, a new component of the plant ESCRT system	45
C 3. VPS23-3 might serve as an additional fourth subunit of the ESCRT-I complex	46
C 4. A model depicting the <i>Arabidopsis</i> ELCH and VPS23-3 mediated protein trafficking	47
Outlook	49
D. Material and Methods	50
D 1. Material	50
D 1.1 Chemicals	50
D 1.2 Enzymes and kits	50
D 1.3 Primers	50

D 1.4 Antibiotics	51
D 1.5 Bacterial strains	52
D 1.6 Cloning vectors	52
D 1.7 Plant lines	53
D 1.8 T-DNA insertion lines	54
D 1.9 Biochemicals and antibodies	54
D 2. Methods	54
D 2.1 Plant work	54
D 2.1.1 Plant growth conditions	55
D 2.1.2 Crossing of plants	55
D 2.1.3 Plant transformation	55
D 2.1.4 Seed surface sterilisation and subsequent plant treatment	55
D 2.1.5 Selection of transformants	56
D 2.2 Genetic analysis	56
D 2.3 Microscopy and Cell biology	56
D 2.3.1 Microscopy	57
D 2.3.2 DAPI staining	57
D 2.3.3 FM4-64 staining	57
D 2.3.4 Arabidopsis cell culture, protoplasting and transfection	57
D 2.4 Molecular biology	58
D 2.4.1 Basic DNA manipulation techniques	58
D 2.4.2 Plasmid DNA preparation from bacteria	59
D 2.4.3 Gateway cloning	59
D 2.4.4 Cloning of promoters	59
D 2.4.5 Bi-molecular fluorescence complementation (Bi-FC)	60
D 2.4.6 Genomic DNA isolation from plants	60
D 2.4.7 RNA isolation and RT-PCR	60
D 2.5 Biochemical methods	61
D 2.5.1 Basic protein techniques	62
D 2.5.2 Protein extraction (denaturing)	63
D 2.5.3 Western blotting	63
D 2.5.4 Ubiquitin binding assay	63
D 2.5.5 Gel filtration/ Size exclusion chromatography	63
D 2.5.6 Radioactive <i>In vitro</i> expression	63

D 2.5.7 Radioactive <i>In vitro</i> co-IPs	63
D 2.5.8 Blue-native PAGE	64
E. Appendix	66
E 1. Genetic analysis of the double knock-out <i>elch vps28-1</i>	66
E 2. Genetic analysis of the double knock-out <i>elch vps28-2</i>	67
E 3. Genetic analysis of the double knock-out <i>elch vps37-1</i>	68
E 4. Genetic analysis of the double knock-out <i>elch vps37-2</i>	69
E 5. Genetic analysis of the triple knock-out <i>elch vps28-2 vps37-1</i>	70
E 6. Statistics of promoter rescue analysis of ELCH under ELCH promoter	71
E 7. Statistics of promoter rescue analysis of VPS23-2 under ELCH promoter	72
E 8. Statistics of promoter rescue analysis of VPS23-3 under ELCH promoter	73
F. References	74
Zusammenfassung	82
Erklärung	83
Lebenslauf	84

Figure/ Table index

- Figure 1:** ESCRTs function in protein sorting to the degradative pathway
- Figure 2:** A model of ESCRT mediated protein trafficking in yeast
- Figure 3:** Model depicting the characterized endosomal trafficking pathways in plants
- Figure 4:** Comparison of different stages of cell division in plant and animal cells
- Figure 5:** Membrane dynamics during cell plate development.
- Figure 6:** ESCRT pathway functions
- Figure 7:** Working model for the function of Mvb12
- Figure 8:** Genetic characterization of ESCRT-I mutants
- Figure 9:** Rescue analysis of ESCRT-I mutants
- Figure 10:** Phenotypic analysis of the ESCRT-I mutants.
- Figure 11:** Phenotypic trichome analysis of putative ESCRT-I mutants
- Figure 12:** Molecular and genetic analysis of dominant-negative VPS23-2.
- Figure 13:** Cluster tree and expression analysis of VPS23-3
- Figure 14:** Protein alignment of the Arabidopsis VPS23 homologs
- Figure 15:** VPS23-3 localized on endosomes
- Figure 16:** VPS23-3 protein binds ubiquitin in vitro
- Figure 17:** VPS23-3 is part of a high molecular weight complex
- Figure 18:** Dominant-negative VPS23-3 shows differential localization
- Figure 19:** Interaction network of ESCRT-I components
- Figure 20:** In vivo interaction between VPS23-3 and VPS28-1 occur on endosomes
- Figure 21:** In vivo interaction between VPS23-3 and VPS28-2 occur on endosomes
- Figure 22:** Radioactive in vitro transcription/ translation assay
- Figure 23:** *vps23-3* knock-out shows a shift in the molecular weight of the complex
- Figure 24:** A model of VPS23-3 and ELCH mediated trafficking of proteins
-
- Table 1:** Homologs of the ESCRT-I complex in yeast, mammals and *Arabidopsis*
- Table 2:** Summary of the rescue experiments
- Table 3:** Summary of genetic analysis of putative ESCRT-I mutants
- Table 4:** Summary of the promoter rescue analysis

Abbreviations List

:	fused to (in the context of reporter-gene fusion constructs)
°	degree Celsius
%	percent
μ	micro
μm	micrometer
μM	micromolar
aa	amino acid
AD	activation domain
<i>A. thaliana</i>	<i>Arabidopsis thaliana</i>
ATP	adenosine triphosphate
Bp	base pairs
bHLH	basic helix-loop-helix
Bi-FC	Bi-molecular fluorescence complementation
<i>CaMV</i>	<i>Cauliflower mosaic virus</i>
CCV	clathrin coated vesicles
cDNA	complementary DNA
CDS	coding sequence
CFP	cyanin fluorescent protein
CLSM	confocal laser scanning microscopy
Co-IP	co-immunoprecipitation
°C	degree Celsius
Da	dalton
DAPI	4',6-Diamidino-2-phenylindol
DNA	deoxyribonucleic acid
DTT	dithiothreitol
DUB	deubiquitinating enzyme
E3	Enzyme 3
EGFP	epidermal growth factor receptor
<i>ELC</i>	<i>ELCH</i>
ESCRT	endosomal sorting complex required for transport
<i>et al.</i>	et alerni [Lat.] and others
FLAG	flagellin
g	gram (s)
x g	gravitation constant (981 cm/s)
GFP	green fluorescent protein
HA	hemagglutinin of <i>influenza virus</i>
HIV	human immunodeficiency virus
IP	immunoprecipitation
K	kilo
Kb	kilobase (s)
K	lysine
kDa	kilodalton (s)
<i>KIS</i>	<i>KIESEL</i>
LAP	lysosomal acid phosphatase
<i>Ler</i>	<i>Landsberg erecta</i>
Mm	milli molar
MPR	manose-6-phosphate receptor
mRNA	messenger ribonucleic acid

MVB	multi-vesicular body
n	number
ORF	open reading frame
PAGE	polyacrylamide gel electrophoresis
pCPS	precursor of CarboxypeptidaseS
PCR	polymerase chain reaction
PFS	planar fenestrated sheet
pH	negative decimal logarithm of H ⁺ concentration
PPB	pre-prophase band
RNA	ribonucleic acid
Rpm	rounds per minute
RT-PCR	reverse transcription PCR
RT	room temperature
<i>STI</i>	<i>STICHEL</i>
T-DNA	transfer DNA
SDS	sodium dodecyl sulfate
T1	seeds that grow on a transformed plant
T2	seeds that grow on a T1 plant
<i>TFC-A</i>	<i>Tubulin-Cofactor A</i>
TOF	time of flight
Tris	Tris-(hydroxymethyl)-aminomethane
<i>TSG101</i>	<i>TUMOR SUSCEPTIBILITY GENE 101</i>
TN	tubular network
TVN	tubulo-vesicular network
UBA	Ubiquitin Associated domain
<i>UBAP1</i>	<i>UBIQUITIN ASSOCIATED PROTEIN1</i>
UEV	Ubiquitin Enzyme Variant domain
V-ATPase	vacuolar-ATPase
Vps23p	yeast nomenclature for protein
<i>VPS</i>	<i>VACUOLAR PROTEIN SORTING</i>
<i>Ws2</i>	<i>Wassilewskija 2</i>
<i>WT</i>	<i>wild type</i>
YFP	yellow fluorescent protein
YFPC/n	C/N terminal sub-fragment on the YFP gene

Gene names are written in italics, in capital letters when referred to wild type and in small letters for the mutant. Protein names are written in capital letters.

Abstract

Recently the *Arabidopsis* *ELCH* gene, a homolog of Vps23/ TSG101 and the key component of the plant ESCRT-I complex has been functionally characterized (Spitzer et al, Development, 2006). The *elch* mutant shows multiple nuclei in various cell types, indicating a role in cytokinesis. VPS28 and VPS37 are other known components of ESCRT-I complex that in combination with *elch* have synergistic phenotypes in double and triple knock-outs suggesting their involvement in ELCH-dependent regulation of cytokinesis. Cytokinesis regulation is therefore a function of the whole ESCRT system in plants and not a special ESCRT unrelated function of ELCH. The role of ESCRT complexes in yeast cytokinesis is unclear but mutations in one or more ESCRT components of mammals and *Arabidopsis* induce cytokinesis defects, suggesting that the role of the ESCRT machinery in cytokinesis might be conserved in multicellular organisms.

A second Vps23 homolog, VPS23-2 (At5g13860) displays high sequence similarity to ELCH (72%). A dominant-negative VPS23-2 construct phenocopies the *elch* mutant and expression of VPS23-2 under ELCH promoter can rescue the *elch* mutant. VPS23-2 is therefore functionally redundant to ELCH.

In addition to ELCH and VPS23-2 a third, dicot-specific Vps23 homolog, VPS23-3 (At2g38830) has been identified. It shows a lesser degree of homology (47%) to *Arabidopsis* ELCH compared to the homology of ELCH to *Oryza sativa* ELCH (66%) and VPS23-2 (72%). Similar to ELCH, VPS23-3 is ubiquitously expressed, localized on endosomes, binds to ubiquitin with its N-terminal UEV domain and part of a high molecular weight complex in gel filtration/size exclusion chromatography assays suggesting that VPS23-3 is a component of the plant ESCRT system. Surprisingly however, VPS23-3 did not rescue the *elch* phenotype, when expressed under ELCH promoter control indicating that it has a cellular function different from the other two Vps23 genes. *vps23-3* knock-out showed a shift in the molecular weight of the complex on blue-native PAGE and differential interaction pattern in bi-molecular fluorescence complementation and *in vitro* transcription/ translation assays suggesting that VPS23-3 might serve as an additional, fourth component of the *Arabidopsis* ESCRT-I complex.

A. Introduction

A 1. The endomembrane system

Endocytosis is a process where integral proteins of the plasma membrane, such as receptors and ion channels at the cell surface are internalized and sorted to three alternative destinations (Figure 1; (Gruenberg and Stenmark 2004; Maxfield and McGraw 2004)). Some membrane proteins, such as the receptors for transferrin and low-density lipoprotein, are recycled to the cell surface, whereas others, such as mannose 6-phosphate receptors, enter the trans-golgi network (TGN). A third group of membrane proteins, such as misfolded proteins and activated growth factor receptors, are transported into the intraluminal vesicles (ILVs) of maturing endosomes, known as multivesicular bodies (MVBs). The ILVs and their contents are degraded when they fuse with late endosomes or lysosomes (Katzmann et al. 2002; Raiborg et al. 2003; Gruenberg and Stenmark 2004). Covalent attachment of ubiquitin on one or several cytosolic lysine residues of the target proteins is the best-characterized sorting signal for lysosomal trafficking of endocytosed membrane proteins (Haglund et al. 2003; Hicke and Dunn 2003). Central to this machinery are the endosomal sorting complexes required for transport, ESCRT-I, -II and -III.

A 2. The ESCRT pathway

Genetic studies in yeast have identified more than 60 gene products involved in vacuolar protein sorting (Vps). These genes encode transport components that function at distinct stages of protein traffic between the golgi complex and the vacuole. A subset of the Vps proteins, the class E Vps proteins, functions in the MVB sorting pathway (Odorizzi et al. 1998; Katzmann et al. 2001; Bowers and Stevens 2005). Class E *vps* mutants accumulate endosomal membranes and exhibit defects in the formation of MVB vesicles. The characterization of these proteins has resulted in the identification of three high-molecular-weight protein complexes that function in the MVB sorting pathway. These complexes are called the ESCRT (endosomal sorting complex required for transport) complexes-I, II, and III (Katzmann et al. 2002; Hicke and Dunn 2003; Morita and Sundquist 2004). MVB sorting starts with the recognition of monoubiquitylated cargo

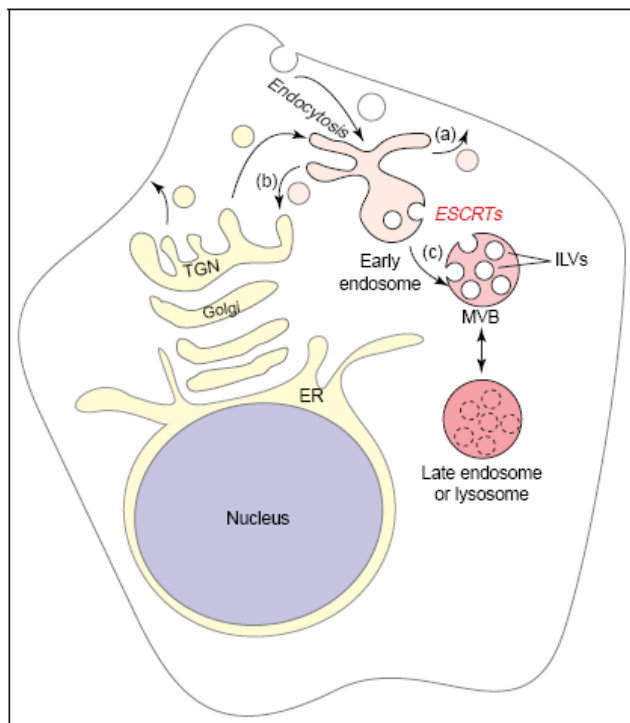


Figure 1. ESCRTs function in protein sorting to the degradative pathway as reviewed by (Slagsvold et al. 2006). Membrane proteins that enter endosomes via endocytosis or biosynthetic trafficking (from the TGN) are transported either to the plasma membrane (a), to the TGN (b) or into ILVs of MVBs, also called 'endosomal carrier vesicles' (c). The ILVs and their content are degraded when the MVB fuses with a lysosome or late endosome. ESCRTs function to sort (ubiquitinated) cargo into ILVs.

by the UIM (ubiquitin interacting motifs) containing the Vps27/Hse1 dimer (ESCRT-0) (Bilodeau et al. 2002; Bilodeau et al. 2003). ESCRT-0 recruits the heterotetrameric ESCRT-I complex consisting of the UEV (ubiquitin E2 variant) domain containing protein Vps23 and Vps28, Vps37 and Mvb12, from the cytosol to the endosomal membrane (Katzmann et al. 2001; Katzmann et al. 2003). The C-terminus of Vps28 is required for interaction with the N-terminus of Vps36, a member of the ESCRT-II complex consisting of Vps36, Vps22 and Vps25 (Teo et al. 2004; Kostelansky et al. 2006; Teo et al. 2006). Finally the cargo is concentrated in certain membrane regions of the endosome by members of the ESCRT-III complex, which consists of four small coiled-coil proteins that likely coat the endosomal membrane in regions that later undergo inward budding (Babst et al. 2002; Babst 2005). Prior to invagination, ubiquitin is removed from the cargo by the deubiquitylase Doa4 (Amerik et al. 2000; Dupre et al. 2001) and the ESCRT components are disassembled from the endosomal surface by the AAA ATPase Vps4/SKD1 (Babst et al. 1997; Finken-Eigen et al. 1997; Babst et al. 1998; Scheuring et al. 1999; Yoshimori et al. 2000; Scheuring et al. 2001) (Figure 2).

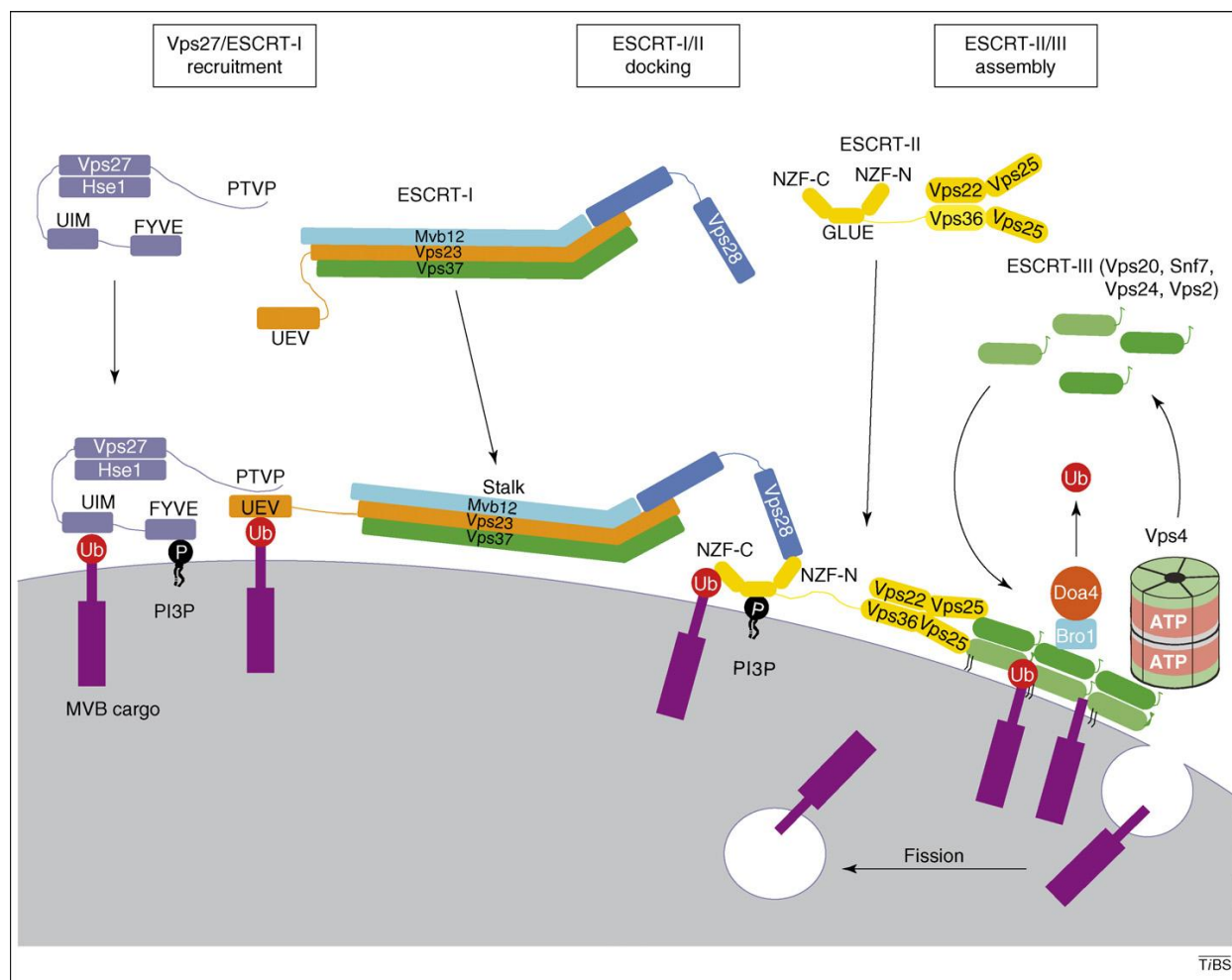


Figure 2. A model of ESCRT mediated protein trafficking in yeast. Adapted from (Saksena et al. 2007). The FYVE domain of Vps27 binds PI3P on the endosomal membrane resulting in membrane docking of the Vps27–Hse1 complex. The UIM domains of Vps27 and Hse1 recognize and bind ubiquitylated cargo for sorting into MVB vesicles. Vps27–Hse1 complex recruits the ESCRT-I complex to the membrane via interactions with the UEV domain of Vps23. Membrane bound ESCRT-I binds ubiquitylated cargo via the UEV domain of Vps23 and recruits ESCRT-II to the membrane via interactions between the Vps28 C-terminus and the NZF-N domain of Vps36 (ESCRT-II). The GLUE domain of Vps36 binds endosomal PI3P, while the NZF-C domain binds ubiquitylated cargo. Membrane-bound ESCRT-II recruits the downstream ESCRT-III complex via interactions between Vps25 and Vps20. The ESCRT-III lattice assembled on the endosomal membrane is disassembled following cargo sorting into MVB vesicles via interactions between the C-terminal MIR region of the ESCRT-III subunit at the leading edge of the lattice and the MIT domain of Vps4.

A 3. The endosomal system in plants

As in animals and yeast cells, endosomes in plants traffic both biosynthetic and endocytic cargo. Recent studies have demonstrated the extraordinary dynamics of the endocytic pathway in plant cells (Ueda et al. 2001; Grebe et al. 2003; Baluska et al. 2005; Haupt et al. 2005; Geldner and Jurgens 2006) (Figure 3). Recent studies have also shown the central role of

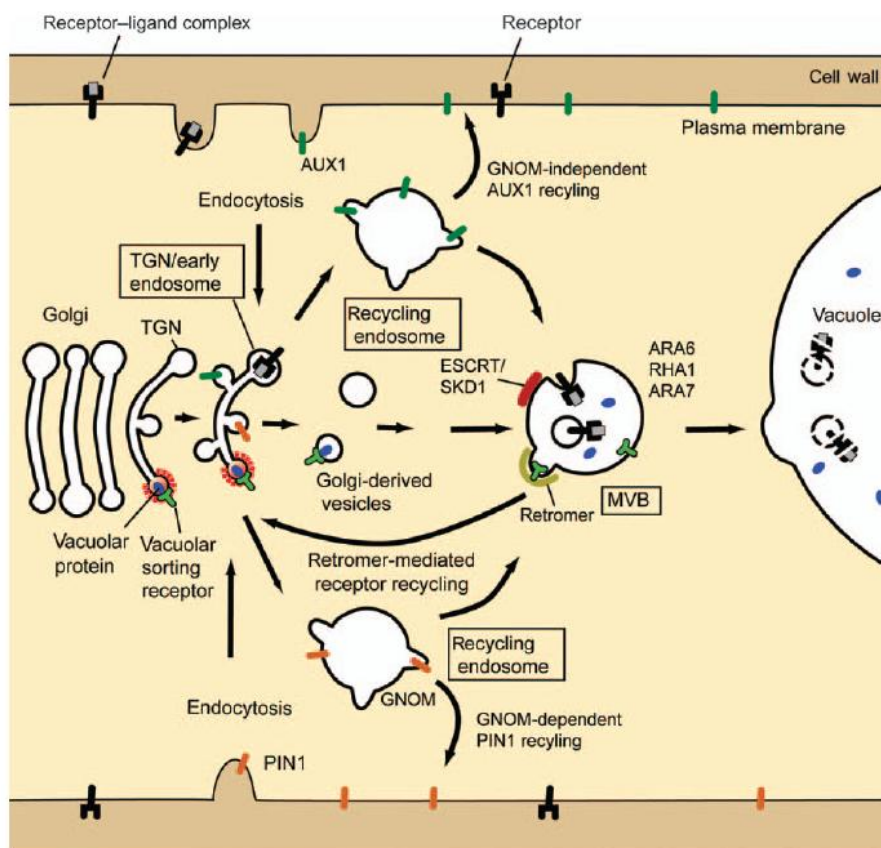


Figure 3: Model depicting some of the characterized endosomal trafficking pathways in plants. Adapted from (Otegui and Spitzer 2008). The TGN or an immediate TGN-derived compartment acts as early endosome receiving plasma membrane cargo internalized by endocytosis. At least two different recycling pathways have been discovered in plants for auxin carriers. PIN proteins are recycled by a mechanism that requires the BFA-sensitive ARF-GEF GNOM, whereas AUX1 is recycled by a BFA-insensitive GNOM independent mechanism. MVBs arise from the fusion of Golgi-derived vesicles carrying newly synthesized vacuolar proteins and, likely, from early/recycling endosomal compartments. Two very important sorting processes take place in MVBs: (i) the recycling of vacuolar cargo receptors mediated by the retromer complex and (ii) the sorting of plasma membrane protein into internal vesicles by the ESCRT machinery. Fusion of MVBs with the vacuole leads to the release of soluble vacuolar proteins and MVB vesicles into the lumen of the vacuole.

endocytosis and endosomes in key plant processes such as embryo differentiation (Geldner and Jurgens 2006; Goh et al. 2007; Jaillais et al. 2008), epidermis differentiation (Tian et al. 2007), guard cell movement (Sutter et al. 2006), cell wall remodeling (Baluska et al. 2002), the regulation of auxin transport (Paciorek et al. 2005; Jaillais and Gaude 2007) and defense responses against pathogens (Robatzek et al. 2006). Though plants possess the common molecular machinery that regulates membrane traffic in other eukaryotes, they have evolved molecular and structural specializations related to plant-specific cellular processes. For example, plants are thought to have specialized mechanisms that allow individual cells to maintain a diversity of vacuolar trafficking pathways (Surpin and Raikhel 2004) and more than one type of vacuole (Frigerio et al. 2008). Putative homologs of all the main ESCRT and ESCRT related proteins have been identified in plants (Spitzer et al. 2006; Winter and Hauser 2006). However, only the endosomal functions of a few of these proteins, such as the ESCRT-I component ELCH and the ESCRT-related proteins SKD1, LIP5/Vta1p and Did2p/CHMP1, have been studied to date.

A 4. Cytokinesis in plants and animals

The spindle segregates the duplicated sets of chromosomes during mitosis in dividing eukaryotic cells. Subsequently, the mother is physically divided into two daughter cells by a process called cytokinesis. Although the spatiotemporal aspects of cell division in plants and animals are regulated via cytoskeleton and membrane trafficking machinery that exist in both, it has generally been considered that cytokinesis is accomplished differently in plants and animals (Guertin et al. 2002). In plants, the division plane is determined early in mitosis before the spindle stage by a circular band of microtubules known as preprophase band (PPB). During early prophase, PPB predicts the cell division plane by encircling the cylindrically shaped plant cells, it then disappears during late prophase leaving some kind of a physical trace at the cortical division site (Pickett-Heaps and Northcote 1966). Later, vesicular fusions build up a juvenile cell wall called the cell plate which grows from the cell center by an 'inside-out' mechanism (Figure 4). This cytokinetic cell plate attaches to the parental cell wall exactly at the cortical division site that was marked earlier by the PPB (Jurgens 2005). In animals, dividing cells assemble an actomyosin ring at the cell periphery by involvement of astral microtubules (D'Avino et al. 2005) and 'outside-in' constriction of this actomyosin ring generates the midbody

channel, which is ultimately closed by the fusion of targeted vesicles (Strickland and Burgess 2004).

In both plant and animal cells, endocytosis has emerged as a key process that is actively participating in cytokinesis (Strickland and Burgess 2004; Albertson et al. 2005; Baluska et al. 2005; Schweitzer et al. 2005; Dhonukshe et al. 2006). In addition to this, participation of Golgi derived secretory vesicles in construction of the cell plate or construction of the plasma membrane is a common feature (Samuels et al. 1995). The Golgi stacks provide the materials needed to build the new cell wall while phragmoplast microtubules provide the infrastructure that transports the Golgi derived vesicles to the forming cell plate. Plant cells assemble a new cell wall by accumulating transport vesicles with cell wall material in the plane of division (Staehelin and Hepler 1996). Vesicle fusion forms the tubulo-vesicular-network (TVN) that is subsequently reduced through the tubular network (TN) to a planar fenestrated sheet (PFS). The PFS matures to the cell plate that will give rise to the new cell wall (Staehelin and Hepler 1996). Though the mechanisms are only roughly defined, the reduction seems to be mediated by budding of clathrin coated vesicles (CCV) from the TVN that are speculated to feed the endosomal/MVB pathway (Samuels et al. 1995; Jurgens 2005; Jurgens 2005). The MVB is then thought to distribute membranes back to the different compartments of the endo-membrane system similar to the way it does during endocytosis (Figure 5). Recently, an additional function of ESCRT proteins has come into focus with the finding that ESCRT proteins are involved in cytokinesis of multicellular organisms (Spitzer et al. 2006; Carlton and Martin-Serrano 2007; Morita et al. 2007). In animals it has been shown that different ESCRT proteins are recruited to the midbody by the centrosomal protein Cep55 and function at the abscission stage (Carlton and Martin-Serrano 2007; Morita et al. 2007) whereas in plants a role in regulating the tubulin cytoskeleton was discussed based on genetic interactions of the *Arabidopsis* TSG101 homolog *ELCH* and the tubulin folding cofactor- A/ *KIESEL* (Spitzer et al. 2006). Apart from *elch* related cytokinesis phenotype little is known about function, architecture and mechanism of ESCRT machinery in plants.

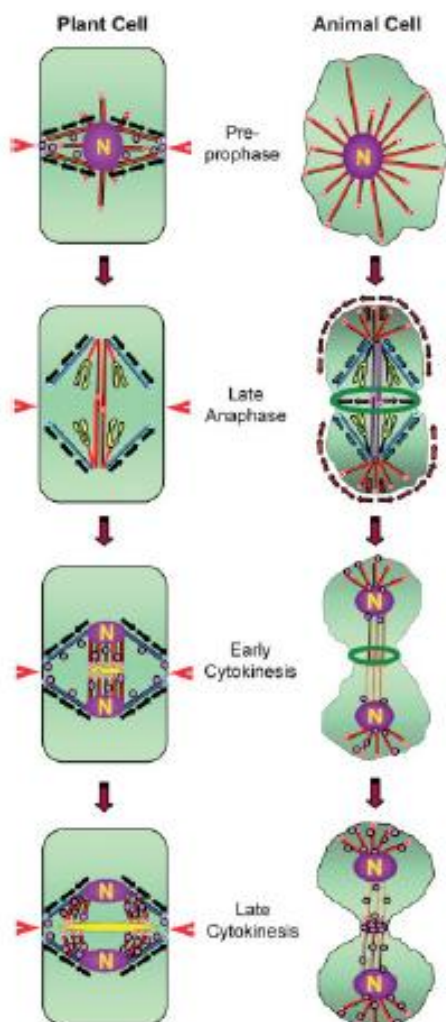


Figure 4. Comparison of different stages of cell division in plant and animal cells. Adapted from (Dhonukshe et al. 2007). In plant cells, the cell division plane (denoted by red arrowheads) is determined by the PPB microtubules at the pre-prophase stage whereas, in animal cells, the cell division plane is determined at the late anaphase. Both in plant and animal cells, the astral microtubules (blue in color and in plants shown by the black arrows and in animals shown as blue Arrow heads) somehow participate in either determining (in animal cells) or executing (in plant cells) the cell division planes. Endocytic vesicles participate both in the formation of cell plates in plant cells and the sealing of the midbody canal in animal cells. The presumed trafficking of these endocytic vesicles via cortically bound astral microtubules and their subsequent motility on the central phragmoplast microtubules (in plant cells) or interzonal microtubules (in animal cells) is shown.

A 5. ESCRT machinery in cytokinesis

Current models propose that the ESCRT-III machinery is recruited by ESCRT-I and ESCRT associated protein ALIX facilitate membrane fission in animals (Hurley and Emr 2006), a function initially characterized in multivesicular body (MVB) formation. ESCRT-I and ALIX bind a series of proteins that localize to centrosomes and midbodies, and function in cytokinesis (Morita et al. 2007) (Figure 6). TSG101 and ALIX deficient cells led to cytokinesis defects manifested by the appearance of multinucleated cells suggesting their essential role in abscission (Carlton and Martin-Serrano 2007). TSG101/ ESCRT-I can localize to centrosomes and midbodies, the downregulation of TSG101 leads to mitotic abnormalities was also reported earlier (Xie et al. 1998). TSG101-VPS28 interaction is essential for complete abscission (Carlton

and Martin-Serrano 2007). EAP20/ ESCRT-II also concentrates at centrosomes (Morita et al. 2007) and negatively regulates maturation of the meiotic spindle pole body (centrosome) in *Schizosaccharomyces pombe* (Jin et al. 2005). Recently the *elch* mutant in *Arabidopsis*, a homolog of yeast Vps23 and mammalian TSG101 showed high levels of multinucleate cells, and this might reflect a cytokinesis defect arising from misregulation of the microtubule cytoskeleton (Spitzer et al. 2006).

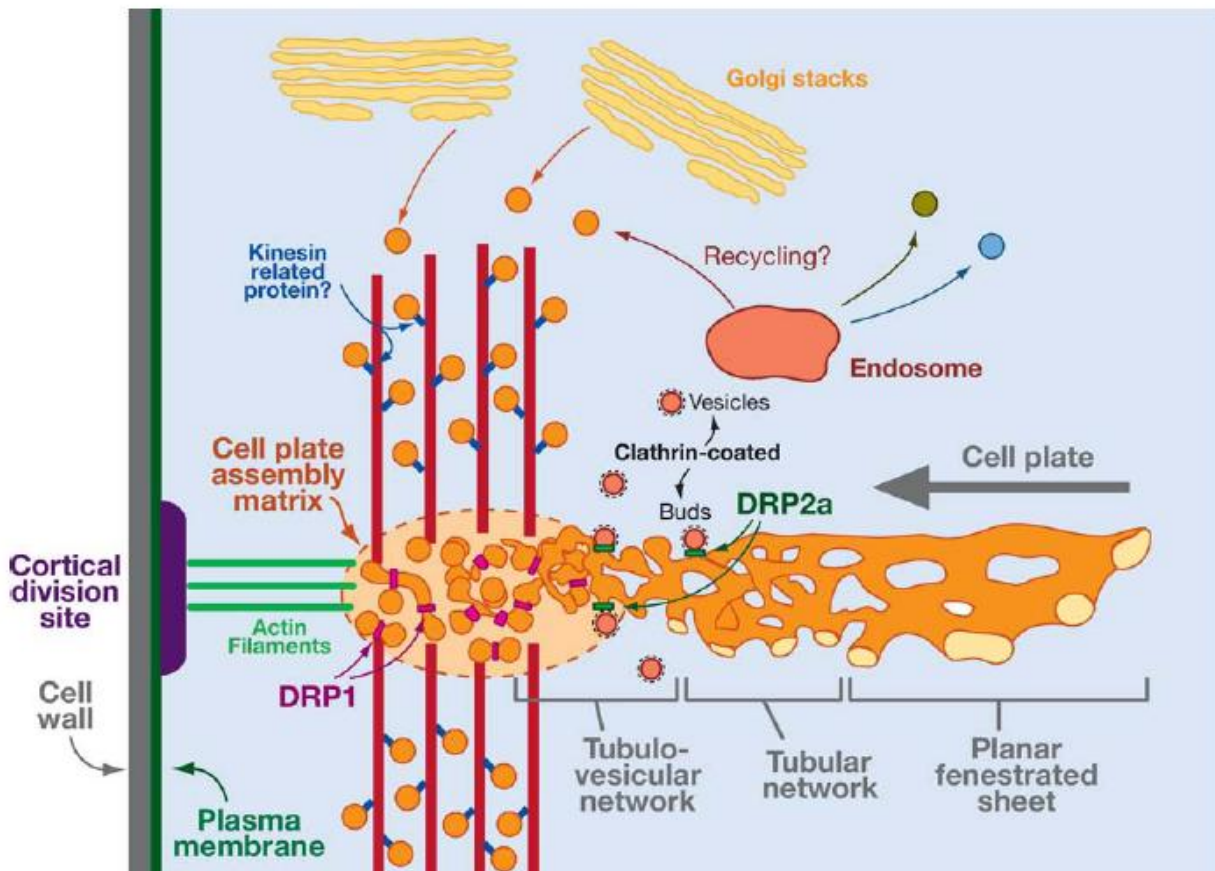


Figure 5. Membrane dynamics during cell plate development. Adapted from (Jurgens 2005). Golgi-derived vesicles (orange) are delivered along phragmoplast microtubules (red), by a putative kinesin-related protein (blue), to the cell plate assembly matrix. Vesicle fusion generates fusion tubes and tubulo-vesicular networks as a result of the constricting activity of class I dynamin-related proteins (DRP1) (magenta). The tubulo-vesicular network is successively transformed into a tubular network and a planar fenestrated sheet. Lateral expansion of the cell plate (large arrow) toward the cortical division site is guided by actin filaments. Endocytosis from the tubulo-vesicular network and tubular network removes excess membrane, which is delivered to endosomes via clathrin-coated buds and vesicles. Dynamin-related protein 2a (DRP2a; green) is involved in the formation of clathrin-coated vesicles. The endosome sorts proteins for trafficking to various destinations (blue, green, orange), possibly including recycling to the margin of the cell plate.

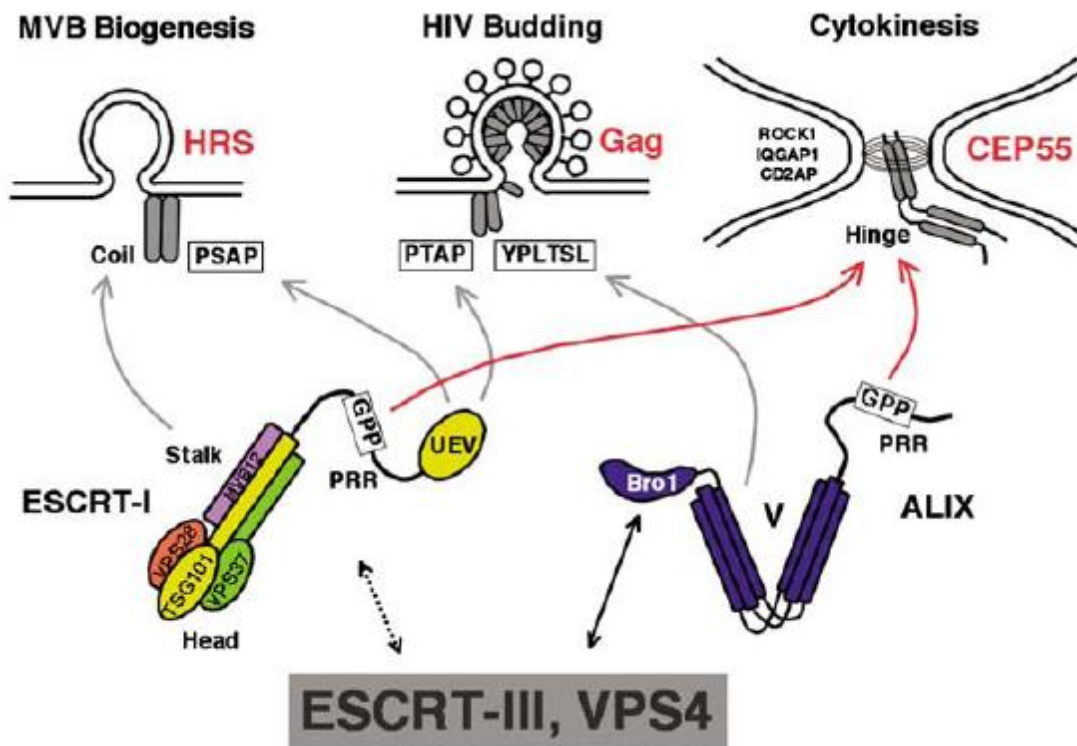


Figure 6. ESCRT pathway functions. Adapted from (Morita et al. 2007). The schematic model illustrates how ESCRT-I, ALIX, and other ESCRT pathway proteins may be recruited by different adaptor proteins (red) to perform similar roles in the terminal membrane fission events of MVB biogenesis, virus budding, and cytokinesis.

A 6. The ESCRT-I complex

ESCRT-I is a core complex of the ESCRT system was originally identified in yeast as a 350kDa heterotrimeric complex which plays a central role in the MVB pathway (Katzmann et al. 2001; Katzmann et al. 2002). ESCRT-I transiently associates with endosomal membranes and acts in the recognition of monoubiquitylated cargo proteins. It comprises Vps23p, Vps28p and Vps37p in yeast and TSG101, VPS28 and one of four isotopes of VPS37 in humans (VPS37 A-D) (Bishop and Woodman 2001; Bache et al. 2004). Vps23p and the human homolog TSG101 contains a ubiquitin-conjugating (UBC)-like domain also known as UEV domain. The UEV domain is similar to the ubiquitin conjugating enzyme E2 UBC but lacks the cysteine residue in the active site. Therefore, Vps23 does not function as an ubiquitin conjugating enzyme and yet is able to bind ubiquitylated proteins. The human Vps23p homolog TSG101, interacts with

VPS27, VPS28 (Eastman et al. 2005) and VPS37 (Stuchell et al. 2004) via its C-terminal coiled-coil domain. In yeast, deletion of any ESCRT-I subunit gives rise to a class E phenotype. In mammalian cells, depletion of TSG101 has a much stronger inhibitory effect on receptor degradation than HRS depletion and causes a strikingly different endosomal morphology (Doyotte et al. 2005; Razi and Futter 2006). On the other hand, depletion of HRS leads to enlarged vacuolar structures with EGFR trapped at the limiting membrane. It was shown that, depletion of TSG101 promotes the accumulation of EGFR and EGF on extensive tubular clusters and induces the formation of multicisternal structures with an internal matrix (Doyotte et al. 2005; Razi and Futter 2006). This phenotype may suggest that, in contrast to HRS, TSG101 (ESCRT-I) is required for the maintenance of the vacuolar morphology of endosomes (Razi and Futter 2006). The *Arabidopsis* ELCH is the functional homolog of the ESCRT-I subunit Vps23p in yeast and TSG101 in mammals, and like its counterparts, the ELCH protein has ubiquitin-binding capacity and forms a complex with other subunits (Spitzer et al. 2006). VPS28s are small proteins of about 200 amino acids and *Arabidopsis* has two putative VPS28 homologs (Table 1) (Winter and Hauser 2006). Using the human VPS37 sequences two putative VPS37 homologs have been identified in the *Arabidopsis* genome (Table 1) (Winter and Hauser 2006).

Table 1. Homologs of the ESCRT-I complex in yeast, mammals and *Arabidopsis*

Yeast	Mammals	<i>Arabidopsis</i>	<i>Arabidopsis</i> locus
Vps23p	TSG101	ELCH	At3g12400
		VPS23-2 (ELCH-like)	At5g13860
Vps28p	VPS28	VPS28-1	At4g21560
		VPS28-2	At4g05000
Vps37p	VPS37A	VPS37-1	At3g53120
	VPS37B	VPS37-2	At2g36680
	VPS37C		
	VPS37D		
Mvb12p	MVB12A	VPS23-3?	At2g38830
	MVB12B		

A 7. A novel fourth component of ESCRT-I complex

ESCRT-I is a 350k.Da protein complex that has been shown to be composed of the three class E Vps proteins: Vps23, Vps28, and Vps37 (Babst et al. 2000; Katzmann et al. 2001). However, the expression of these subunits in *Escherichia coli* does not result in the formation of a 350k.Da complex, suggesting that additional unidentified subunits might be necessary for the formation of the ESCRT-I in yeast (Kostelansky et al. 2006; Teo et al. 2006). Therefore recently a fourth subunit of the yeast ESCRT-I complex, called Mvb12p has been functionally characterized (Curtiss et al. 2007). Mvb12p, localizes on endosomes and loss of Mvb12p results in a partial defect in MVB sorting and the mistargeting of ESCRT-I to the vacuolar lumen suggesting its requirement for efficient cargo sorting and the release of ESCRT-I from the MVB (Curtiss et al. 2007). Mvb12 has also been suggested to regulate ESCRT-I/ ESCRT-II interactions by stabilizing an inactive oligomeric state of ESCRT-I in the cytosol (Chu et al. 2006) (Figure 7). Yeast ESCRT-I form a complex with a 1:1:1:1 stoichiometry both in solution and in the crystal. The structure reveals a globular domain composed of the core heterotrimeric ESCRT-I complex (Kostelansky et al. 2006; Teo et al. 2006; Williams and Urbe 2007), which attaches to an extended stalk formed by helical segments from Vps23p, Vps37p, and Mvb12p. Mvb12p contains a short N-terminal helix that interacts with the globular core, followed by a long extended conformation and a C-terminal helix that stabilizes the stalk by forming a triple-stranded coiled coil together with Vps23p and Vps37p. Its mode of interaction with ESCRT-I suggests that Mvp12p is indeed an integral part of the ESCRT-I complex. Mvb12p does not seem to be evolutionarily conserved as homologs are missing in multicellular organisms (Chu et al. 2006; Curtiss et al. 2007).

Off late, Morita and colleagues have identified metazoan orthologs of Mvb12p by proteomic analyses (Morita et al. 2007). They found two forms, MVB12A and B in humans, which are both substantially larger than Mvp12p and exhibit no apparent sequence homology to the yeast protein. Both MVB12A and B participate in the formation of the mammalian ESCRT-I complex, which shows the same 1:1:1:1 stoichiometry as the yeast complex. Consistent with the structural data from yeast ESCRT-I, human MVB12A interacts through its conserved C terminus with a binary complex composed of TSG101 and VPS37. However, human ESCRT-I is more complicated than its yeast counterpart, because the existence of different paralogs of VPS37 and MVB12 allows the assembly of eight different forms of ESCRT-I, which may play distinct

or overlapping roles in sorting (Morita et al. 2007). ESCRT-I is transiently recruited to endosomal membranes and subsequently released by the ATPase Vps4p. In the absence of active Vps4p, yeast ESCRT-I becomes entrapped on enlarged endosomal structures called class E compartments (Katzmann et al. 2002; Williams and Urbe 2007). Contrary to the proposal by Emr and coworkers (Chu et al. 2006) who suggested that Mvb12p-containing yeast ESCRT-I complexes are mainly cytosolic, mammalian ESCRT-I containing MVB12A found to be trapped in the class E compartment in the presence of dominant-negative VPS4 (Morita et al. 2007).

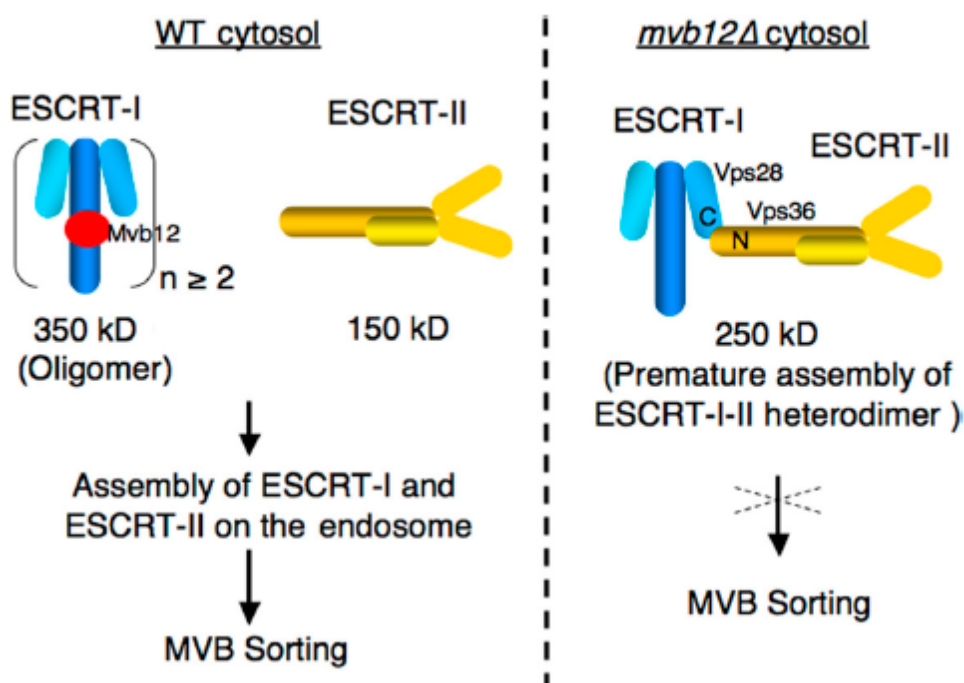


Figure 7. Working model for the function of Mvb12 as proposed by (Chu et al. 2006). In the cytosol, Mvb12 associates with and stabilizes ESCRT-I in an oligomeric, inactive state so that ESCRT-I cannot interact with ESCRT-II. Once recruited to the endosome, ESCRT-I assembles with ESCRT-II, leading to the activation of the downstream ESCRT machinery and cargo sorting into the MVB pathway. In the absence of Mvb12, the assembly of ESCRT-I and -II occurs prematurely in the cytosol, resulting in a defect in MVB sorting.

Very recently a fourth subunit of ESCRT-I complex in *C. elegans* named MVB-12 has been identified and functionally characterized (Audhya et al. 2007). MVB-12 is conserved

among metazoans, but is, three fold larger and bears no clear sequence similarity to the yeast protein Mvb12p. Hydrodynamic analysis of endogenous and recombinant ESCRT-I reveals that both are stable heterotetrameric complexes, with a native molecular weight of,125 kD, reflecting a 1:1:1:1 association of the four subunits. Depletion of MVB-12 slows the kinetics of cell surface receptor downregulation, consistent with a function in ESCRT-mediated MVB sorting (Audhya et al. 2007). Until now the presence and functionality of fourth subunit of ESCRT-I complex in plants is not known.

Aim

The *Arabidopsis ELCH* gene, a homolog of Vps23/ TSG101 and the key component of the plant ESCRT-I complex has been functionally characterized. The *elch* mutant shows multiple nuclei in various cell types, indicating a role in cytokinesis regulation (Spitzer et al. 2006). Therefore the first major objective was to elucidate whether the cytokinesis regulation is a special ESCRT unrelated function of ELCH or it is the function of the whole ESCRT system in plants as discussed for mammalian ESCRT machinery. In order to achieve this objective, genetic characterization of VPS28 and VPS37, the other important components of ESCRT-I complex have been performed.

A second Vps23 homolog, VPS23-2 (At5g13860) displays high sequence similarity to ELCH (72%). The functionality of this gene was determined by dominant-negative approach and promoter swapping experiment.

Very recently a novel fourth subunit of ESCRT-I complex has been identified and functionally characterized in yeast (Mvb12p), human (MVB12A and MVB12B), and *C. elegans* (MVB-12) which play a crucial role in MVB sorting pathway. In addition to *Arabidopsis* ELCH and VPS23-2, a third, dicot-specific Vps23 homolog, VPS23-3 encoded by At2g38830 has been identified. It shows a lesser degree of homology (47%) to *Arabidopsis* ELCH compared to the homology of ELCH to *Oryza sativa* ELCH (66%) and VPS23-2 (72%). Therefore the second major aim was to determine if this novel VPS23-3 is a component of the plant ESCRT system. If so, does it serves as an additional fourth subunit of ESCRT-I complex in plants? In order to analyse this, a detailed molecular and biochemical characterization of VPS23-3 was performed.

B. Results

B 1. Genetic characterization of the ESCRT-I components

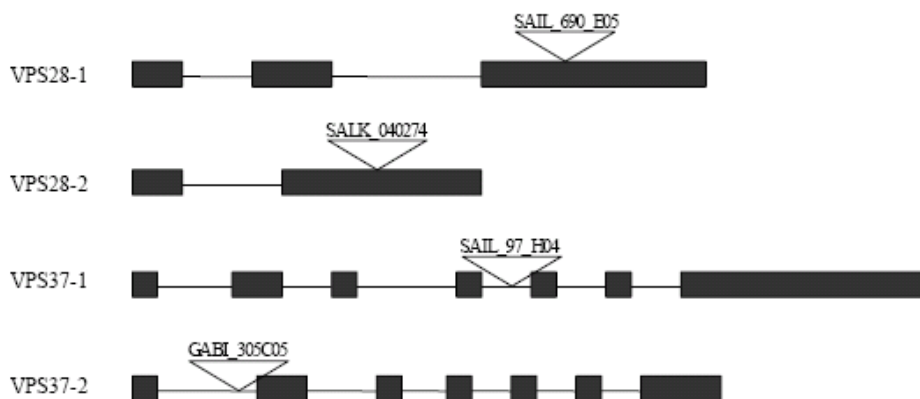
Recently the *Arabidopsis* ELCH (VPS23-1) a component of ESCRT-I complex and a homolog of yeast Vps23 and mammalian TSG101 has been isolated and functionally characterized (Spitzer et al. 2006). To date, the *elch* mutant (*elc*, *vps23-1*) is the only characterized mutant of the *Arabidopsis* ESCRT component. The *elch* mutant showed cytokinesis defects in all tested cell types resulting in multinucleated cells indicating that ELCH is involved in regulating plant cytokinesis (Spitzer et al. 2006). VPS28 and VPS37 are the other known components of ESCRT-I complex (Winter and Hauser 2006) (Table 1). From yeast it is known that Vps23 acts in concert with Vps37 and Vps28 in the ESCRT-I complex. Consistent with this both *Arabidopsis* VPS37 and VPS28 paralogs were co-immunoprecipitated with HA tagged ELCH (Spitzer et al. 2006). It remained unclear whether the cytokinesis regulation is a function of the whole ESCRT system in plants as discussed for mammalian ESCRT machinery (Carlton and Martin-Serrano 2007; Carlton et al. 2008) or represents a special ESCRT unrelated function of ELCH. Therefore a detailed genetic analysis of ESCRT-I homologs of *Arabidopsis* has been performed.

B 1.1. Genetic analysis of VPS28 and VPS37

At least one T-DNA insertion mutant for each of the two paralogs of *VPS28* and *VPS37* were isolated. The T-DNA insertion lines of *VPS28-1* (SAIL_690_E05, inserted on third exon), *VPS28-2* (SALK_040274, inserted on second exon), *VPS37-1* (SAIL_97_H04, inserted on fourth intron) and *VPS37-2* (GABI_305C05, inserted on first intron) (Figure 8 A) were screened by PCR using primer combinations LP RP for WT and RP LB for homozygous lines. In order to check the knock-out status of the isolated homozygous lines of *VPS28* and *VPS37*, RT-PCR was performed using appropriate primer combinations. RT-PCR analysis of homozygous mutant plants showed that in none of the four mutant lines full length mRNA of the respective gene was present (Figure 8 B). To test whether the isolated mutants represent complete knock-outs, RT-PCR with primer pairs that are located on 5' of the respective insertions was performed. In the

vps28-1 and *vps37-2* lines, the expressions of the fragment 5' to the insertion were detected (Figure 8 B). The lines *vps28-2* and *vps37-1* did not show any expression of the fragment 5' of the respective insertion and were therefore likely to represent complete knock-outs (Fig 8 B).

A



B

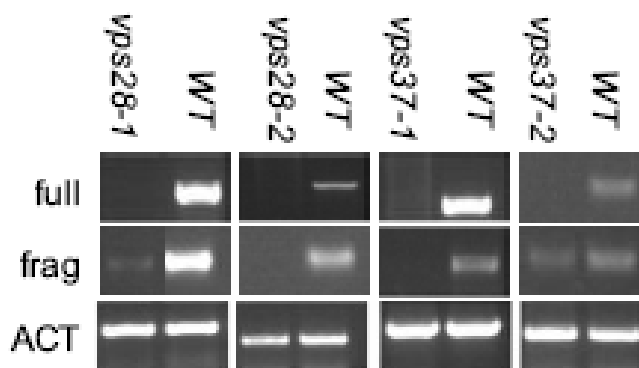
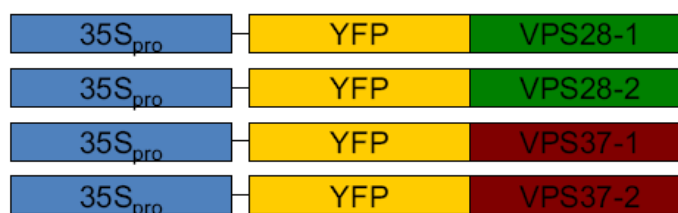


Figure 8: Genetic characterization of ESCRT-I mutants. A. Genomic structures of the VPS28 and VPS37 homologs. Exons are shown as bold lines; introns are represented by thin lines. The positions of the respective insertions are indicated by triangles. **B.** RT PCR analysis of the expression of *VPS28-1*, *VPS28-2*, *VPS37-1* and *VPS37-2* genes in homozygous lines of the respective mutants (WT= wild type, ACT= ACTIN, frag= 5' fragment to insertion, full= full length cDNA).

B 1.2. *vps28-1 vps28-2* and *vps37-1 vps37-2* are lethal

None of the four single mutants displayed any recognizable phenotype. As this was most likely due to redundancy, generation of the double knock-outs *vps28-1 vps28-2* and *vps37-1 vps37-2* were tried. In both cases homozygous double mutants could not be identified in populations of 48 (*vps37-1 vps37-2*) and 96 (*vps28-1 vps28-2*) F2 plants. As the examined numbers were too low to exclude the possibility of missed double mutants, the plants from each F2 population that were homozygous for one of the copies and heterozygous for the other were isolated and allowed to self. In the resulting F3 generations (50 plants tested each), there are no double knock-outs identified by PCR screen. This indicates that complete loss of function of *VPS28* or *VPS37* is lethal for the plant. To prove that lethality is due to the lack of *VPS28* or *VPS37* activity, rescue experiments were performed by transforming plants derived from F2 generations of the crosses *vps37-1* with *vps37-2* and *vps28-1* with *vps28-2* with constructs expressing fusions of the respective VPS genes fused to YFP under the control of the 35S promoter (Figure 9 A). The resulting T1 plants were PCR screened for plants that were genotypically double mutant, indicating rescue of the lethal effect of the double mutant by expression of the respective YFP fusion. In none of the four transformed populations any double mutant plants were found. To exclude that this was a statistic effect due to the low number of plants in the respective T1 generations one plant from each T1 that was homozygous mutant for the isoform it was transformed with and heterozygous for the other were selected. After selfing the T2 generation lines were screened expecting one quarter of double mutant plants in case of a rescue. For each combination the double knock-out genotypes were identified (Figure 9 B; Table 2) indicating the rescue of the double mutant lethality. The lethality is due to the total loss of *VPS28* or *VPS37* activity.

A



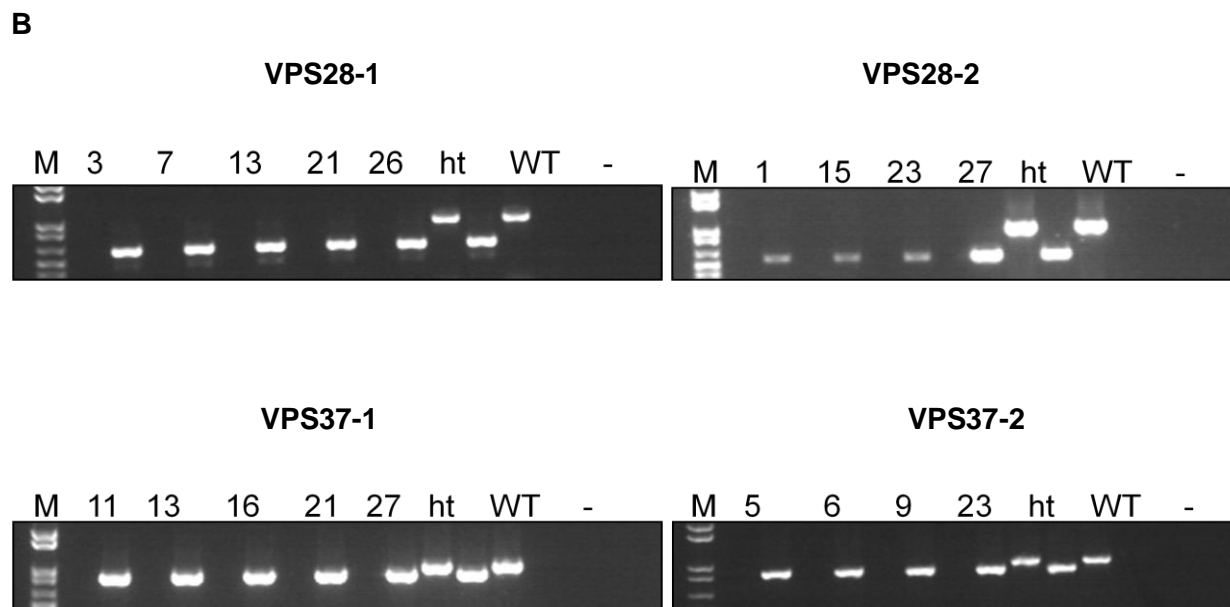


Figure 9: Rescue analysis of ESCRT-I mutants. A. Constructs used for the rescue experiments. **B.** Identification of genotypically homozygous lines for the four T-DNA insertion mutants (M=marker, ht= heterozygous lines, WT= wildtype, -= negative control without DNA, numbers= individual lines).

Table 2. Summary of the rescue experiments.

Fusion protein	Transformed into cross	Homozygous mutants in T2 generation	Number of plants tested
YFP:VPS28-1	<i>vps28-1 x vps28-2</i>	5	30
YFP:VPS28-2	<i>vps28-1 x vps28-2</i>	4	53
YFP:VPS37-1	<i>Vps37-1 x vps37-2</i>	5	57
YFP:VPS37-2	<i>Vps37-1 x vps37-2</i>	4	30

B 1.3. Double knock-outs *elch vps28-1*, *elch vps28-2* and *elch vps37-1* show synergistic phenotype

To test whether cytokinesis regulation is a function of all ESCRT-I components, double knock-outs were generated. For generating double knock-outs the *elch* mutant was used as a male

partner with each of the four other ESCRT-I single mutants as female partners for crossings. Seeds were collected in F1 generation and double homozygous lines were selected in F2 generation by PCR screen. The double knock-outs were scored for enhancement of the *elch* phenotype. The advantage of the correlation of the *elch* cytokinesis phenotype with an aberration in leaf trichome shape was taken into account. Plants with mutations in the *ELCH* gene exhibit 2% leaf trichomes with multiple nuclei (Spitzer et al. 2006). In addition these trichomes develop two stems that undergo normal branching giving them the overall appearance of antlers. Therefore the appearance of antler like trichomes is an easily observable direct measure of the *elch* dependent cytokinesis defect. Each of the double mutants with exception of *elch vps37-2* displayed a significantly enhanced antler frequency compared to the *elch* single mutant (Table 3). The double knock-outs *elch vps37-1* (4%) and *elch vps28-2* (3,8%) showed a stronger enhancement of the phenotype than *elch vps28-1* (2,5%) indicating that *vps37-1* and *vps28-2* are complete knock-outs and *vps28-1* could be still partly functional (Figure 8 B).

B 1.4. ESCRT-I members are involved in cytokinesis regulation

As the double knock-outs *elch vps37-1* and *elch vps28-2* are showing a strong trichome phenotype, the triple knock-out was generated by crossing the *elch vps37-1* as female partner and *elch vps28-2* as male partner. Seeds were collected in F1 and triple knock-out *elch vps37-1 vps28-2* was selected in F2 generation by PCR screen. In the triple knock-out *elch vps37-1 vps28-2*, 10.9% of the trichomes appear as antlers (Table 3; Figure 11) that typically have more than two stems and nuclei (Figure 10 d & e and i & j). In addition to this a synthetic phenotype was also observed. Triple knock-out plants were strongly reduced in growth and siliques were extremely small compared to WT, *elch* and *elch vps37-1* (Figure 10 C-E) highlighting the general importance of the pathway. In summary, the results of genetic analysis of ESCRT-I components indicate that VPS28 and VPS37 are functionally associated with ELCH-dependent cytokinesis regulation. The phenotype is dependent on the function of the ELC protein as other ESCRT-I double mutants do not display *elch*-like antlers (Table 3). Therefore the *Arabidopsis* ESCRT-I proteins are working together in regulating cytokinesis and it is not just a special ESCRT unrelated function of ELCH.

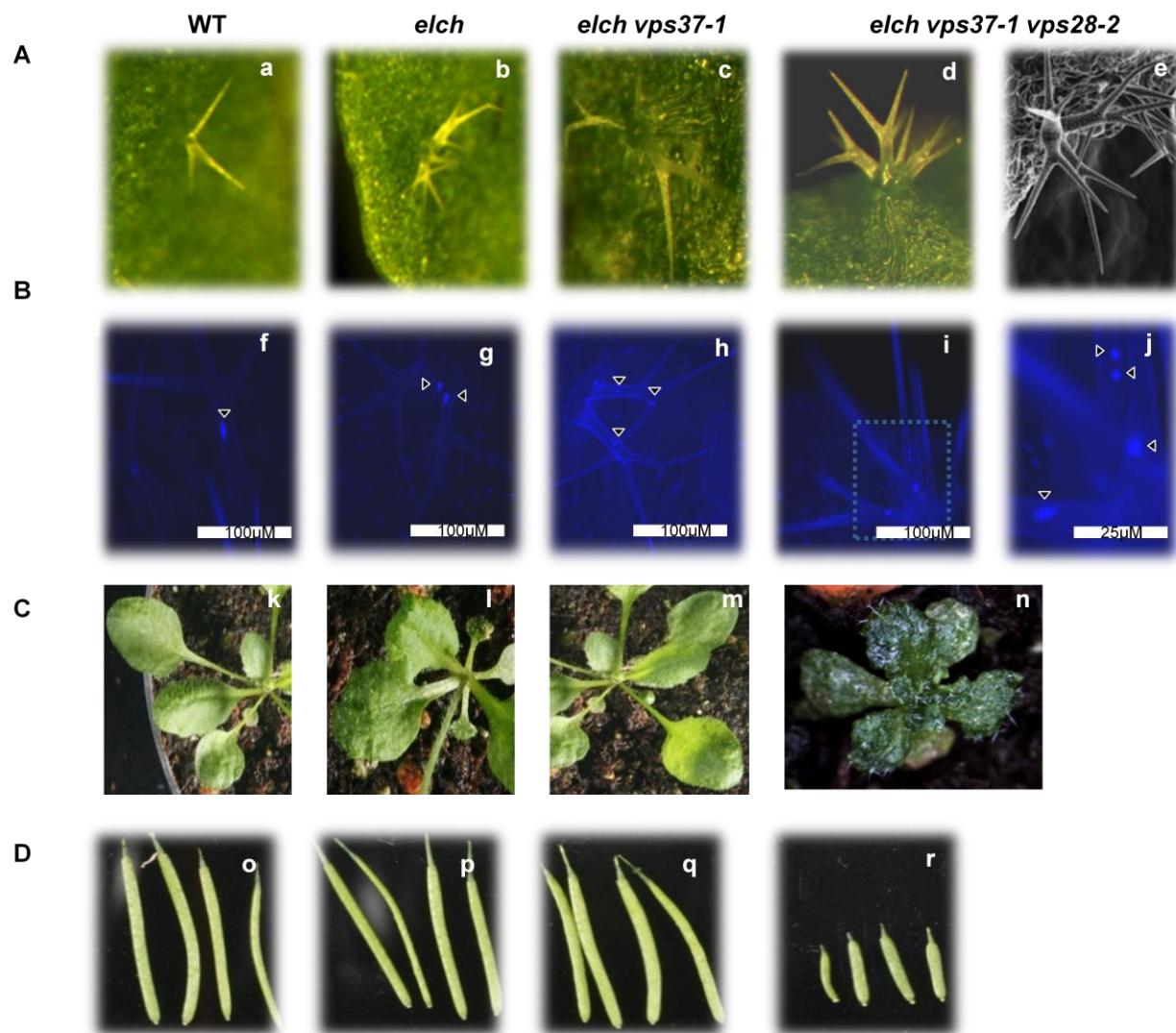


Figure 10: Phenotypic analysis of the ESCRT-I mutants. **A.** WT, single knock-out *elch*, double knock-out *elch vps37-1* and triple knock-out *elch vps37-1 vps28-2* as binocular images. 'e' is a scanning electron microscope (SEM) image of triple knock-out showing cluster trichomes. **B.** WT, single knock-out *elch*, double knock-out *elch vps37-1* and triple knock-out *elch vps37-1 vps28-2* as DAPI stained images. Arrows depict the multiple nuclei in a single trichome cell (j). **C.** Rosettes of WT, single knock-out *elch*, double knock-out *elch vps37-1* and triple knock-out *elch vps37-1 vps28-2*. **D.** Siliques of WT, single knock-out *elch*, double knock-out *elch vps37-1* and triple knock-out *elch vps37-1 vps28-2*. WT (a,f,k,o), *elch* (b,g,l,p), *elch vps37-1* (c,h,m,q) and *elch vps37-1 vps28-2* (d,e,l,j,n,r).

Table 3. Summary of genetic analysis of putative ESCRT-I mutants

Genotype	Antler frequency [%]	N	P
<i>Ws-0</i>	0	6052	
<i>Col-0</i>	0	5910	
<i>Elch</i>	1.84	4207	
<i>vps28-1</i>	0	5705	
<i>vps28-2</i>	0	5932	
<i>vps37-1</i>	0	7102	
<i>vps37-2</i>	0	7745	
<i>vps28-1 vps28-2</i>	Nd		
<i>vps37-1 vps37-2</i>	Nd		
<i>vps37-1 vps28-2</i>	0	5488	
<i>vps37-2 vps28-1</i>	0	5942	
<i>elch vps28-1</i>	2.48	5439	<0,05 ^a
<i>elch vps28-2</i>	3.80	5351	<0,001 ^a
<i>elch vps37-1</i>	4.01	5410	<0,001 ^a
<i>elch vps37-2</i>	1.98	5761	n.s. ^a
<i>elch vps28-2 vps37-1</i>	10.91	4564	<0,001 ^{a,b,c}

^a Cross tab test against *elch*

^b Cross tab test against *elch vps28-2*

^c Cross tab test against *elch vps37-1*

n.s.: not significant

nd: not done

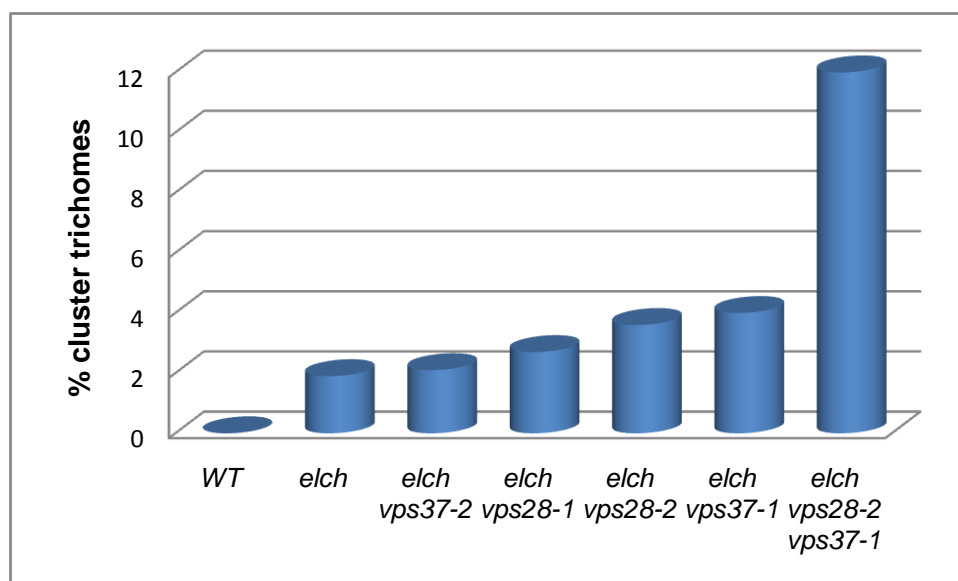


Figure 11: Phenotypic trichome analysis of putative ESCRT-I mutants and combinations. Graph showing the synergistic phenotypes of double and triple knock-outs.

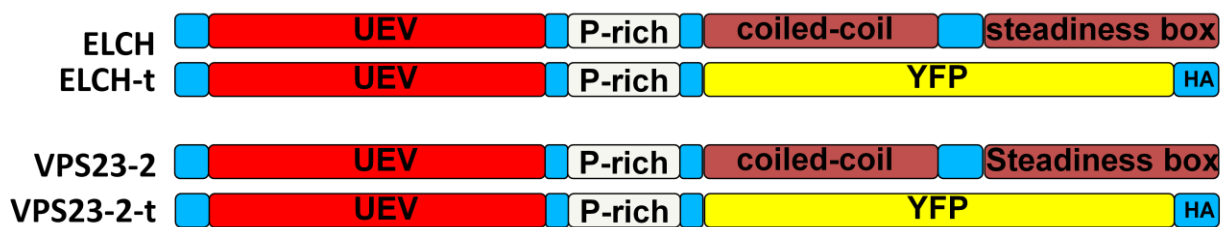
B 2. Functional analysis of VPS23-2

The ELCH protein is similar to yeast Vps23p. It shows moderate similarity to yeast Vps23 gene and mammalian TSG101 (Spitzer et al. 2006). It has a N-terminal UEV domain without a conserved cysteine residue in all UBC domains. The central region of the protein contains a coiled-coil domain as predicted by the COILS program and the homology comparison (Lupas et al. 1991). At the C-terminal end a conserved domain that was named steadiness box because it is involved in the control of the stability of TSG101 (Feng et al. 2000) and the interaction with Vps28p and Vps37 in yeast (Kostelansky et al. 2006). *Arabidopsis* VPS23-2 is a close homolog of ELCH (72% identity) encoded by At5g13860. It also shares similar domain structure and lacks the critical cysteine residue in the UEV domain (Figure 14). The main differences are two small deletions in the first half of the protein that do not affect the UEV- or the coiled-coil domain (Figure 14).

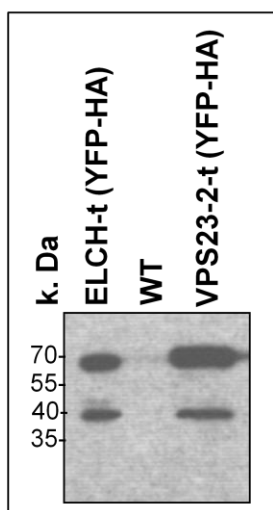
B 2.1 Dominant-negative VPS23-2 (VPS23-2-t) phenocopies the *elch* mutant

The deletion of the central coiled-coil domain of Vps23 affects the interaction with Vps28p and Vps37 in yeast (Kostelansky et al., 2006) and deletion of the C-terminal steadiness box affects the stability of TSG101 (Feng et al., 2000). Taken this advantage a dominant-negative ELCH (ELCH-t) construct with deleted central coiled-coil domain and C-terminal steadiness box and fused with HA tag was expressed under the control of the 35S promoter rescued the *elch* mutant (ELCH-t construct was prepared, analyzed and kindly provided by Dr. Swen Schellmann; Figure 12 A-D). In order to functionally characterize VPS23-2, generating the knock-out of VPS23-2 was tried by screening T-DNA insertion lines SALK_114460 (inserted on 1000-promoter region) and SAIL_237_G05 (inserted on exon), but both lines showed expression of mRNA transcript in RT-PCR analysis (not shown). Other suitable insertion lines were not available for analysis. As VPS23-2 possesses a similar domain structure of ELCH at

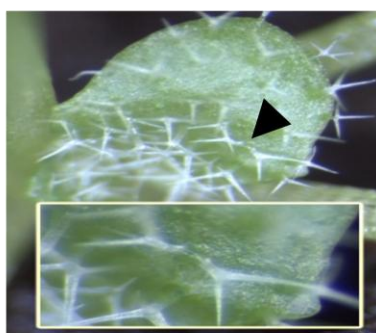
A



B



C



D



E

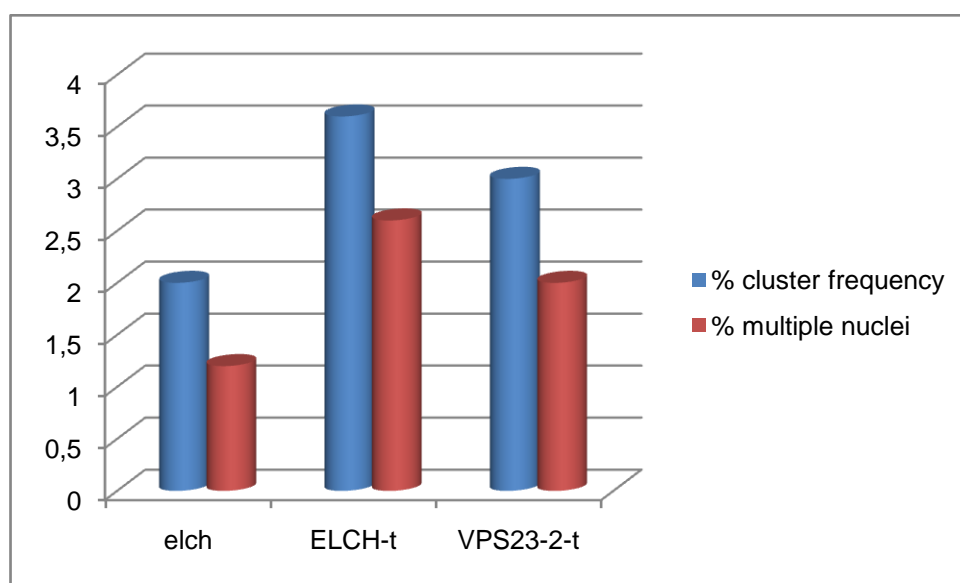


Figure 12: Molecular and genetic analysis of dominant-negative VPS23-2. **A.** Protein structure of full length and dominant-negative ELCH and VPS23-2. **B.** Western blot of dominant-negative versions of ELCH and VPS23-2 probed with anti-HA antibody. **C and D.** Dominant-negative versions phenocopying the *elch* mutant. **E.** Graph showing the percent cluster trichomes and multiple nuclei in *elch* and dominant-negative ELCH and VPS23-2. (**A, C and D** are kindly provided by Dr. Swen Schellmann).

protein level, a similar truncated construct of VPS23-2 was created by deleting the coiled-coil domain and steadiness box (VPS23-2-t) and fused with HA tag and expressed under the control of the 35S promoter with and transformed into Col-0 plants by *Agrobacterium* mediated transformation. The transgenic T1 plants were selected by spraying the BASTA herbicide and the phenotypic analysis was performed in the T2 generation. The presence of protein in stable transformed plants was confirmed by immunoblot with anti-HA antibody (Figure 12 B). The presence of additional bands in immunoblot suggests the importance of the steadiness box in maintaining the stability of the proteins. The dominant-negative VPS23-2 phenocopied the *elch* mutant and showed higher percentage of clustered trichomes and multiple nuclei compare to *elch* mutant (Figure 12 E) suggests the functional redundancy of VPS23-2 with ELCH.

B 2.2 VPS23-2 expressed under the *ELCH* promoter rescues the *elch* mutant

In order to confirm the functionality of *VPS23-2*, a promoter-swapping experiments were performed by expressing *VPS23-2* under the control of *ELCH* promoter and the construct was transformed to the *elch* mutant lines by *Agrobacterium* mediated transformation. The construct in that *ELCH* is expressed under the *ELCH* promoter was used as a positive control. The transgenic T1 plants were selected on hygromycin and the phenotypic analysis was performed in the next generation. No trichome showed an *elch* phenotype among the observed 3560 trichomes in plants bearing the p*ELCH*:*VPS23-2* and they all look like wildtype (Table 4). Similarly in the plants transformed with control construct none of the observed trichomes showed the *elch* phenotype among the 3600 trichomes suggesting the presence and functionality of the construct (Table 4). Promoter swapping experiments confirmed the functional redundancy of *VPS23-2* with *ELCH*.

B 3. Functional characterization of the *Arabidopsis* ELCH homolog VPS23-3

Recently *Arabidopsis* *ELCH* gene corresponds to yeast Vps23 has been characterized (Spitzer et al. 2006). VPS23-2 is a close homolog of ELCH which are functionally redundant as previously described. In order to analyze the ESCRT pathway in detail in *Arabidopsis*, BLAST search was conducted and a dicot specific *Arabidopsis* *ELCH* homolog VPS23-3 encoded by At2g38830 was found. VPS23-3 shows a lesser degree of homology (47%) to *Arabidopsis* ELCH compared to the second homolog VPS23-2 which shows 70% homology to *Arabidopsis* ELCH. In a cluster tree the rice ELCH (OsELCH) show close homology (61%) to *Arabidopsis* ELCH compared to VPS23-3 (Figure 13 A). Hence it was very interesting to know the role of this novel gene in the context of the ESCRT pathway in plants. Therefore molecular and biochemical characterization of VPS23-3 was performed to address two major questions. First, is VPS23-3 a component of the plant ESCRT system? Second, is it functionally different from ELCH?

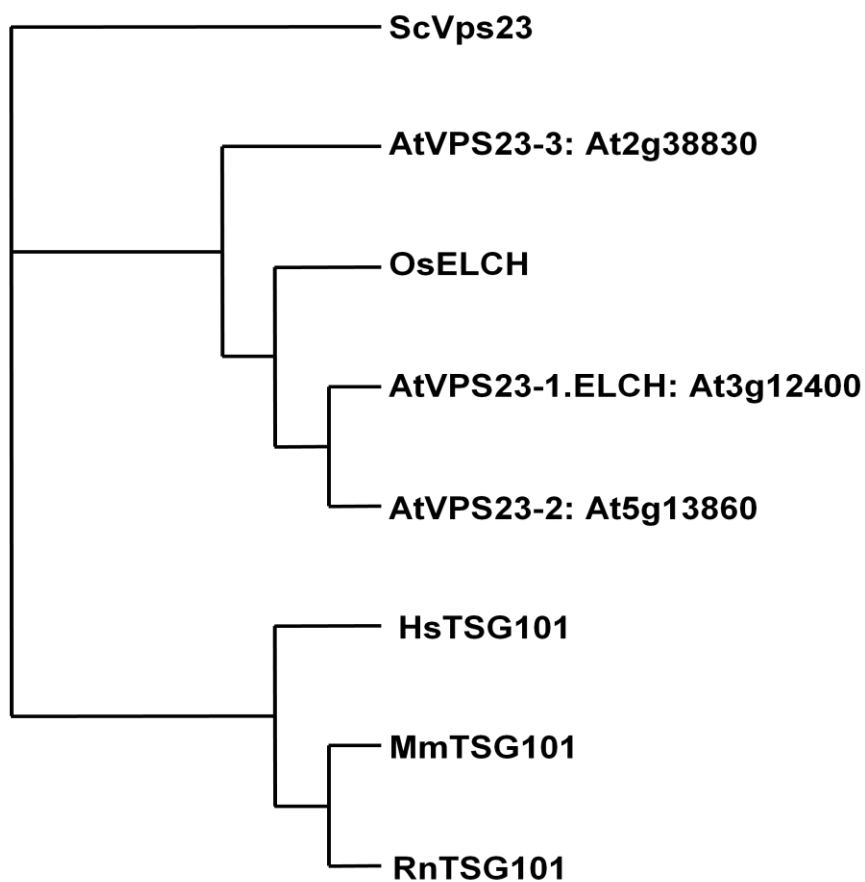
B 3.1 The *Arabidopsis* ELCH homolog VPS23-3 is a component of the plant ESCRT system

In order to investigate if VPS23-3 is a component of the *Arabidopsis* ESCRT-I complex, molecular, cell biological and biochemical analysis were performed.

B 3.1.1 VPS23-3 expressed ubiquitously

Expression analysis of VPS23-3 was performed by RT-PCR. RNA was extracted from different organs like cauline and rosette leaves, stems, flowers and siliques of WT (Col-0) plants. As VPS23-3 has no introns, RT-PCR was performed with and without the reverse transcriptase. PCR was performed using VPS23-3 specific primers and actin primers were used as control (Figure. 13 B). VPS23-3 show expression in all tested organs suggesting its ubiquitous expression.

A



B

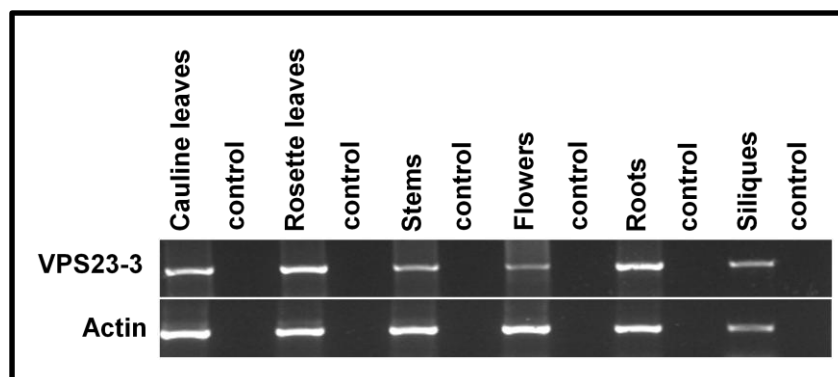


Figure 13: **A.** Cluster tree showing the VPS23 homologs in *Arabidopsis*, rice, yeast and mammals (note that OsELCH showing close homology to *Arabidopsis* ELCH compare to VPS23-3). **B.** Expression analysis of *VPS23-3* by RT-PCR analysis. Actin used as positive control. *VPS23-3* showed ubiquitous expression in all the organs tested. (control=RT-PCR without reverse transcriptase).

AtVPS23 -1-ELCH-3g12400	1	MVPPPS NPQQVQFLSSALSQRGPSSVPEE.SNKWLIRQHLLNLISSYPSLEPKTASF M
AtVPS23 -2-5g13860	1	MAPPPAKMDEIHQFLSSALTQRGPSALPYAE.NTKSLIRQHLLNLISSY TSLDPKTATFT
AtVPS23 -3-long-At2g38830	1	MAASSSSSSQVKFIEKALLATGSFATSYTDPDQKWLIRKHLTSLLDQYFNFELSDTTFN
		UEV-domain
AtVPS23 -1-ELCH-3g12400	60	HNDGRSVNLLQADGTIPMPFHGVTYN.IPVIIWLLESYP RHPPCVYVNPADMIIKRPH A
AtVPS23 -2-5g13860	60	HNDGRSV ILLQADGTIPMPF QGVSYN.IPVVIWLLESYP QYPPCVYVNP RDMIKRPH S
AtVPS23 -3-long-At2g38830	60	HNNGAKVQIFCLEGLSLRIRSSTTQLPTVQLTIWIHENYELTPIIVFINFN.SIPIRNNHP
		UEV-domain
AtVPS23 -1-ELCH-3g12400	119	H VTPSGLVSLPYLQNWVYPPSSNLVDLVS DLSAAFARDPPLYS RRRPQPPFPSPPTVYDSS
AtVPS23 -2-5g13860	119	N VSPSGLVSLPYLQNWYPPSSNLVDL ASHLSAAFSDPPLYS QRRP.PPQPSP.....
AtVPS23 -3-long-At2g38830	119	F INSSGYTKSR YIETWEHPCRNLLD FTRNLKKVLANDHFFLHTDSLIPTRNQS.....
		UEV-domain
AtVPS23 -1-ELCH-3g12400	179	LSRPP SADQSLRPFPPSPYGGVSRVQVQHVVHQQ QSDDAAEVFKRNAINKVMEMVH SD
AtVPS23 -2-5g13860	171 SIGSGYSRFLPP.....R QTDDAAEVYKKNAINRIVEMVH GD
AtVPS23 -3-long-At2g38830	172 VSRTEALDRLATSLHYD
		Coiled-coil-domain
AtVPS23 -1-ELCH-3g12400	239	LVSMMRAREAEAEELLSLQA GLKRREDELN IGLKEMV EKETLEQQLQII SMNTDILDSW
AtVPS23 -2-5g13860	208	IVLMRSAREVETEGLLSLQSDLKRREEIN NFKEMVIEKETLEQQLQVI AMNTDVLGSW
AtVPS23 -3-long-At2g38830	189	VLTIMERSDEEIEENWKLQSEVKQRSESVKSIITELEIERGTIKVRALKIKEDSDVLTW
		Coiled-coil-domain
AtVPS23 -1-ELCH-3g12400	299	VRENQGKTAN.LVDLDVDNAFECGDTLSKQMLECTALDLAIED AIYSLDKSF QDCVVPFD
AtVPS23 -2-5g13860	268	IRENQGKAKDLVDLDVD DSFECIDSLKQMLECTALDLAIEDVVYSMDKSF RDCSLPFD
AtVPS23 -3-long-At2g38830	249	VEMNYLKLTS...MDMGRIEMFIEES..EVEGLAGDDAIEDVLRVLEEAERCELEIG
		Coiled-coil-domain
		Steadiness box
AtVPS23 -1-ELCH-3g12400	358	QYLRNVRLLSREQFFHRATGSKVR AAQMEVQVA AIAGRLHS
AtVPS23 -2-5g13860	328	QYLRNVRLLSREQFFHRATA EKVREIQMDAQVA SIAARLHS
AtVPS23 -3-long-At2g38830	303	S YLKQVRVLAREQFF LKHLSEFKTQNFHI.....0
		Steadiness box

Figure 14: Protein alignment of the *Arabidopsis* VPS23 homologs. N-terminal UEV domain is underlined in red lines, central coiled-coil domain is underlined in white lines and C-terminal steadiness box is underlined in green lines.

B 3.1.2 VPS23-3 is localized on endosomes

In order to test the intracellular localization, VPS23-3 was fused to YFP under the control of the 35S promoter and expressed in *Arabidopsis* protoplasts. Dotted structures of YFP fluorescence were observed. To check if the observed dots were endosomes, YFP:VPS23-3 was co-expressed with the endosomal markers ARA6, ARA7 and the MVB marker Pep12 fused to CFP. YFP:VPS23-3 showed partial co-localization with all the three markers suggesting that VPS23-3 is localized on endosomes (Figure 15 A-L). To test if VPS23-3 co-localizes with ELCH, YFP:VPS23-3 was co-expressed with CFP:ELCH in *Arabidopsis* protoplasts (Figure 15 M-P). VPS23-3 also showed co-localization with ELCH indicating that VPS23-3 is localized in the same complex as ELCH.

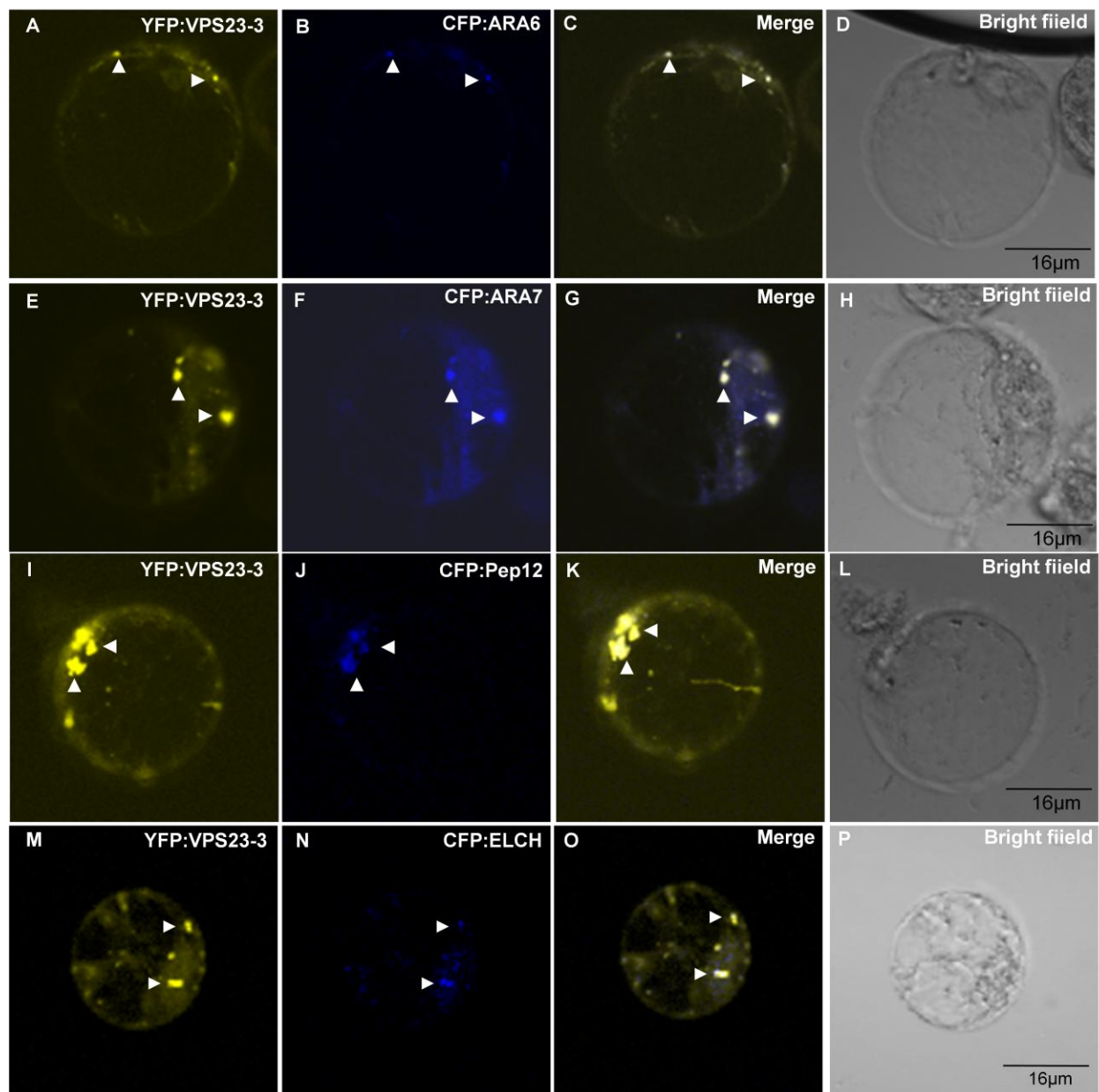


Figure 15: VPS23-3 is localized on endosomes. The *Arabidopsis* protoplasts transformed with YFP:VPS23-3 (A, E, I, M) were co-localized with endosomal markers ARA6:CFP (B), CFP:ARA7 (F), CFP:Pep12 (J) and also with CFP:ELCH (N). C, G, K, O are the respective merged images and D, H, L, P are the respective bright field images. Arrows indicate the co-localization. Bar 16 μ m.

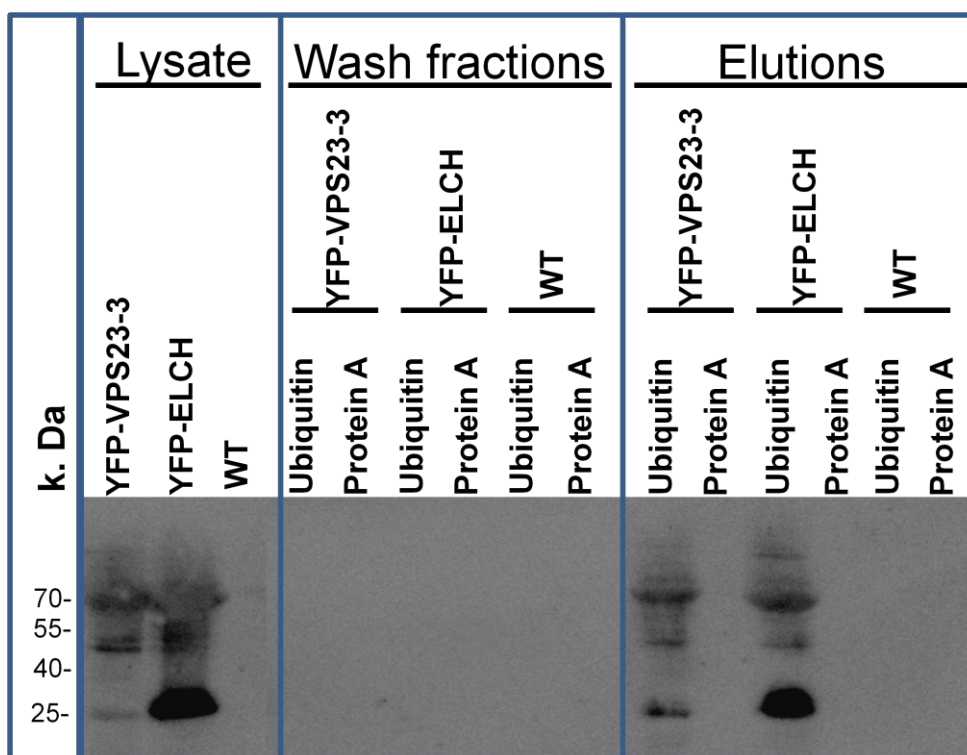
B 3.1.3 YFP:VPS23-3 binds to ubiquitin *in vitro*

The major role of the Vps23-3/ TSG101 in the ESCRT-I complex appears to be binding to the ubiquitylated target proteins. To test whether VPS23-3 has the ability to bind ubiquitin, pull-down experiments were performed using ubiquitin agarose (Figure 16 B). Protein extracts from YFP:VPS23-3 plants were incubated with ubiquitin agarose and immunoblotting was performed using GFP antibody. Protein G agarose was used as a negative control. YFP:VPS23-3 binds to ubiquitin but not to protein G agarose.

A



B



C

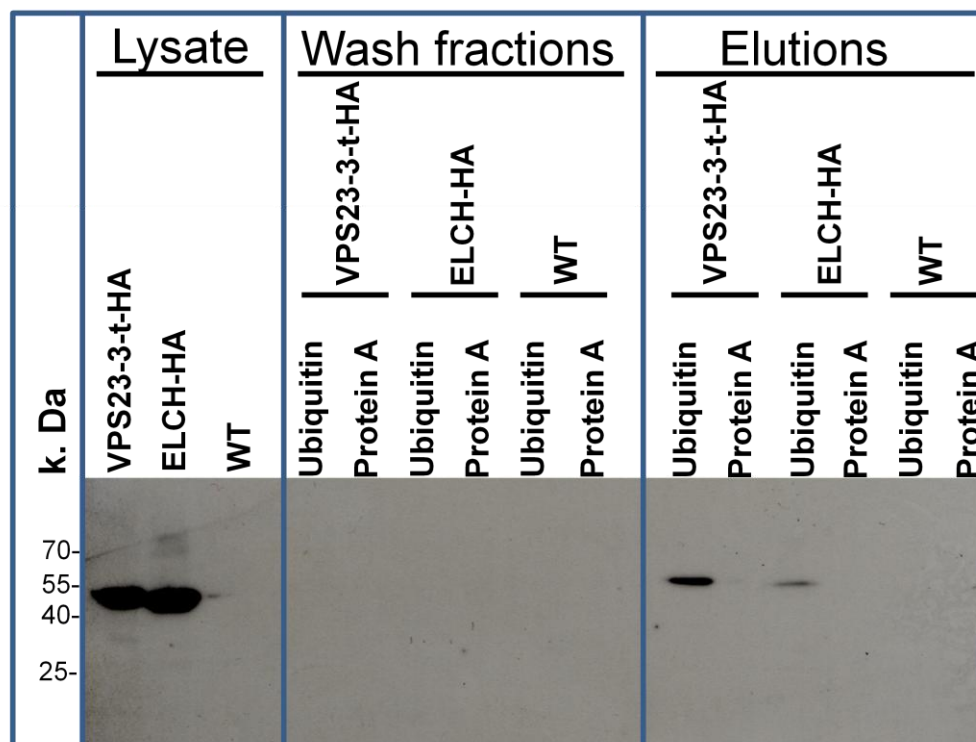


Figure 16: VPS23-3 protein binds ubiquitin *in vitro*. **A.** Full length VPS23-3 protein and dominant-negative VPS23-3 (lacking central coiled-coil domain and C-terminal steadiness box fused to YFP-HA tags). **B.** YFP-VPS23-3 was pulldown with ubiquitin agarose and protein G beads and immunoblotting with GFP antibody. YFP-ELCH was used as a positive control and WT as negative control. **C.** Dominant-negative VPS23-3-t-HA lines were pulldown with ubiquitin agarose and protein G agarose beads and western with HA antibody. ELCH-HA was used a positive control and WT as negative control. Binding of dominant-negative VPS23-3 lacking the coiled-coil and steadiness box to ubiquitin suggesting the importance of UEV domain for ubiquitin binding.

B 3.1.4 N-terminal UEV domain is necessary for ubiquitin binding

In the protein alignment of the *Arabidopsis* VPS23 homologs, VPS23-3 shows about 47% similarity to the N-terminal UEV domain, central coiled-coil domain and C-terminal steadiness box of ELCH (Figure 14). Therefore to test which domain of VPS23-3 is important for ubiquitin binding, the central coiled-coil and C-terminal steadiness box were deleted and the N-terminal domain was fused to the HA tag (Figure 16 A). Pull-down experiments were performed using ubiquitin agarose and protein G agarose beads. This N-terminal domain of VPS23-3 (VPS23-3-

t) was still binding to the ubiquitin (Figure 16 C). This suggests that the N-terminal UEV domain is necessary for binding to the ubiquitylated cargo.

B 3.1.5 YFP:VPS23-3 protein is part of a high molecular weight complex

The ESCRT pathway in yeast and mammals was shown to consist of a protein network with distinct sub-complexes. ELCH-HA protein as a part of a high molecular weight complex has been shown (Spitzer et al. 2006). To determine whether VPS23-3 is also a part of high molecular weight complex, gel filtration/ size exclusion chromatography of YFP:VPS23-3 was performed using supherose 6 column. Protein extracts from YFP:VPS23-3 lines were ultra centrifuged and loaded into the column, fractions were collected, SDS-PAGE followed by immunoblot was performed using anti-GFP antibody. YFP:VPS23-3 eluted in the 11th fraction with a strong band which was equivalent to about 350k.Da indicating that VPS23-3 is part of a high molecular weight complex (Figure 17).



Figure 17: VPS23-3 is part of a high molecular weight complex. Gel filtration assay on supherose 6 column using protein extract from transgenic CaMV 35S::YFP-VPS23-3 plants. Protein size markers are indicated in the top in kilodaltons. The expected size of YFP-VPS23-3 is approximately 65 k.Da judged from SDS PAGE. The column was calibrated with standard marker proteins 1. Thymoglobulin (660 kDa), 2. Ferritin (440 kDa), 3. Aldolase (158 kDa), 4. Ovalbumin (43 kDa). Protein extracts from YFP-VPS23-3 lines were run on supherose 6 column, fractions were collected and SDS-PAGE followed by immunoblot was performed using GFP antibody. There is a strong band in the 11th fraction at about 350k.Da indicating that VPS23-3 is part of a high molecular weight complex.

B 3.2 VPS23-3 is functionally different from ELCH

Ubiquitous expression, endosomal localization, ubiquitin binding and being part of a high molecular weight complex suggests that VPS23-3 is a component of the plant ESCRT system. In order to check the functionality of VPS23-3 with the ELCH, expression of truncated VPS23-3 in stable plants, promoter rescue analysis and interaction assays were performed.

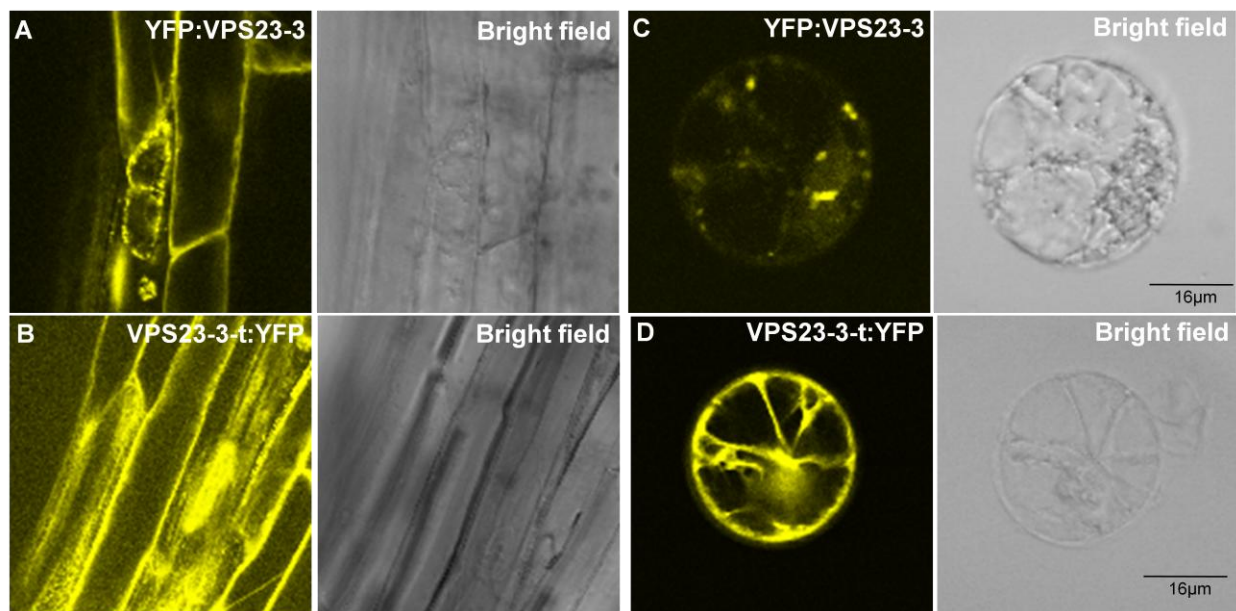


Figure 18: Truncated VPS23-3 (VPS23-3-t) shows differential localization. YFP:VPS23-3 shows endosomal localization in epidermal cells of stable transformed plants (A) and in protoplasts (C). Truncated VPS23-3-t:YFP shows cytosolic localization in epidermal cells of stable transformed plants (B) and in protoplasts (D). Bar 16 μ m.

B 3.2.1 The truncated VPS23-3 (VPS23-3-t) does not phenocopy the *elch* mutant

As described previously dominant negative VPS23-2, a close homolog of ELCH phenocopies the *elch* mutant. Taken this advantage similar truncated construct of VPS23-3 (VPS23-3-t) was prepared by deleting the central coiled-coil domain and C-terminal steadiness box and fused to YFP-HA tag under the control of the 35S promoter and was transformed into stable plants by *Agrobacterium* mediated transformation (Figure 16 A). Unlike VPS23-2-t, VPS23-3-t did not

phenocopy the *elch* mutant. The only difference observed in VPS23-3-t compared to the full length VPS23-3 was a different localization both in transient assays and in stable transformed plants. YFP:VPS23-3 is localized in dotted structures on endosomes (Figure 18 A and C) whereas YFP:VPS23-3-t shows mostly cytosolic localization (Figure 18 B and D). This gave a primary hint that VPS23-3 is not functionally redundant to ELCH.

B 3.2.2 VPS23-3 expressed under the *ELCH* promoter did not rescue the *elch* mutant

To test if the expression of VPS23-3 under the *ELCH* promoter rescues the *elch* mutant, promoter swapping experiment was performed by expressing the VPS23-3 under the control of the *ELCH* promoter and transformed into *elch* mutant lines by *Agrobacterium* mediated transformation. On average of about 1,8% of the observed 3660 trichomes showed the *elch* phenotype (Table 4). Expression of the ELCH under the control of the *ELCH* promoter was used as a control where none of the observed 3600 trichomes showed the *elch* phenotype (Table 4). Promoter swapping experiment suggests that VPS23-3 is functionally different from ELCH.

Table 4. Summary of the promoter rescue analysis

promoter	gene	No. of WT trichomes in T2	No. of <i>elch</i> trichomes in T2	% <i>elch</i> trichomes	Rescue Status
ELCH	ELCH	3600	0	0	rescued
ELCH	VPS23-2	3560	0	0	rescued
ELCH	VPS23-3	3557	63	1,8	no rescue

B 3.3 VPS23-3 might serve as a fourth component of the *Arabidopsis* ESCRT-I complex

In yeast the core ESCRT machinery consists of ten proteins that build three sub complexes, ESCRT I-III. In the *Arabidopsis* genome at least one sequence homolog of each member of the

ESCRT complexes was found (Spitzer et al. 2006; Winter and Hauser 2006). Three recent publications have identified a new fourth component of the *S. cerevisiae* ESCRT-I complex, Mvb12p. Mvb12p does not seem to be evolutionarily conserved as homologs are missing in multicellular organisms (Chu et al. 2006; Curtiss et al. 2007; Oestreich et al. 2007). However, a fourth component of ESCRT-I has also been reported in *C. elegans*. It has two human homologs and was named Mvb12 although it is lacking recognizable sequence similarity to yeast Mvb12p (Morita et al. 2007; Shi et al. 2007). According to BLAST analysis neither the yeast nor the human type of MVB12 proteins is present in plants. In order to determine if VPS23-3 serves as a fourth subunit of ESCRT-I complex, protein-protein interaction assays and blue native-PAGE experiments were performed.

B 3.3.1 VPS23-3 show differential interaction pattern

In an extensive and systematic yeast two hybrid assay, using each gene as bait and as prey with every other ESCRT member, Mojgan Shahriari has shown that VPS23-3 was interacting only with VPS28 homologs of ESCRT-I complex and not with any other components of the ESCRT system. Whereas ELCH was interacting with VPS37 homologs and not with VPS28 homologs of ESCRT-I complex and it served as a central molecule of the ESCRT system by interacting with the upstream and downstream components of the ESCRT system. In addition ELCH was showing self interactions unlike VPS23-3 which did not show self interactions (Mojgan Shahriari, PhD thesis, 2008). In order to verify the yeast two hybrid interactions independently and to check whether the interactions observed in a heterologous system also take place in the plant, VPS23-3 and other ESCRT members were fused to the N- and C-terminal sub-fragments of the *YFP* gene in a vector allowing the transient expression of the fusion proteins *in planta* and used these constructs to perform a bimolecular fluorescence complementation assay (Bi-FC) in protoplast cells of *Arabidopsis thaliana* (Bi-FC constructs of ESCRT-II and ESCRT-III members were prepared and analyzed by Aneta Saboljevic and Mojgan Shahriari respectively). The Bi-FC (also known as "split YFP") assay is based on the observation that the N- and C-terminal sub-fragments of the YFP (YFP_n and YFP_c respectively) do not spontaneously reconstitute a functional fluorophore. However, if fused to interacting proteins, the two non-functional halves of the fluorophore are brought into tight contact, refold together and generate *de novo* fluorescence. Thus, by Bi-FC, the interaction status of two proteins can be easily monitored *via* fluorescence emission upon excitation with a suitable

wavelength (Bhat et al. 2006). Similar results were observed in Bi-FC analysis where VPS23-3 was interacting only with VPS28-1 and VPS28-2 of the ESCRT-I complex and not with any other ESCRT member (Figure 19; Mojgan Shahriari, PhD thesis, 2008).

B 3.3.2 *In vivo* interactions between VPS23-3 and VPS28 homologs occur on endosomes

The Bi-FC method provide the possibility to explore where the interactions between VPS23-3 and its interactors (VPS28-1 and VPS28-2) take place in the cell. Therefore triple transformations of *Arabidopsis* protoplasts with the interacting partners (VPS23-3 with VPS28-1 and VPS23-3 with VPS28-2) and ARA6:CFP, CFP:ARA7 and CFP:Pep12 as endosomal markers were performed. In all cases partial co-localization of interacting partners with ARA6, ARA7 and Pep12 were found suggesting that the interaction occurs on endosomes (Figure 20; 21).

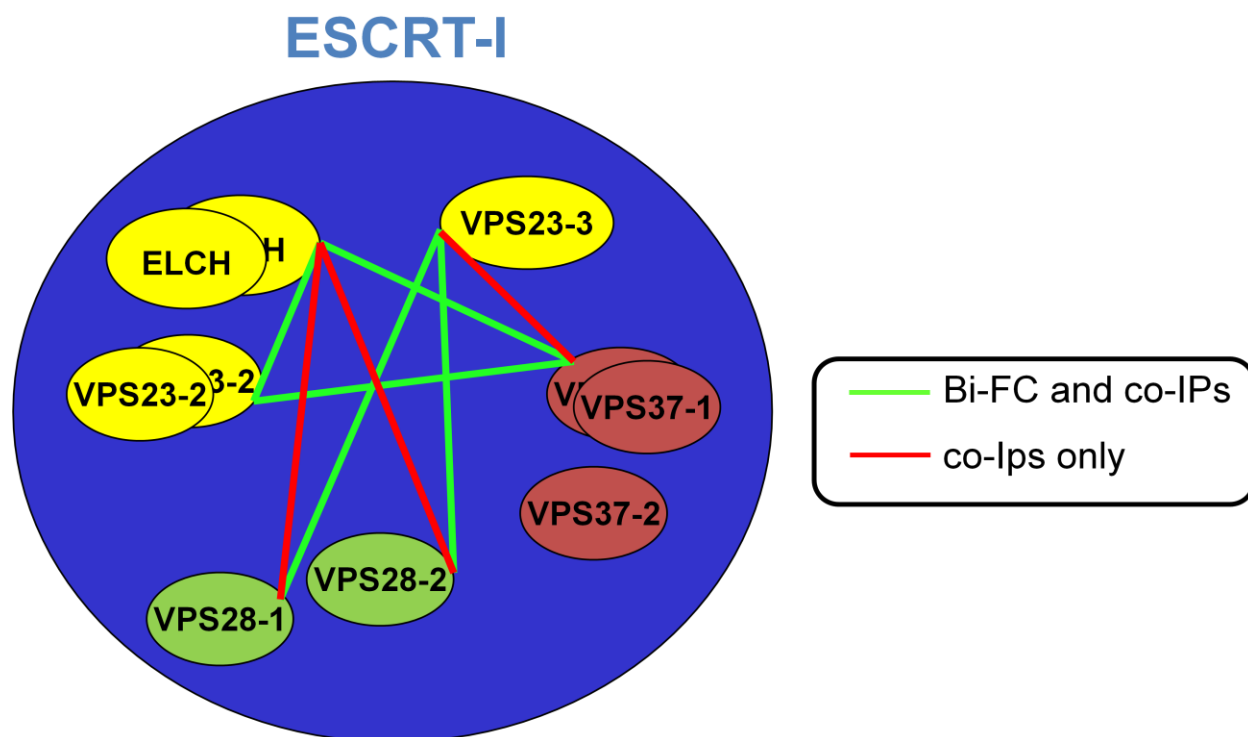


Figure 19: Interaction map of ESCRT-I components. Green lines represent the positive interactions in both Bi-molecular fluorescence complementation (Bi-FC) and radioactive *in vitro* co-IPs. Red lines represent the positive interactions only in radioactive *in vitro* co-IPs.

B 3.3.3 VPS23-3 interacts with VPS37 and ELCH interacts with VPS37 in *in vitro* co-IPs

As VPS23-3 was showing interaction with only VPS28 homologs and ELCH with VPS37 of ESCRT-I complex in both yeast two hybrid and Bi-FC assays, the specificity of interactions was tested by a third biochemical interaction assay called radioactive *in vitro* co-IPs. The *in vitro* expression of each protein was necessary to perform this interaction assay. Therefore *in vitro* expression of all the ESCRT-I proteins were performed by cloning each of them into separate gateway expression vectors with and without gal-4 activation domain (GAD) and radioactively expressed by complete labeling. All the ESCRT-I members showed the *in vitro* expression although expression of VPS23-3 was weaker compared to other members (Figure 22 A). First the interaction of VPS23-3 with other ESCRT-I members were tested by using VPS23-3 as a bait by partially labeled with radioactive S35 and all other ESCRT-I members as prey proteins by completely labeled with radioactive S35. Bait and prey proteins were treated with α -GAD antibody and pulldown with protein A beads and magnetically separated. Supernatant and

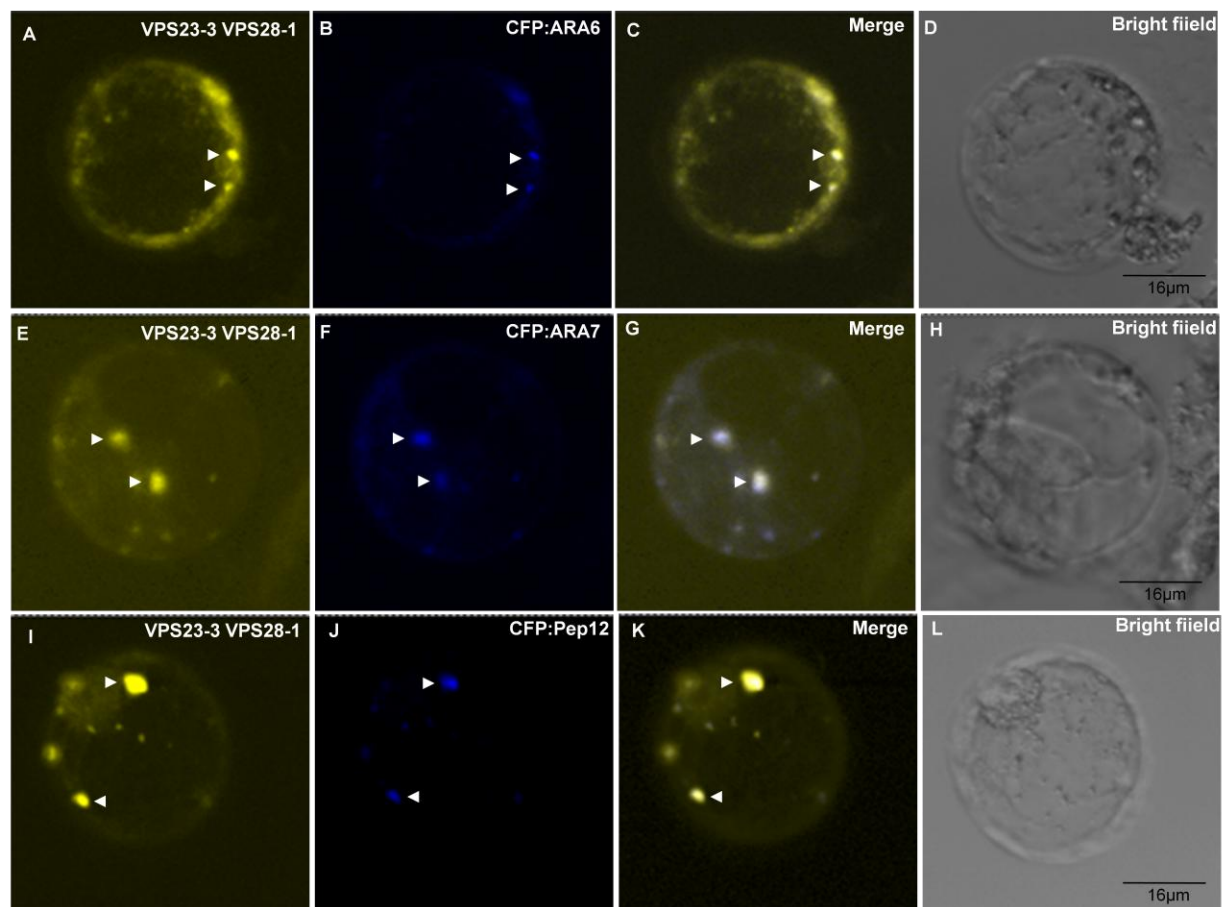


Figure 20: In vivo interaction between VPS23-3 and VPS28-1 occur on endosomes. A series of four pictures is shown for each co-localization: The first depicts the localization of Bi-FC interaction of VPS23-3 and VPS28-1 (**A, E, I**), second depicts the marker localization (**B, F, J**), the third an overlay of the respective first two pictures (**C, G, K**) and the fourth a bright field image of the respective protoplast (**D, H, L**). Co-localization of the interactions between VPS23-3 and VPS28-1 with the endosomal markers ARA6:CFP (**A-D**), CFP:ARA7 (**E-H**) and CFP-Pep12 (**I-L**) is shown. Arrows indicate the co-localizations. Bar 16µm.

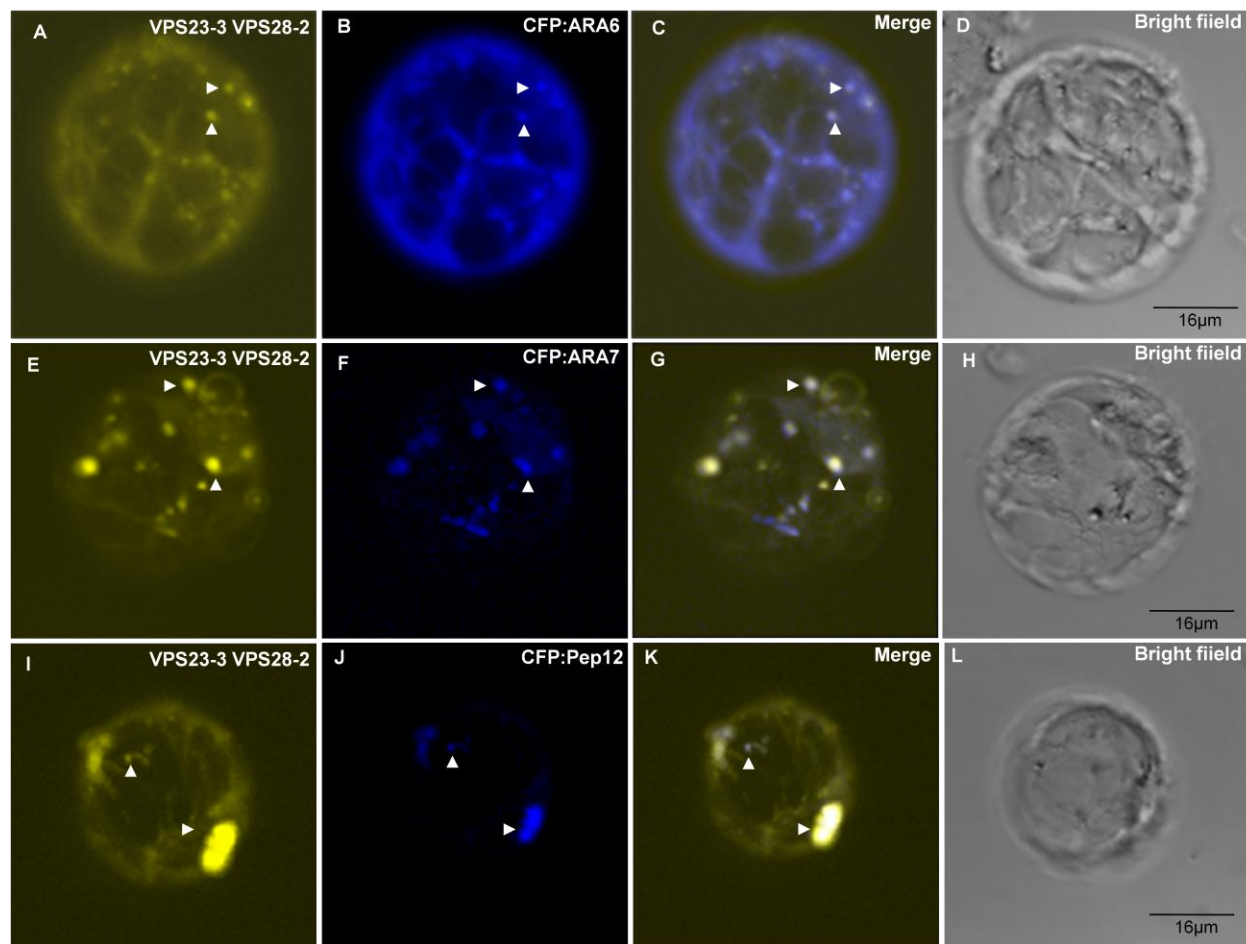
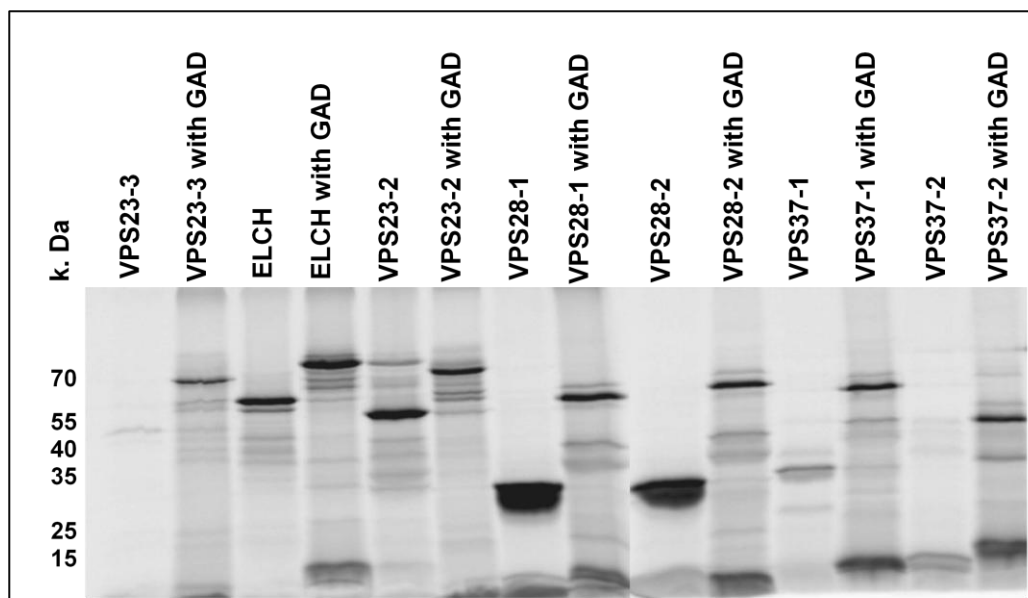


Figure 21: In vivo interaction between VPS23-3 and VPS28-2 occur on endosomes. A series of four pictures is shown for each co-localization: The first depicts the localization of Bi-FC interaction of VPS23-3 and VPS28-2 (**A, E, I**), second depicts the marker localization (**B, F, J**), the third an overlay of the respective first two pictures (**C, G, K**) and the fourth a bright field image of the respective protoplast (**D, H, L**). Co-localization of the interactions between VPS23-3 and VPS28-2 with the endosomal markers ARA6:CFP (**A-D**), CFP:ARA7 (**E-H**) and CFP-Pep12 (**I-L**) is shown. Arrows indicate the co-localizations. Bar 16 μ m.

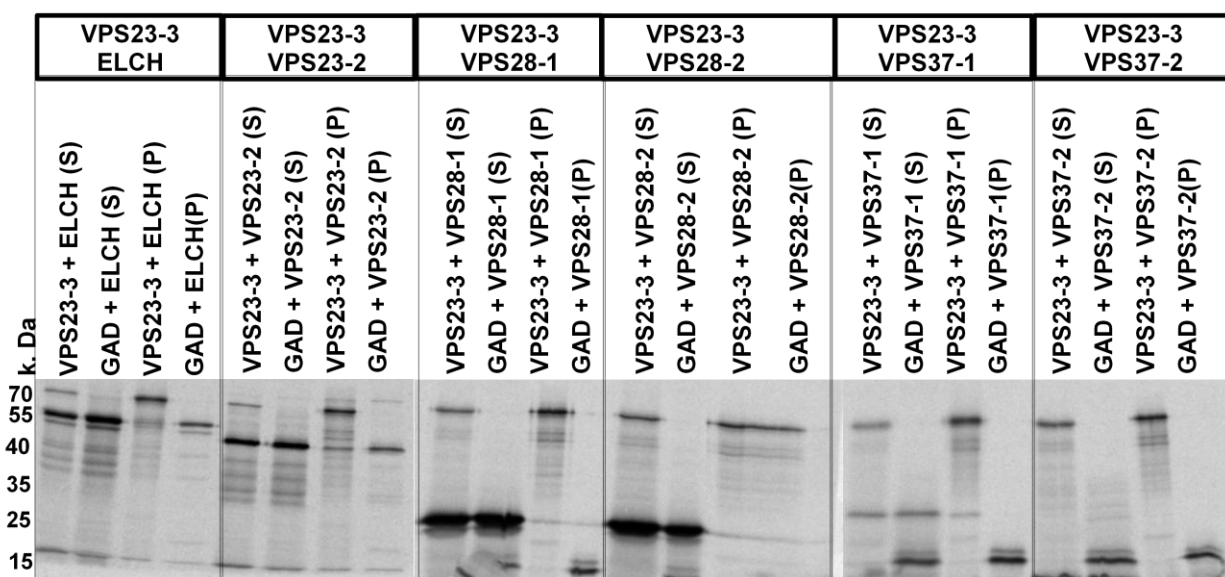
pellet of each interaction were loaded on SDS-PAGE and the radioactivity was visualized by phosphor imaging. Empty vector with GAD treated with each respective prey proteins were used as negative control. The interaction results were in accordance with yeast two hybrid and Bi-FC results, in addition VPS23-3 also shows interaction with VPS37-1 (Figure 22 B). Similarly the interaction of ELCH with other ESCRT-I members were tested by using ELCH as a bait by partially labelling with radioactive S35 and all other ESCRT-I members as prey proteins by completely labelling with radioactive S35. Here also the interaction results were similar to yeast

two hybrid and Bi-FC results, in addition ELCH also shows strong interaction with VPS28-1 and VPS28-2 (Figure 22 C). The observed interactions of VPS23-3 with ESCRT-I members were weaker compared to the interactions of ELCH with other ESCRT-I members could be due to the weaker *in vitro* expression of VPS23-3 compared to ELCH. The bands of the weaker interactions were quantified and found significant (data not shown). To summarize the

A



B



C

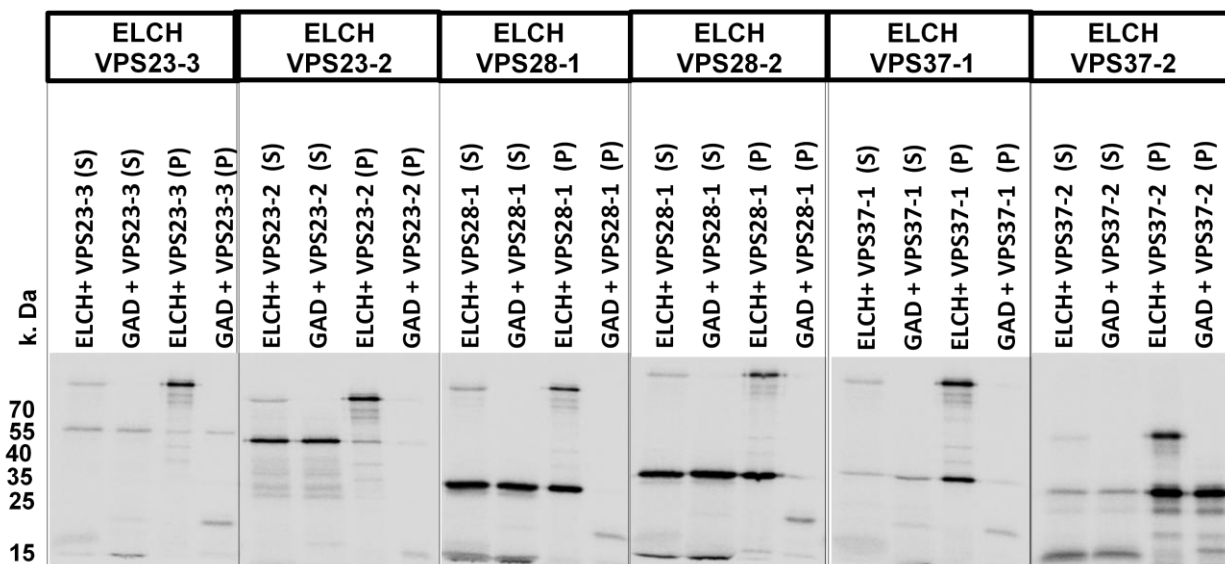


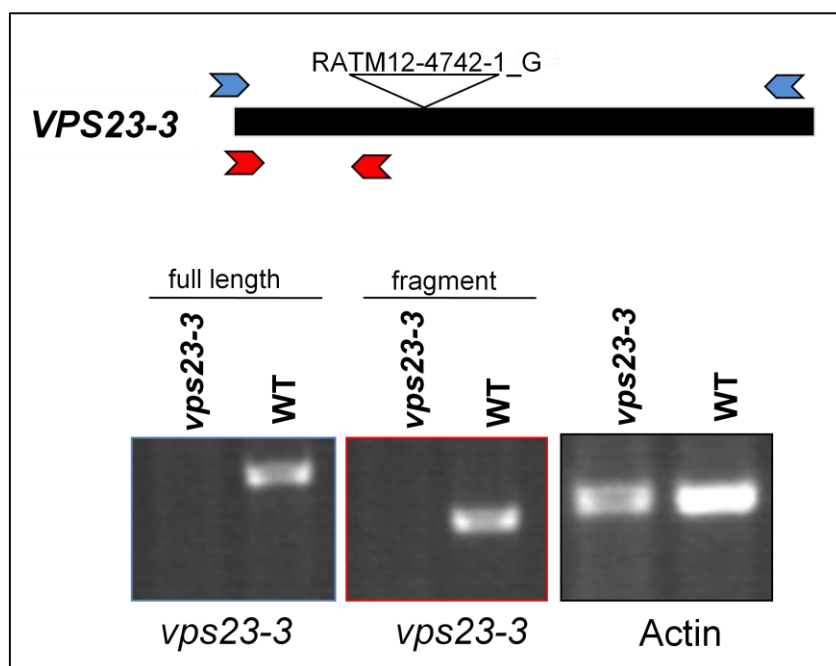
Figure 22: Radioactive *in vitro* co-IPs. A. *in vitro* expression of ESCRT-I proteins followed by phosphor imaging. **B.** S35 labelled radioactive *in vitro* co-IPs. VPS23-3 was partially labeled with S35 and used as a bait protein and other ESCRT-I proteins were completely labeled with S35 and used as prey proteins. Bait and prey proteins were treated with α -GAD antibody and pulldown with protein A beads and magnetically separated and used for SDS-PAGE followed by phosphor imaging. VPS23-3 shows no interaction with ELCH, VPS23-2 and VPS37-2 and show interaction with VPS28-1, VPS28-2 and VPS37-1. **C.** ELCH was partially labelled with s35 and used as a bait protein and other ESCRT-I proteins were completely labeled with s35 and used as prey proteins. ELCH show no interaction with VPS23-3 but interacts with other ESCRT-I proteins. **B and C.** (S)= supernatant, (P)= pellet. Third lane of each interaction panel represents the respective interacting partners and fourth lane of each interaction panel represents respective negative controls. For weaker interactions the bands were quantified and found significant.

interaction results, in none of the three interaction assays tested VPS23-3 showed interaction with either ELCH or VPS23-2. ELCH was interacting with VPS28 and VPS37. Similarly VPS23-3 was also interacting with VPS28-1, VPS28-2 and VPS37-1 of ESCRT-I complex. Therefore interaction results suggest that VPS23-3 might function at the same time as ELCH in the complex and might serve additional ESCRT function.

B 3.3.4 *vps23-3* knock-out show a shift in the molecular weight of the complex on blue native-PAGE

In order to determine if VPS23-3 functions at the same time as ELCH in the complex, a T-DNA insertion mutant for VPS23-3 was isolated. In the insertion line RATM12-4742-1_G the T-DNA is inserted in exon was screened by PCR using the primer combinations LP RP for WT and RP LB for homozygous lines. The knock-out status of the isolated homozygous lines was tested by RT-PCR using the primer combinations for full length and 5' of the insertion region. In both cases expression of mRNA transcript was not detected and represents a complete knock-out (Figure 23 A). Protein extracts from the *vps23-3* knock-out line and WT were ultra centrifuged at 100,000 g for 60 minutes and solubilized with 0,6% digitonin, separated on 6-12% gradient blue-native PAGE and immunoblot was performed using VPS28 antibody (VPS28 antibody was a gift from Peter Pimpl group, Heidelberg, Germany). *vps23-3* knock-out showed a clear shift in the molecular weight of the complex compared to WT (Figure 23 B). This suggests that VPS23-3 function at the same time in the complex as ELCH and it might serve as a fourth component of the ESCRT-I complex.

A



B

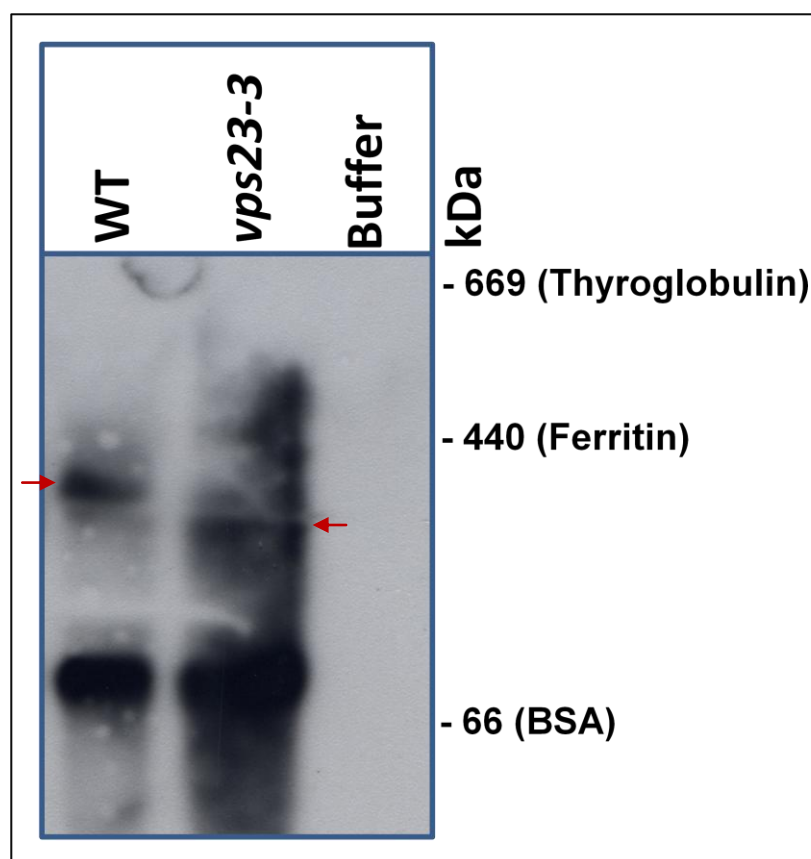


Figure 23: *vps23-3* knock-out shows a shift in the molecular weight of the complex. A. Gene structure and T-DNA insertion region of VPS23-3. Red and blue arrows indicate the primers used for RT-PCR. The transcript was absent in both combinations suggesting the complete knock-out. **B.** One-dimensional blue native PAGE (BN-PAGE) of WT and *vps23-3* knock-out using 0.6% digitonin followed by western probed with VPS28 antibody. Thyroglobulin (669k. Da), Ferritin (440k. Da) and BSA (66k. Da) were used as marker proteins. *vps23-3* knock-out show a shift in the molecular weight of the complex suggests that VPS23-3 function at the same time in the complex and it might serve as a fourth component of the ESCRT-I complex.

C. Discussion

C 1. ESCRT components function together in regulating cytokinesis in plants

To gain further understanding of the cytokinesis phenotype of the *elch* mutant, a genetic characterization of ESCRT-I components were performed. The analysis was confined to ESCRT-I components because VPS28 and VPS37 are the known components of *Arabidopsis* ESCRT-I complex (Winter and Hauser 2006). Studies in yeast show that Vps23 acts in concert with Vps37 and Vps28 in the ESCRT-I complex. Consistent with this both *Arabidopsis* VPS37 and VPS28 paralogs were co-immunoprecipitated with HA tagged ELCH in *Arabidopsis* (Spitzer et al. 2006). Single mutants of each of the studied genes *vps28-1*, *vps28-2*, *vps37-1* or *vps37-2* did not display any significant phenotype suggesting the strong redundancy in the function of the homologous pairs. Therefore the double knock-outs with *elch* were generated and scored for an *elch* like phenotype. The appearance of antler like trichomes is an easily observable direct measure of the *elch* dependent cytokinesis defect. The advantage of the correlation of the *elch* cytokinesis phenotype with an aberration in leaf trichome shape was taken into account for phenotypic analysis of double knock-outs. The strong synergistic phenotype observed in double knock-outs *elch vps28-2* and *elch vps37-1* must be because *vps28-2* and *vps37-1* were complete knock-outs compared to *elch vps28-1* and *elch vps37-2* in which *vps28-1* and *vps37-2* are still partially functional. The triple knock-out *elch vps28-2 vps37-1* showed a high degree of synergistic phenotype with respect to clustered trichomes and multiple nuclei. The severity of the phenotypes of the double mutants of homologous ESCRT-I components and the *elch vps28-2 vps37-1* triple knock-out shows the general importance of the ESCRT pathway for the plant. The synergistic phenotypes of the double knock-outs suggest that VPS28 and VPS37 are functionally associated with the ELCH-dependent cytokinesis regulation. The double knock-outs between *vps28-1 vps28-2* and *vps37-1 vps37-2* were unable to identify because of the lethality and the lethality is due to the lack of VPS28 or VPS37 was confirmed by rescue experiments. This indicates that complete loss of function of VPS28 or VPS37 is lethal for the plant. The lack of genetic interaction between *elch* and *vps37-2* mutants could be explained by the presence of two splice variants of VPS37-2 that are published in EST databases. The splice variant that used in this study contains a deletion of five base pairs that results in a frameshift and a premature STOP after 139 amino acids. It is therefore unlikely to be fully functional. However,

the genetic analysis indicates that this truncation exhibits at least residual VPS37 activity as over-expression of the YFP:VPS37-2 fusion could rescue the lethality of the *vps37-1 vps37-2* double knock-out. In this study the lethality of VPS28 or VPS37 double knock-outs was represented at genotypic level. The next step of experiments would be to analyse the lethality at phenotypic level and in particular the stage at which the lethality occurs. Is this rather in the gametophyte, the embryo or a seedling phase? Does the observed lethality include cytokinesis defects? Further analysis of the plants rescued by the 35S expression. Given that the single mutants of each of the studied genes show no phenotype one can assume strong redundancy in the function of the homologous pairs as evident from the analysis of VPS23-2, a close homolog of ELCH which rescued the *elch* mutant when it was expressed under the control of the *ELCH* promoter and the dominant-negative VPS23-2 phenocopied the *elch* mutant. In this respect it will be interesting to see the phenotype of the *elch vps23-2* double mutant that has not been created for this study, because a suitable insertion-line of VPS23-2 was not available at the time. The *Arabidopsis* ESCRT associated protein AtSKD1 (VPS4) is involved in regulating the cytokinesis as the dominant-negative versions of AtSKD1 show clustered trichomes and multiple nuclei (Mojgan Shahriari, PhD thesis). This is in accordance with mammalian ESCRT associated protein ALIX which functions in cytokinesis regulation (Morita et al. 2007; Carlton et al. 2008). Taken together the results of genetic characterization of the ESCRT-I components indicate that the ESCRT components function together in regulating cytokinesis in plants.

In animals, it is shown that the localization of TSG101 is cell cycle-dependent, occurring in the nucleus and golgi complex during interphase, and in mitotic spindles and centrosomes during mitosis (Xie et al. 1998). TSG101 play an important role in cell division as evident from the finding that mutations in TSG101 lead to genomic instabilities and a series of mitotic abnormalities including multiple microtubule organizing centers, aberrant mitotic spindles, abnormal distribution of metaphase chromatin, aneuploidy, and nuclear anomalies (Xie et al. 1998). The preliminary evidence comes from the result of the expression of the *Arabidopsis* ELCH under the control of the *KNOLLE* promoter in the *elch* background rescued the *elch* mutant (data not shown). This gave a primary hint that ELCH might be expressed during the cell plate formation. KNOLLE is a cytokinesis specific syntaxin that localizes to the plane of cell division and mediates cell-plate formation (Volker et al. 2001). Therefore the initial experiment in this direction would be to analyse the localization of ELCH and other ESCRT proteins during the cell plate formation by co-localizing them with KNOLLE in the *Arabidopsis* cell suspension culture cells. As the VPS28 antibody is available, the cell-cycle dependent localization of ESCRT-I components can be checked by synchronizing the *Arabidopsis* suspension cells at

different stages of the cell cycle followed by staining with anti-VPS28 antibody. In order to test if ESCRT components function in mitotic stage of cell division, the *Arabidopsis* cell lines of *elch vps28-2* and *elch vps37-1* double knock-outs and *elch vps28-2 vps37-1* triple knock-out can be prepared and stained with anti-tubulin antibody and mitotic abnormalities can be analysed in these lines.

The initial piece of evidence which came from *elch* phenotype is reminiscent of mutants defective in regulation of the microtubule cytoskeleton (Kirik et al. 2002; Kirik et al. 2002; Steinborn et al. 2002; Twell et al. 2002) and synergistic phenotype of *elch tfc-a* double knock-out suggests the link between ELCH and microtubule dependent processes and ELCH might be involved in regulation of microtubule cytoskeleton in plants (Spitzer et al. 2006). As the double knock-outs of ESCRT-I in combination with *elch* have shown a strong cytokinesis phenotype, the possible experiment in order to clearly interpret the role of plant ESCRT system in regulating microtubule cytoskeleton would be generating *elch vps37-1 tfc-a* and *elch vps28-2 tfc-a* triple knock-outs and visualization of microtubules in double and triple knock-outs. Using *elch vps37-1 vps28-2* triple knock-out for generating *elch vps37-1 vps28-2 tfc-a* quadruple knock-out would be an ideal choice but getting a quadruple knock-out is unlikely as ESCRT-I triple knock-out itself shows severe defects in germination, growth and development and reproductive stages. The higher frequency of trichome cluster formation and aberrant cell morphology compared to the individual mutants should facilitate the determination of differences. Paclitaxel (Taxol) is a microtubule stabilizing drug especially in dividing cells (Jordan and Wilson 1998). Oryzalin is a drug that in contrast to Paclitaxel destabilizes microtubules by slowing down microtubule assembly (Hugdahl et al. 1993). Nocodazole is known as antimitotic agent that disrupts microtubules by binding to β -tubulin and preventing formation of some of the disulfide linkages (Ludueno and Roach 1991). MAP-4:GFP is a microtubule marker which nicely decorates the microtubules. Treatment of double and triple knock-outs of ESCRT-I with microtubule influencing drugs and crossing of these knock-out lines with MAP-4:GAP marker line and analyzing the mitotic abnormalities in different cell types can give further indication of role of the ESCRT pathway in regulation of the microtubule cytoskeleton in plants.

Recent publications have addressed regulation of cytokinesis by ESCRT components in animal cells (Dhonukshe et al. 2007; Morita et al. 2007). It was shown that ESCRT proteins are involved in regulating the final stages of abscission, a process that shows remarkable similarities to plant cytokinesis (Dhonukshe et al. 2007). However, the mechanism involved in animal cells requires the recruitment of the ESCRT components to the midbody via the midbody resident protein Cep55 (Carlton and Martin-Serrano 2007; Morita et al. 2007). This protein

cannot be found in plants. Therefore, although the phenotypes of ESCRT mutants in animals and plants are similar the underlying mechanisms must deviate substantially. Hence, it would be important to identify and characterize the functional homolog of *Cep55* in plants and further analyse if it recruits the plant ESCRT machinery during final stages of cytokinesis.

The role of ESCRT complexes in yeast cytokinesis is unclear but mutations in one or more ESCRT components of mammals and *Arabidopsis* induce cytokinesis defects, suggesting that the role of the ESCRT machinery in cytokinesis might be conserved in multicellular organisms.

C 2. VPS23-3, a new component of the plant ESCRT system

As described in this thesis *VPS23-2*, a close homolog of *ELCH* is functionally redundant to *ELCH*. The newly identified *VPS23-3* (At2g38830) is dicot specific and unlike *VPS23-2* it shows a lesser degree of homology (47%) to *Arabidopsis* *ELCH* and even the rice *ELCH* (*OsELCH*) shows higher homology (61%) to *Arabidopsis* *ELCH* compared to *VPS23-3*. This gave an initial hint that *VPS23-3* might not be simply redundant to *ELCH*. *VPS23-3* is ubiquitously expressed and localized to early and late endosomes/MVBs/pre-vacuolar compartments as evident from co-localization studies with early and late endosomal markers *ARA6*, *ARA7* and *AtPep12*. This is in accordance with yeast *Mvb12p* which transiently localizes to MVBs (Curtiss et al. 2007). In addition yeast *Mvb12p* and human *MVB12* proteins also showed cytoplasmic localization (Audhya et al. 2007; Curtiss et al. 2007) whereas in case of *VPS23-3* the localization is always confined to the dotted endosomal compartments. *VPS23-3* also shows co-localization with *ELCH*. This suggests that both *VPS23-3* and *ELCH* are localized in the same complex. *VPS23-3* binds to ubiquitin when YFP:*VPS23-3* was pulldown with ubiquitin agarose beads. This is similar to the observation as *ELCH* (Spitzer et al. 2006). In an independent experiment pulldown of truncated *VPS23-3* (*VPS23-3-t*) lacking the coiled-coil domain and steadiness box also showed ubiquitin binding. This indicates that the N-terminal UEV domain is necessary for binding to the ubiquitylated cargo. In order to confirm the importance of UEV domain for ubiquitin binding, more refined experiment would be to delete the N-terminal UEV domain of *VPS23-3* and show that it is not binding to the ubiquitin in absence of UEV domain. In a gel filtration/size exclusion chromatography experiment on supherose-6 column, *VPS23-3* showed a strong band in the molecular weight range of about 350k.Da. This indicates that *VPS23-3* is a part of high molecular weight complex. This result is in accordance with the *Arabidopsis* *ELCH*

(Spitzer et al. 2006), yeast Mvb12p (Curtiss et al. 2007) and human MVB12 proteins (Morita et al. 2007). Taken together these results indicate that VPS23-3 is a new component of the plant ESCRT system.

C 3. VPS23-3 might serve as an additional fourth subunit of ESCRT-I complex

In a promoter swapping experiment, expression of VPS23-3 under the control of the *ELCH* promoter did not rescue the *elch* mutant. This indicates that VPS23-3 performs different function than ELCH. Because of the dicot specificity of identified VPS23-3 one can assume that either VPS23-3 is not needed in monocots or the functional role of VPS23-3 might be taken over by ELCH or VPS23-2 in monocots.

Neither *vps23-3* single knock-out nor double knock-out with *elch* (*vps23-3 elch*) or with *vps28-2* (*vps23-3 vps28-2*) display any cytokinesis phenotype unlike other ESCRT-I mutants (data not shown). These results indicate that VPS23-3 might not have a functional role in cytokinesis regulation in plants.

In yeast two hybrid and bi-molecular fluorescence complementation interaction assays, ELCH played a central role in the interaction network by interacting with upstream and downstream ESCRT machinery. In addition ELCH showed self interactions (Mojgan Shariari, PhD thesis, 2008). In contrast VPS23-3 showed interactions only with VPS28 homologs of the ESCRT-I complex, but not with any other ESCRT components. This suggests that VPS23-3 might function in close association with components of the ESCRT-I complex. Even within the ESCRT-I complex both in yeast two hybrid and Bi-FC assays VPS23-3 showed only positive interactions with VPS28-1 and VPS28-2 whereas ELCH was interacting with only VPS37 and VPS23-2. The *in vivo* interactions between VPS23-3 and VPS28 take place on endosomes as the positive interactors show co-localizations with early and late endosomal markers. This together with localization results suggests the endosomal/MVB function of VPS23-3. In addition to the above interactions, interaction of VPS23-3 with VPS37 and interaction of ELCH with VPS28-1 and VPS28-2 were confirmed in an independent radioactive *in vitro* co-IPs. In none of the interaction assays (yeast two hybrid, Bi-FC and *in vitro* co-IPs) the interaction between VPS23-3 and ELCH was found. VPS23-3 also did not show interaction with VPS23-2 in any of the interaction assays whereas ELCH was interacting with VPS23-2 in all three assays. This indicates that although VPS23-3 and ELCH are present in the same complex their functions seem to be independent. Unlike ELCH-t and VPS23-2-t, the truncated VPS23-3 (VPS23-3-t)

lacking the central coiled-coil domain and C-terminal steadiness box did not phenocopy the *elch* mutant. This might be due to low degree of homology of functional domains of VPS23-3 compared to ELCH and VPS23-2. In order to know the importance of these domains, it will be interesting to look for the interaction pattern of VPS23-3-t with the ESCRT components.

The interaction results gave an indication that VPS23-3 might function independently at the same time as ELCH in the complex. This is confirmed by a blue native PAGE experiment followed by immunoblot with VPS28 antibody where *vps23-3* knock-out showed a shift in the molecular weight of the complex compared to WT. In order to further confirm these results and to clearly interpret the proposed model as discussed later, the important experiment underway is crossing of the ELCH-HA lines into the *vps23-3* knock-out lines and gel filtration analysis of the ELCH-HA lines in WT and the *vps23-3* knock-out background. This has to be independently confirmed by one and two dimensional blue native-PAGE experiment. Taken together the results of interaction assays and BN-PAGE analysis indicate that VPS23-3 functions at the same time as ELCH in the complex and therefore it might serve as an additional fourth component of the ESCRT-I complex in plants.

C 4. A model depicting the *Arabidopsis* ELCH and VPS23-3 mediated protein trafficking

Based on the results of promoter swapping, interaction assays and BN-PAGE analysis a working schematic model depicting the ELCH and VPS23-3 mediated protein trafficking was proposed. According to this model VPS23-3 functions at the same time as ELCH in the complex in MVB cargo sorting. ELCH interacts with VPS28 and VPS37 via its central coiled-coil domain and binds to mono-ubiquitylated cargo with its N-terminal UEV domain and gets sorted the cargo through ESCRT-II and ESCRT-III machinery into MVB. VPS23-3 functions independent of ELCH at the same time in the complex by interacting with VPS28 and VPS37 via its central coiled-coil domain and binds to a different/ specific mono-ubiquityated cargo with its N-terminal UEV domain and gets sorted the cargo through ESCRT-II and ESCRT-III complexes into the MVB (Figure 24). Although it is a tentative model, the potential targets of VPS23-3 and ELCH mediated trafficking is needed to unravel the actual role of these components in MVB sorting pathway in plants (Figure 24).

The role of Mvb12p in yeast and MVB12 A and B in mammals in ESCRT/MVB sorting pathway is well characterized (Curtiss et al. 2007; Morita et al. 2007). Although the results of

cell biological and biochemical experiments give an indirect evidence of endosomal function of VPS23-3 in plants, the actual role of VPS23-3 in MVB sorting pathway is not known yet. The crucial step in this direction will be identification and genetic and biochemical characterization of a potential interacting partner in other words a suitable target of VPS23-3 and analysis of MVB sorting defects of this target in *vps23-3* knock-out.

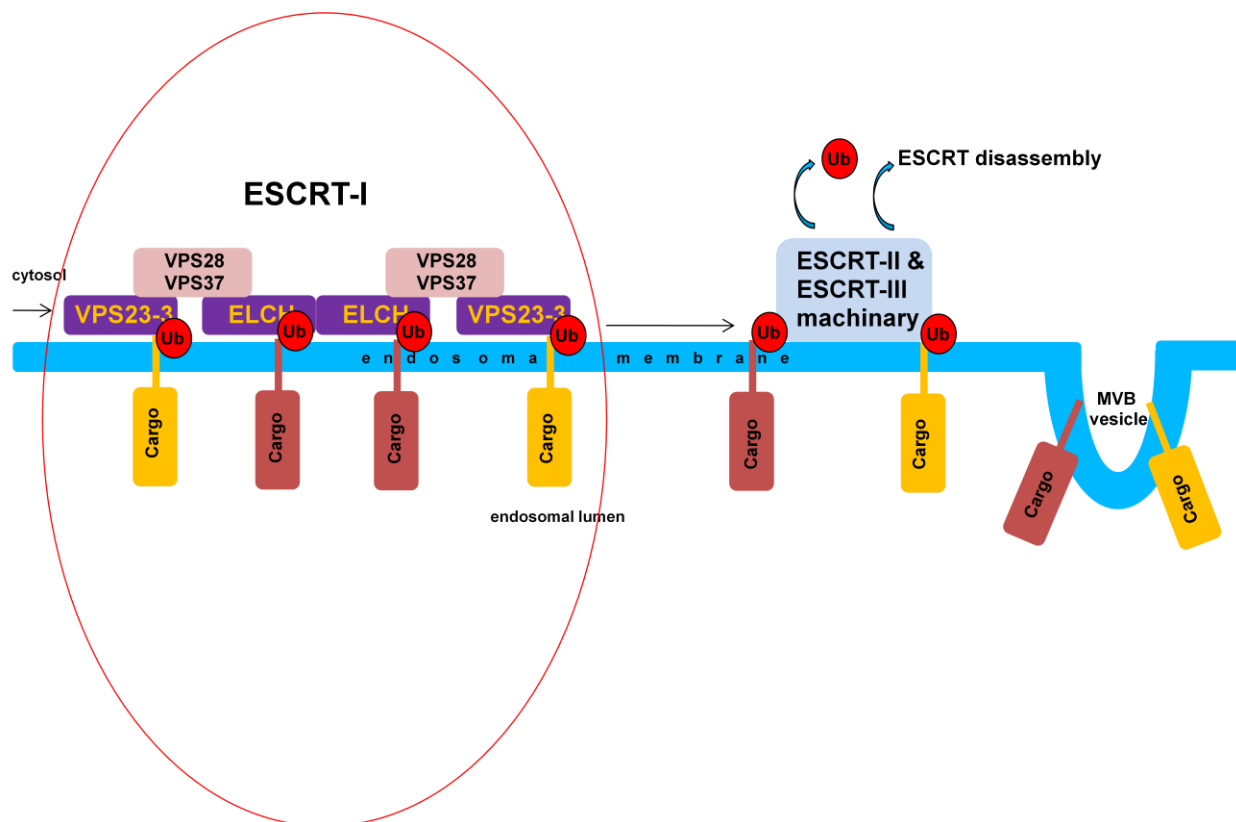


Figure 24: A model depicting the VPS23-3 and ELCH mediated trafficking of proteins. VPS23-3 functions at the same time as ELCH in the complex. With its coiled-coil domain ELCH interacts with VPS28 and VPS37 and binds to mono-ubiquityated cargo with its N-terminal UEV domain and sorts through ESCRT-II and ESCRT-III machinery into MVB. VPS23-3 function at the same time as ELCH in the complex by interacting with VPS28 and VPS37 with its coiled-coil domain and binds to a different/ specific mono-ubiquityated cargo with its N-terminal UEV domain and sorts the cargo through ESCRT-II and ESCRT-III complexes into the MVB.

Outlook

Although the genetic characterization shows the role of ESCRT system in cytokinesis regulation in plants, a number of basic questions need to be addressed. It is important to determine the stage at which the ESCRT components play a role in cytokinesis. Though the initial results suggests the role of ELCH in regulation of microtubule cytoskeleton. This has to be clearly interpreted more strongly with other ESCRT components.

The lethality of the VPS28/VPS37 double knock-outs has to be addressed at the phenotypic level as well especially the stage at which the lethality occur. Is this rather a gametophytic, an embryo or a seedling lethal phenotype? Does the observed lethality include cytokinesis defects and analysis of the phenotype of the plants rescued by 35S expression.

With more and more evidences indicating that the ESCRT machinery is functional in plants the main tasks will be the determination of whether plant ESCRT system fulfills similar functions like yeast and/ or animal ESCRTs and what are the functional differences between plant ESCRT machinery and other systems.

VPS23-3 found to be a novel component of ESCRT system in plants, which might serve as an additional fourth subunit of ESCRT-I complex. Further experimental evidences are needed to strengthen this model and determine the specific role of VPS23-3 in MVB sorting pathway in plants. In this direction identification of potential cargos of VPS23-3 and ELCH mediated ESCRT trafficking is very important.

The analysis of ESCRT dependent MVB sorting in plants seems, however, to be more difficult than in yeast. First, the mutant analysis is complicated by the fact that phenotypes are either masked by redundancy or double mutant combinations are lethal. Second, so far no marker for ubiquitin dependent vacuolar sorting has been established in plants. Therefore to analyse sorting functions of plant ESCRT proteomic experiments identifying putative cargos will be crucial.

D. Material and Methods

D 1. Material

D 1.1 Chemicals

All used chemicals were analytically pure according to the manufacturers and were obtained from Roche (Mannheim, Germany, www.roche.de), Fluka (Buchs, CH and www.sigmaaldrich.com), Merck (Darmstadt, Germany, www.merck.de) and Sigma (Muechen, Germany, www.sigmaaldrich.com), Duchefa (Haarlem, Netherlands, www.duchefa.com) and Qiagen (www.qiagen.de, Hilden, Germany).

D 1.2 Enzymes and kits

All restriction enzymes were purchased from MBI-fermentas (St.Leon-Rot, Germany, www.mbifermentas.de) and New England Biolabs (Frankfurt/Main, Germany). Kits were supplied from peqlab (Erlangen, Germany, www.peqlab.de), Roche (Mannheim, Germany, www.roche.de) and QIAGEN (Hilden, Germany). Proof readings Taq-polymerases were provided from Biorad (www.biorad.com), Stratagene (www.stratagen.com) and Qiagen (www.qiagen.de, Hilden, Germany). Reverse transcription Superscript kits were bought from Invitrogen (www.invitrogen.com) and MBI-fermentas (St.Leon-Rot, Germany, www.mbifermentas.de).

D 1.3 Primers

Primers were generated by using VectorNTI software and purchased from Invitrogen (Karlsruhe) and SIGMA (Deisenhofen).

Primer name	Primer sequence
CK_VPS28-1_LP	TCATTGGGTTTTCTCCATTTTC
CK_VPS28-1_RP	TACCAGCATTAGGCAAAGCAG
CK_VPS28-2_LP	TCAAATTAATAAAAATTTTACGGTCC
CK_VPS28-2_RP	GACAAACGCGAAAGAGAGATG
CK_VPS37-1_LP	TGGAGGATCTGATGGAGAATG
CK_VPS37-1_RP	TCCTGAGTTCATCCACGCTAC
CK_VPS37-2_LP	TGACATGAAATCATTATCAAGTAAGATG
CK_VPS37-2_RP	CAGCACAACTTCATGAGCATAG
CK_VPS23-3_LP	TAAACTTCCACGAAACAACGG
CK_VPS23-3_RP	CATCTTCAATGGCGTCATCTC
CK_LBb1_SALK	GCGTGGACCGCTTGCTGCAACT
CK_LB_SAIL	GCCTTTTCAGAAATGGATAAATAGCCTTGCTTCC
CK_LB_GABI	CCCATTTGGACGTGAATGTAGACAC
CK_VPS28-1_RT_F	TCGTGATCTAATCTCTCCATCTGAA
CK_VPS28-1_RT_R	GAGCCTGCTGCTCAGTGAGTT
CK_VPS28-2_RT_F	TCAAATTAATAAAAATTTTACGGTCC
CK_VPS28-2_RT_R	GACAAACGCGAAAGAGAGATG
CK_VPS37-1_RT_F	TCAGGAAGCTTCTTCACAGTCGCCAT
CK_VPS37-1_RT_R	TCAAATGTTTTGACGTTTTAGCGGCA
CK_VPS37-2_RT_F	TCTCCAGAAGCTTCTGCAACACCG
CK_VPS37-2_RT_R	TCAGCCAATAGATGAAGTTTTAGCAGCG
CK_VPS23-3_RT_F	ATGGCGGCATCATCATCATCT
CK_VPS23-3_RT_R	CTCTCCGCAGCTTCTTCCA
CK_ACT_F	GGATAGCATGTGGAAGTGCATAC
CK_ACT_R	TGCGACAATGGAAGTGGAAATG

D 1.4 Antibiotics

Antibiotic	dissolved in	Stock conc.	Final conc.
Kanamycin	H ₂ O	50mg/ml	50 µg/ml
Ampicillin	H ₂ O	100mg/ml	50 µg/ml
Carbenicillin	50% EtOH	100mg/ml	50 µg/ml (<i>E. Coli</i>)
			100 µg/ml (<i>A. tumefaciens</i>)
Hygromycin		50mg/ml	50 µg/ml
Chloramphenicol	50% EtOH	10mg/ml	10 µg/ml (<i>E. Coli</i>)
			75 µg/ml (<i>A. tumefaciens</i>)
Rifampicin	DMSO	30mg/ml	150 µg/ml (<i>A. tumefaciens</i> <i>GV3101</i>)
			20 µg/ml (<i>A. tumefaciens</i> <i>LBA4404</i>)
Gentamycin	H ₂ O	30mg/ml	25 µg/ml (<i>A. tumefaciens</i> <i>GV3101</i>)
			40 µg/ml (<i>A. tumefaciens</i> <i>LBA4404</i>)
Tetracyclin	EtOH	5mg/ml	5µg/ml
Spectinomycin	H ₂ O	100mg/ml	100 µg/ml

D 1.5 Bacterial strains

For standard cloning, the *Escherichia coli* strain DH5α was used. For gateway cloning of destination vectors the DB3.1 strain was used which was resistant to the *ccdB* gene. For cell culture transformation *Agrobacterium tumefaciens* strain LBA4404 was used and for stable plant transformation *Agrobacterium tumefaciens* strains GV3101 was used.

D 1.6 Cloning vectors

Vector	Source	Purpose
p-GEM-T easy	Promega	PCR product cloning
pDONR201/207	Invitrogen	Gateway entry cloning
pENSG-YFP and pENSG-CFP	Invitrogen	Gateway destination cloning
pEXSG-YFP and pEXSG-CFP	Invitrogen	Gateway destination cloning
pSPYNE and pSPYCE	(Walter et al. 2004)	Gateway destination cloning
pEarlyGate101	Early et al 2006	Gateway destination cloning
pJIC26 and pJIC39	Coupland, MPIZ, Cologne	Gateway destination cloning
pEarlyGate101	www.pgreen.ac.uk	promoter cloning

D 1.7 Plant lines

Plant material	Purpose
<i>Arabidopsis thaliana</i> ecotype Col-0	Used as a source wild type (WT) DNA, mRNA and genotype background for creation of transgenic plants
<i>Arabidopsis thaliana</i> ecotype Ler	Used as a source wild type (WT) DNA, mRNA and genotype background for creation of transgenic plants
<i>Arabidopsis thaliana</i> ecotype Ws-2	Used as a source wild type (WT) DNA, mRNA and genotype background for creation of transgenic plants
<i>Arabidopsis thaliana</i> ecotype Noessen	Used as a source wild type (WT) DNA, mRNA and genotype background for creation of transgenic plants
T-DNA insertion lines	Used to study a loss-of-function of a single protein. Insertion lines obtained from the Nottingham <i>Arabidopsis</i> Stock Center (NASC, ref. Alonso <i>et al.</i> , 2003), Syngenta <i>Arabidopsis</i> Insertion lines (SAIL), GABI-KAT and RIKEN Center, Japan.
<i>Arabidopsis</i> protoplasts	Used for transient assays
<i>Arabidopsis</i> cell suspension culture	Used for transient assays

D 1.8 T-DNA insertion lines

Gene	AGI code	T-DNA insertion line	T-DNA insertion region
VPS28-1	At4g21560	SAIL_690_E05	EXON
VPS28-2	At4g05000	SALK_040274	EXON
VPS37-1	At3g53120	SAIL_97_H04	INTRON
VPS37-2	At2g36680	GABI_305C05	INTRON
VPS23-3	At2g38830	RATM12-4742-1_G	EXON

D 1.9 Biochemicals and antibodies

Biochemical/ Antibodies	Source
Complete protease inhibitor	Roche
Protein G agarose	Roche
Ubiquitin agarose	Sigma
Supherose 6 10/300 GL	Amersham
Protein A dynabeads	Invitrogen
Page ruler protein ladder	Fermentas
Rat anti HA antibody	Roche
Mouse anti GFP antibody	Roche
GAL-4 antibody	Santa Cruz
VPS28 antibody	Hiedelberg

D 2. Methods

D 2.1 Plant work

D 2.1.1 Plant growth conditions

Arabidopsis seeds were germinated by sowing directly onto moist soil. Seeds were cold treated by placing pots on a tray covered with a lid and incubated in the dark at 4°C for three to four days. Trays were subsequently transferred to a controlled environment growth chamber, covered with a propagator lid and maintained under long day conditions (16 h photoperiod and 24°C). Propagator lids were removed when seeds had germinated. Plants were protected from various herbivores by applying 10 mg/l Confidor® WG 70 (Bayer, Germany). The solution was applied by watering the plants.

D 2.1.2 Crossing of plants

Using fine-tweezers the anthers of flowers at a stage when the petals grew out of the sepals were removed. All remaining older and younger flowers were removed and the prepared flower was fixed on a wooden stick. After one to three days the stigma of the carpels were pollinated.

D 2.1.3 Plant transformation

Plants were transformed according to the “floral dip” method (Clough and Bent 1998). To gain strong plants, they were grown at 18°C and till the first flowers appeared at stalks of approximately 10 cm in length. Four days before plant transformation a 5 ml pre-culture in YEB medium of the agrobacterial culture was incubated for two days at 29°C and 1 ml of this pre-culture was used to inoculate the final 200 ml culture. This culture was incubated again for two days at 29°C and afterwards precipitated at 5800 rpm for 12 minutes. The pellet was resuspended in a 5% Sucrose solution containing 0.05% Silwett L-77. Plants were dipped for approximately 20 seconds and afterwards covered with a lid. The lid was removed after two days and the plants were treated as usual.

D 2.1.4 Seed surface sterilisation and subsequent plant treatment

Before placing seeds on MS-agar-plates (1% Murashige-Skoog salts, 3% sucrose, 0.7% agar-agar, pH5.7, when required: with kanamycin (50µg/ml) or hygromycin (25µg/ml) they were incubated for two minutes in 95% Ethanol (Rotisol), five minutes in 70% Ethanol and afterwards incubated for 15 minutes in a 3% NaClO₃ solution containing 0.1% triton X-100. Then the seeds were washed two times with 0.01% Triton-X100 and finally the seeds were washed twice with sterile double distilled water.

D 2.1.5 Selection of transformants

The seeds of transgenic plants were selected on MS-Agar plates with 50µg/ml kanamycin or 25 µg/ml hygromycin, based on the respective resistance. Transgenic plants containing the BASTA resistance were grown on soil for 10 to 15 days. The seedlings were sprayed with a 0.001% BASTA solution, the spraying was repeated after three to seven days.

D 2.2 Genetic analysis

To identify mutants of *VPS28-1*, *VPS28-2*, *VPS37-1*, *VPS37-2* and *VPS23-3* the SiGnAL database (<http://signal.salk.edu/cgi-bin/tdnaexpress>) was searched for insertions in exons or introns of the genes of interest. Primers for mutant isolation were generated with the SiGnAL isect tools. Homozygous lines of the respective mutants were isolated by PCR screening. All crosses with *elch* were performed using *elch* as male partner. Double mutants were identified by PCR screening in the F₂ generation. In cases where no homozygous double mutant could be found plants homozygous for one crossing partner and heterozygous for the other were selected and allowed to self. The progeny was again PCR screened. All comparisons with wildtype were done with *Ws-0* and *Col-0*. For generation of the triple knock-out *elch vps28-2 vps37-1* the double mutants *elc vps37-1* and *elc vps28-2* were crossed each other. Triple mutants were identified in the F₂ generation by PCR.

D 2.3 Microscopy and Cell biology

D 2.3.1 Microscopy

Light and epifluorescence microscopy was performed using a LEICA-DMRE microscope using DIC optics (LEICA). Images were taken using a high resolution KY-F70 3-CCD JVC camera and a frame grabbing DISKUS software (DISKUS, Technisches Büro, Königswinter). Confocal microscopy was done using a TCS SP2, Leica, Wetzlar, Germany. Adobe Photoshop CS2 software was used to adjust brightness, contrast and levels of the pictures and for producing the merged pictures.

D 2.3.2 DAPI staining

DNA was stained with 4',6-Diamidino-2-phenylindol (DAPI). Solid DAPI was diluted to 10 mg/ml in H₂O (stock solution). For DAPI staining, leaves were incubated in DAPI solution (40 µg/ml final concentration) for 15 minutes under vacuum (0,6 bar). Leaves were washed in 70% EtOH at 4°C to reduce background and visualized by epifluorescence microscopy [excitation filter (BP 340-380), emission filter (LP425)].

D 2.3.3 FM4-64 staining

FM4-64 staining of transformed protoplasts was done according to (Ueda et al. 2001). After 16 h of incubation in MS cell culture medium containing 0.34 M glucose mannitol, protoplasts were collected by centrifugation, resuspended in the same medium supplemented with 50 µM FM4-64, and placed on ice for 10 min. After labeling, cells were washed twice, resuspended in the same medium without FM4-64 and examined by fluorescence microscopy with the appropriate filters (Leica).

D 2.3.4 The *Arabidopsis* cell culture, protoplasting and transfection

Arabidopsis cells were cultured in suspension culture (Columbia ecotype; grown in MS medium supplemented with 0.5 mg/l NAA and 0.1 mg/l KIN) as described (Mathur and Koncz 1998; Mathur and Koncz 1998). Protoplasts were isolated and transformed by polyethylene glycol-mediated transfection according to (Mathur and Koncz 1998; Mathur and Koncz 1998) with little modifications. To prepare the protoplasts, 50 mL of cell suspension culture (MS powder: 4,3g, sucrose: 30g, vitamin B5: 4 mL, NAA: 0,5 mg, kinetin 0,1 mG, pH 5,5) was spinned down at 1500 rpm for 5 minutes. 50 mL of enzyme solution (1% cellulase, 0,2% macerozyme in MS-0,34M Glucose mannitol medium (MS powder 4,3 g, glucose 30,5 g, mannitol: 30,5g, pH 5,5) was added to the pellet in two steps of 25 mL each. The suspension was transferred to two large petridishes and shaken in dark for 4 hours at 50 rpm. Subsequently, the protoplasts were transferred to two Falcon tubes and were spinned down at 800 rpm. The pellets were resuspended in 25 mL MS-0,34M Glucose manitol medium and spinned down as described previously. The pellet was resuspended in 5mL of MS-0,28M sucrose medium (MS powder: 4,3g.L-1, 0,28M sucrose, pH 5,5) and centrifuged at 800 rpm for 5 minutes. The supernatant containing the protoplasts was then ready for transformation. Each transformation required to mix 50 μ L of protoplasts and 15 μ g of DNA with 150 μ L PEG solution (25% PEG 6000, 0,45 M mannitol, 0,1M Ca(NO₃)₂, pH 9) in a 2 mL Eppendorf tube. The mix was incubated 20 minutes in dark and the PEG was washed away by the means of two subsequent additions of 500 μ L of 0,275 M Ca(NO₃)₂. The transformed protoplasts were centrifuged at 800 rpm for 7 minutes and transferred to 500 μ L MS 0,34 M glucose mannitol solution. The transformed cells were incubated at room temperature in dark for 16-24 hours before microscopic observation.

D 2.4 Molecular biology

D 2.4.1 Basic DNA manipulation techniques

Plasmid preparations from bacteria, DNA digestion, agarose gel electrophoresis, Polymerase Chain Reactions etc. are performed according to "Molecular Cloning: A Laboratory Manual (Third Edition) By Joseph Sambrook, and Peter MacCallum Cancer Institute, Melbourne, Australia; David Russell, University of Texas Southwestern Medical Center, Dallas". All polymerase-chain reaction (PCR)-amplified fragments were sequenced prior to further

investigation. Sequencing reactions were performed using Big-Dye kit v1.1/v3.1 (Perkin Elmer Applied Biosystems, Foster City, CA). PCR-Primers and constructs were designed using the VectorNTI-suite 7.1 software (InforMax, Paisley PA4 9RF United Kingdom).

D 2.4.2 Plasmid DNA preparation from bacteria

Plasmid DNA from *E.coli* was prepared according to the manufacturer's protocol using a column pEQ-LAB Plasmid Miniprep Kit (PEQLAB Biotechnology GmbH, Erlangen) to obtain plasmid concentrations of up to 200 ng/μL or using HiSpeed Plasmid Purification Kit (Sigma) to obtain concentrations of up to 400 ng/μL. Plasmid DNA from *Agrobacteria* was isolated using Qiagen plasmid miniprep kit.

D 2.4.3 Gateway cloning

Gene specific primers incorporating *attB1* and *attB2* sequences were purchased from Invitrogen. The coding sequences of the VPS genes were amplified by PCR reactions with primers incorporating *attB1* and *attB2* sequences (Invitrogen) and introduced into the pDONR201 by BP clonase reaction according to the manufacturer's instructions (Invitrogen). The resulting pDONR201 clones were transformed into the *E. coli* strain DH5-alpha and sequenced. DNA fragments were transferred to the destination vectors pENSG-YFP and pENSG-CFP or pEXSG-YFP and pEXSG-CFP or pEarlyGate101 by LR clonase reaction according to the manufacturer's instructions (Invitrogen). The product of recombination reaction (LR reaction) was used to transform *Arabidopsis* protoplasts as described earlier.

D 2.4.4 Cloning of promoters

NOS terminator cassette digested with EcoRI and EcoRV was ligated into the multiple cloning site of pGreen0179 vector digested with EcoRI and SmaI. In the second step the complete recombination cassette was spliced out using EcoRV and ligated into pGreen0179 vector also digested with EcoRV. In the third step the complete promoter sequence of the target gene was amplified with 5' KpnI site and 3' XhoI site and ligated into pGreen vector just before the recombination cassette and the correct orientation was checked by digestion with appropriate

restriction enzyme (EcoRI). Finally the corresponding swapping genes were cloned by gateway approach using LR recombination reaction.

D 2.4.5 Bi-molecular fluorescence complementation (Bi-FC)

All genes were fused to the N-terminus of the split-YFP parts and were therefore amplified without stop-codon and introduced into pDONR201. After sequencing the resulting clones were used for LR recombination reaction into the destination vectors pSPYNE and pSPYCE (Walter et al. 2004) and subsequent transformation into *Arabidopsis* protoplasts. Negative controls were carried out for each experiment by co-transforming an empty vector containing only the appropriate split-YFP part together with the respective gene:split-YFP fusion and by expression of the non-interacting transcription factors AtMYB51 (At1g18570) in pSPYNE and bHLH133 (At2g20095) in pSPYCE to exclude non-specific association caused by high local concentrations of non interacting partners (Gigolashvili et al. 2007; Lalonde et al. 2008). Interactions were scored as positive if the fraction of fluorescent cells was similar to usual transformation efficiency of ten percent. Experiments were performed in a reciprocal manner at least three times.

D 2.4.6 Genomic DNA isolation from plants

Genomic DNA was isolated with the CTAB method (Rogers et al. 1988). Modifications are described. A small amount of fresh tissue (one-two young leaves) was ground in 200µl 2xCTAB buffer (2 % Cetyltriethylammoniumbromid; 100 mM Tris-HCl (pH 8,0); 20 mM EDTA; 1,4 M NaCl; 1 % Polyvinylpyrrolidon) mixed thoroughly and incubated for at least one hour under agitation at 65°C. 200µl of CI (Chloroform:Isoamylalcohol, 24:1) was added, mixed thoroughly and centrifuged for 15 minutes. 150µl of the upper phase was transferred to a new 1.5 ml reaction tube, mixed with 200µl 2-Propanol and incubated for five minutes at RT. DNA was precipitated at 13000 x g, washed in 70% EtOH for 5 minutes at 13000 x g and air dried until no traces of EtOH are left. It is not recommended to dry the pellet extensively. DNA was resuspended in 20µl of sterile double distilled H₂O.

D 2.4.7 RNA isolation and RT-PCR

RNA was isolated according to the TrizolR protocol from Invitrogen (Cat. No. 15596- 026). TriReagentR from Molecular Research Center (TR 118) was used. All material used was treated to prevent RNA contamination. Plants were ground in liquid nitrogen and processed according to the manufactures instructions. The RNA was dissolved in 50µl of DEPC water and treated with RNase inhibitor from the Fermentas cDNA synthesis kit (Cat# K1612) and DNase from Ambion (Cat# 1906). Equal amounts of RNA from all the tested samples were used for first strand synthesis using the Invitrogen SuperScript™ First- Strand Synthesis System (Cat# 11904-018) according to the manufactures instructions. Respective primers were designed and used for PCR analysis. Actin primers were used as positive and loading controls.

D 2.5 Biochemical methods

D 2.5.1 Basic protein techniques

Basic biochemical techniques were performed according to “Molecular Cloning: A Laboratory Manual (Third Edition) By Joseph Sambrook, Peter MacCallum Cancer Institute, Melbourne, Australia; David Russell, University of Texas Southwestern Medical Center, Dallas”.

D 2.5.2 Protein extraction (denaturing)

The plant samples were ground in 20 µL of extraction buffer/ cracking buffer (50 mM Tris pH 6,8, 2% SDS, 36% Urea, 30 % Glycerin) and 1 µL of mercaptoethanol. Then, the suspension was incubated for 10 minutes at 95 °C and centrifuge at 12000 rpm for 30 seconds. The supernatant was transferred to a fresh eppendorf tube and kept frozen until usage. Upto 15 µL was loaded on SDS-PAGE.

D 2.5.3 Western blotting

The extracted protein was loaded on SDS-PAGE separation gel (7,5% acrylamide, 1M Tris pH 8,8 and 10% SDS, 10% APS) and ran for 60 minutes at 20 mA. The blot was carried under semi-dry conditions on a Roti-PVDF membrane (Carl Roth GmbH, Karlsruhe) according to the manufacturer's instructions. The membrane was blocked overnight at 4°C in 5% skimmed milk powder (sukofine) dissolved in phosphate buffered saline-tween (PBST: 8 g of NaCl 0.2 g of KCl, 1.44 g of Na_2HPO_4 , 0.24 g of KH_2PO_4 , 2 ml of tween-20 in 1L of H₂O; pH 7,2). The blot was treated with primary antibody with appropriate dilution over night at 4°C in 5% skimmed milk in PBST. The blot was washed three to four times in PBST for every fifteen minutes. Then the blot was treated with secondary antibody with appropriate dilution at room temperature for 90 minutes in 5% skimmed milk in PBST. The blot was again washed three to four times in PBST for every fifteen minutes. Finally, the detection was performed with the kit ECL Western Blotting Analysis system (Amersham Biosciences, UK) following the instructions given by the manufacturers. Alternatively the blot was also detected on BIORAD chemiluminescence western detection machine.

D 2.5.4 Ubiquitin binding assay

Native protein was extracted from WT and respective transgenic lines at 4°C. Four plants (4-5th leaf) from selection plates were ground in PPB [50 mM Phosphate buffer, 150mM NaCl; 0,5% NP40/CA630; 0,5mM DTT; 2,5% Complete] and centrifuged at 500 x g for one minute. Equal amounts of Ubiquitin- and Protein G agarose (approximately 70µl) were equilibrated. The beads were centrifuged at 500 x g and resuspended in 100µl PPB (repeat three times). 80µl of PPB and 150µl of native protein extract was added and incubated for 3 hours under slight agitation. Beads were centrifuged at 500 x g and resuspended carefully in 100 µl PPB (repeated three times). All the above steps were performed at 4°C. 50µl cracking buffer was added, heated to 99°C for 10 minutes and used for SDS-PAGE. PAGE was performed using 12% polyacrylamide gels.

D 2.5.5 Gel filtration/ Size exclusion chromatography

Native proteins were extracted from WT and respective transgenic lines at 4°C. Nine plants (4-5th leaf) from selection plates were ground in 600µl P150 [50 mM Phosphate buffer, 150mM NaCl]. 200 µl Complete-150 (one tablet Complete in 2ml P150) was added immediately. The homogenate was centrifuged at 16000 x g for two minutes and the supernatant was transferred to a fresh tube and centrifuged two more times for 37 and 5 minutes respectively. Each time a fresh tube was used. Then the supernatant was ultra-centrifuged at 100, 000 x g for 60 minutes and supernatant was collected. Protein concentration was measured with Bradford reagent using calorimetry. The Superose™ 6 10/300 GL column was equilibrated with two column volumes of P150. The column was then stepwise calibrated with 50µl of thyroglobulin (5mg/ml), 3µl ferritin (0.3mg/ml), 40µl aldolase (4mg/ml) and 40µl ovalbumin (4mg/ml). After washing with three column volumes of P150, 100µl of native protein extract was loaded and run under the same conditions like the standard (25ml, 0,25ml/min). Fractions of a volume of 0,5 ml were collected, precipitated by speed vaccum and suspended in cracking buffer. SDS- PAGE was performed using 12% polyacrylamide gels and western was performed using respective antibody.

D 2.5.6 Radioactive *in vitro* expression

The ESCRT-I proteins in pDONR201 vector was cloned into gateway destination vectors pJIC26 and pJIC39 (a gift from George Coupland group, MPI, Cologne, Germany) using gateway cloning strategy (Invitrogen). The *in vitro* expression was performed using the Promega TNT Quick Coupled Transcription/ Translation System kit according to the manufacturer's instructions. Radioactive S35 obtained from HARTMANN ANALYTIC, Germany was used for labeling. The whole experiment was performed in radioisotope lab with prior instructions. A mixture of 0,25µg of respective DNA, 0,5µl S35, 10µl TNT mix was incubated at 30°C for 90 minutes. 20 µl 2x laemmli buffer (composition of 5x laemmli buffer: 310mM Triss pH 6.8, 10% SDS, 50% glycerin, 0,5% bromophenol blue and 500mM DTT) with 200mM DTT was added to the mix. Samples were boiled at 95°C for 5 minutes and seperated on 12% SDS-PAGE at 20mAmps for 60 minutes and destained the gel using 50% MeOH and 7% Acetic acid. The gel

was dried for 2 hours and exposed with phosphor imager cassette in dark overnight. The signal was detected using phosphor imager detection system (FUJI-FLA7000).

D 2.5.7 Radioactive *in vitro* co-immunoprecipitation

The bait protein was partially labeled with S35 and the corresponding prey proteins were completely labeled with S35. The *in vitro* binding assay was performed using the Promega TNT Quick Coupled Transcription/ Translation System according to the manufacturer's instructions. The separate mix of bait and prey proteins were incubated at 30°C for 90 minutes. 11,5µl of prey protein and 11,5µl of bait protein was added into an eppendorf tube containing 200µl of co-IP buffer (20mM Tris pH 7,5; 150mM NaCl and 0,1% Tween 20) with 200mM DTT. Samples were incubated for 3 hours on the rotator at 4°C. 2µl of α-GAD antibody (purchased from Santacruz Biotech) was added and incubated for 30 min on the rotator at 4°C. 8µl of prewashed ProteinA dynabeads (invitrogen) were added to the mix and again incubated for 30 min at 4°C on a rotator. Samples were placed in the magnet and about 30µl of supernatant fractions were collected and equal amount of 2x laemmli buffer with 200µl of DTT was added. Pellets were washed three times with 1ml ice cold co-IP buffer and were resuspended in 30µl 1x laemmli buffer with 100µl DTT. Both supernatant and pellet fractions were incubated at 95°C for 5 minutes. Pellet samples were again placed in magnet and the supernatant was transferred to a new reaction tube. The supernatant and corresponding pellet fractions were loaded on 12% SDS-PAGE separated at 20mAmps for 60 minutes and destained the gel using 50% MeOH and 7% Acetic acid. Dried the gel for 2 hours and exposed with phosphor imager cassette in dark overnight. The signal was detected using phosphor imager detection system (FUJI-F7000).

D 2.5.8 Blue-native PAGE

Native protein was extracted from WT and knock-out lines at 4°C. Nine plants (4-5th leaf) from selection plates were ground in 600µl P150 [50 mM Phosphate buffer, 150mM NaCl]. 200 µl Complete-150 (one tablet Complete in 2ml P150) was added immediately. The homogenate was centrifuged at 16000x g for two minutes. Supernatant was transferred to a fresh tube and centrifuged two more times for 37 and 5 minutes respectively. Then the supernatant was ultra-centrifuged at 100, 000x g for 60 minutes and supernatant was collected. Protein concentration

was measured with Bradford reagent using calorimetry. The proteins were solubilized using 0,6% digitonin (Sigma-Aldrich) for 15 minutes at 4°C. Meanwhile 6%-12% gradient blue-native gels were prepared as described in (Swamy et al. 2006). The solubilized proteins were loaded on Blue-native PAGE along with standard marker mix (Thyroglobulin, 10mg/ml; Ferritin, 10mg/ml; BSA, 10mg/ml). Inner chamber was filled with cathode buffer (Biss-triss, 15mM; Tricine, 50mM; Coomassie blue G250, 0,02%) and outer and lower chamber was filled with anode buffer (Biss-triss, 50mM). 100V of voltage was given until the samples have entered the separating gel and voltage was increased to 180V and ran until the dye front reaches end of the gel. The gel was electroblotted on PVDF membrane, western blot was performed using VPS28 antibody and bands were detected on BIORAD chemiluminescence western detection machine.

E. Appendix

E 1. Genetic analysis of the double knock-out *elch vps28-1*

	A	B	C	D	E	F	G	H	I	J	K	L
	1	3	128	0	108	0	120	0	98	1	102	2,94
		4	123	0	104	0	110	0	103	1,9	100	2
2	3	3	123	0	138	0	160	0	104	1,9	98	2,04
		4	124	0	136	0	140	0	103	1,9	90	2,22
3	3	3	126	0	130	0	114	0	100	2	87	2,3
		4	123	0	132	0	62	0	102	2,1	94	2,13
4	3	3	114	0	109	0	96	0	98	2	112	2,68
		4	116	0	106	0	144	0	96	1	117	2,56
5	3	3	109	0	119	0	92	0	101	2	118	2,54
		4	106	0	118	0	89	0	107	2,8	114	1,75
6	3	3	113	0	126	0	118	0	98	1,1	127	2,36
		4	112	0	124	0	115	0	99	1	131	2,29
7	3	3	117	0	132	0	119	0	116	2,5	102	1,96
		4	112	0	134	0	148	0	114	1,7	109	2,75
8	3	3	129	0	130	0	140	0	113	1,7	111	1,8
		4	123	0	131	0	126	0	112	1,8	112	1,79
9	3	3	134	0	119	0	115	0	124	2,4	93	1,08
		4	130	0	116	0	130	0	120	1,6	37	5,41
10	3	3	139	0	112	0	105	0	116	1,7	127	2,36
		4	132	0	114	0	93	0	104	1,9	114	1,75
11	3	3	136	0	109	0	100	0	100	2	110	2,73
		4	138	0	106	0	102	0	102	2,1	119	2,52
12	3	3	129	0	112	0	111	0	112	1,7	119	1,68
		4	123	0	113	0	109	0	113	2,6	111	2,7
13	3	3	119	0	123	0	99	0	99	1	84	2,38
		4	118	0	129	0	98	0	94	2,1	86	2,33
14	3	3	104	0	128	0	120	0	100	2	134	2,24
		4	107	0	125	0	121	0	102	2,1	137	2,19
15	3	3	112	0	120	0	108	0	104	2,2	131	3,05
		4	119	0	119	0	104	0	103	2,1	129	3,1
16	3	3	123	0	123	0	117	0	90	1,1	120	3,33
		4	125	0	126	0	116	0	94	2,1	110	2,73
17	3	3	129	0	138	0	128	0	118	1,8	118	2,54
		4	121	0	131	0	134	0	114	1,7	101	2,97
18	3	3	116	0	116	0	109	0	103	2,1	108	1,85
		4	111	0	114	0	108	0	102	2,1	111	2,7
19	3	3	117	0	113	0	113	0	112	1,8	121	3,31
		4	113	0	118	0	116	0	113	1,8	117	2,56
20	3	3	120	0	102	0	121	0	100	2	100	2
		4	121	0	101	0	122	0	104	2,1	121	2,48
n					5910		5705		4207		5439	
M										1,84		2,48
p												<0,05*

A= plant number

B= leaf number

C= trichome number per leaf (Ws)

D= % cluster frequency (Ws)

E=trichome number per leaf (col-0)

F= % cluster frequency (Col-0)

G= trichome number per leaf (vps28-1)

H= % cluster frequency (vps28-1)

I= trichome number per leaf (elch)

J= % cluster frequency (elch)

K= trichome number per leaf (elch vps28-1)

L= % cluster frequency (elch vps28-1)

M= % cluster frequency(average)

*= crosstab test against elch

E 2. Genetic analysis of the double knock-out *elch vps28-2*

A	B	C	D	E	F	G	H	I	J	K	L
1	3	108	0	128	0	138	0	98	1	101	3,9
	4	104	0	123	0	134	0	103	1,9	100	4
2	3	138	0	123	0	128	0	104	1,9	108	3,7
	4	136	0	124	0	124	0	103	1,9	94	4,2
3	3	130	0	126	0	120	0	100	2	112	4,4
	4	132	0	123	0	124	0	102	2,1	110	3,6
4	3	109	0	114	0	125	0	98	2	94	4,2
	4	106	0	116	0	126	0	96	1	84	4,7
5	3	119	0	109	0	118	0	101	2	105	3,8
	4	118	0	106	0	114	0	107	2,8	104	3,8
6	3	126	0	113	0	113	0	98	1,1	114	4,3
	4	124	0	112	0	112	0	99	1	111	3,6
7	3	132	0	117	0	109	0	116	2,5	121	3,3
	4	134	0	112	0	104	0	114	1,7	122	3,2
8	3	130	0	129	0	125	0	113	1,7	104	3,8
	4	131	0	123	0	120	0	112	1,8	101	3,9
9	3	119	0	134	0	140	0	124	2,4	108	3,7
	4	116	0	130	0	134	0	120	1,6	103	2,9
10	3	112	0	139	0	108	0	116	1,7	118	4,2
	4	114	0	132	0	104	0	104	1,9	116	3,4
11	3	109	0	136	0	109	0	100	2	116	3,4
	4	106	0	138	0	106	0	102	2,1	114	3,5
12	3	112	0	129	0	112	0	112	1,7	119	4,2
	4	113	0	123	0	111	0	113	2,6	113	3,5
13	3	123	0	119	0	114	0	99	1	112	4,4
	4	129	0	118	0	112	0	94	2,1	107	3,7
14	3	128	0	104	0	118	0	100	2	111	3,6
	4	125	0	107	0	119	0	102	2,1	112	3,5
15	3	120	0	112	0	125	0	104	2,2	109	3,6
	4	119	0	119	0	126	0	103	2,1	104	2,8
16	3	123	0	123	0	133	0	90	1,1	108	3,7
	4	126	0	125	0	131	0	94	2,1	103	3,8
17	3	138	0	129	0	134	0	118	1,8	111	4,5
	4	131	0	121	0	131	0	114	1,7	114	3,5
18	3	116	0	116	0	118	0	103	2,1	102	3,9
	4	114	0	111	0	114	0	102	2,1	98	3
19	3	113	0	117	0	112	0	112	1,8	100	4
	4	118	0	113	0	111	0	113	1,8	94	3,1
20	3	102	0	120	0	104	0	100	2	101	3,9
	4	101	0	121	0	103	0	104	2,1	96	3,1
N		5910		6052		5932		4207		5410	
M									1,84		3,8
P											<0,001*

A= plant number

B= leaf number

C= trichome number per leaf (Ws)

D= % cluster frequency (Ws)

E=trichome number per leaf (col-0)

F= % cluster frequency (Col-0)

G= trichome number per leaf (vps28-1)

H= % cluster frequency (vps28-1)

I= trichome number per leaf (elch)

J= % cluster frequency (elch)

K= trichome number per leaf (elch vps28-1)

L= % cluster frequency (elch vps28-1)

M= % cluster frequency(average)

*= crosstab test against elch

E 3. Genetic analysis of the double knock-out *elch vps37-1*

	A	B	C	D	E	F	G	H	I	J	K	L
1	3	108	0	128	0	130	0	98	1	125	4	
	4	104	0	123	0	135	0	103	1,9	118	4,2	
2	3	138	0	123	0	124	0	104	1,9	130	4,6	
	4	136	0	124	0	130	0	103	1,9	129	3,9	
3	3	130	0	126	0	121	0	100	2	112	4,5	
	4	132	0	123	0	122	0	102	2,1	110	3,6	
4	3	109	0	114	0	129	0	98	2	94	4,2	
	4	106	0	116	0	130	0	96	1	93	4,3	
5	3	119	0	109	0	118	0	101	2	105	4,8	
	4	118	0	106	0	116	0	107	2,8	104	3,8	
6	3	126	0	113	0	115	0	98	1,1	114	4,4	
	4	124	0	112	0	118	0	99	1	111	4,5	
7	3	132	0	117	0	108	0	116	2,5	121	4,1	
	4	134	0	112	0	103	0	114	1,7	122	4,1	
8	3	130	0	129	0	125	0	113	1,7	104	3,8	
	4	131	0	123	0	121	0	112	1,8	101	3,9	
9	3	119	0	134	0	140	0	124	2,4	108	3,7	
	4	116	0	130	0	139	0	120	1,6	103	3,9	
10	3	112	0	139	0	111	0	116	1,7	118	4,2	
	4	114	0	132	0	112	0	104	1,9	116	3,4	
11	3	109	0	136	0	109	0	100	2	116	3,4	
	4	106	0	138	0	117	0	102	2,1	114	4,4	
12	3	112	0	129	0	112	0	112	1,7	119	5	
	4	113	0	123	0	115	0	113	2,6	113	3,5	
13	3	123	0	119	0	114	0	99	1	112	3,6	
	4	129	0	118	0	116	0	94	2,1	107	3,7	
14	3	128	0	104	0	106	0	100	2	111	4,5	
	4	125	0	107	0	109	0	102	2,1	112	3,6	
15	3	120	0	112	0	125	0	104	2,2	109	3,7	
	4	119	0	119	0	122	0	103	2,1	104	3,9	
16	3	123	0	123	0	140	0	90	1,1	108	4,6	
	4	126	0	125	0	144	0	94	2,1	103	3,9	
17	3	138	0	129	0	130	0	118	1,8	111	4,5	
	4	131	0	121	0	131	0	114	1,7	114	4,4	
18	3	116	0	116	0	117	0	103	2,1	102	3,9	
	4	114	0	111	0	124	0	102	2,1	98	3	
19	3	113	0	117	0	120	0	112	1,8	100	4	
	4	118	0	113	0	111	0	113	1,8	94	3,2	
20	3	102	0	120	0	104	0	100	2	101	4	
	4	101	0	121	0	109	0	104	2,1	96	4,2	
N			5910		6052		7102		4207		5761	
M									1,84		4,01	
P												<0,001*

A= plant number

B= leaf number

C= trichome number per leaf (Ws)

D= % cluster frequency (Ws)

E=trichome number per leaf (col-0)

F= % cluster frequency (Col-0)

G= trichome number per leaf (vps28-1)

H= % cluster frequency (vps28-1)

I= trichome number per leaf (elch)

J= % cluster frequency (elch)

K= trichome number per leaf (elch vps28-1)

L= % cluster frequency (elch vps28-1)

M= % cluster frequency(average)

*= crosstab test against elch

E 4. Genetic analysis of the double knock-out *elch vps37-2*

	A	B	C	D	E	F	G	H	I	J	K	L
	1	3	108	0	128	0	169	0	98	1	125	2,40
		4	104	0	123	0	131	0	103	1,9	120	2,50
	2	3	138	0	123	0	146	0	104	1,9	118	1,69
		4	136	0	124	0	152	0	103	1,9	119	1,68
	3	3	130	0	126	0	101	0	100	2	124	1,61
		4	132	0	123	0	150	0	102	2,1	127	1,57
	4	3	109	0	114	0	150	0	98	2	120	2,50
		4	106	0	116	0	156	0	96	1	123	2,44
	5	3	119	0	109	0	161	0	101	2	102	1,96
		4	118	0	106	0	115	0	107	2,8	109	1,83
	6	3	126	0	113	0	153	0	98	1,1	104	1,92
		4	124	0	112	0	115	0	99	1	108	1,85
	7	3	132	0	117	0	181	0	116	2,5	111	1,80
		4	134	0	112	0	146	0	114	1,7	117	1,71
	8	3	130	0	129	0	196	0	113	1,7	87	2,30
		4	131	0	123	0	180	0	112	1,8	84	2,38
	9	3	119	0	134	0	154	0	124	2,4	83	2,41
		4	116	0	130	0	149	0	120	1,6	88	2,27
	10	3	112	0	139	0	138	0	116	1,7	94	2,13
		4	114	0	132	0	163	0	104	1,9	90	2,22
	11	3	109	0	136	0	150	0	100	2	79	1,27
		4	106	0	138	0	122	0	102	2,1	81	1,23
	12	3	112	0	129	0	236	0	112	1,7	107	1,87
		4	113	0	123	0	171	0	113	2,6	109	1,83
	13	3	123	0	119	0	173	0	99	1	112	1,79
		4	129	0	118	0	200	0	94	2,1	115	1,74
	14	3	128	0	104	0	192	0	100	2	119	1,68
		4	125	0	107	0	190	0	102	2,1	124	1,61
	15	3	120	0	112	0	133	0	104	2,2	125	2,40
		4	119	0	119	0	156	0	103	2,1	127	2,36
	16	3	123	0	123	0	236	0	90	1,1	94	2,13
		4	126	0	125	0	191	0	94	2,1	97	3,09
	17	3	138	0	129	0	89	0	118	1,8	99	2,02
		4	131	0	121	0	130	0	114	1,7	98	2,04
	18	3	116	0	116	0	183	0	103	2,1	104	1,92
		4	114	0	111	0	197	0	102	2,1	109	1,83
	19	3	113	0	117	0	127	0	112	1,8	127	2,36
		4	118	0	113	0	164	0	113	1,8	123	2,44
	20	3	102	0	120	0	178	0	100	2	141	2,13
		4	101	0	121	0	162	0	104	2,1	147	2,04
n			5910		6052		7745		4207		5761	
M										1,84		1,98
p												<n.s*

A= plant number

B= leaf number

C= trichome number per leaf (Ws)

D= % cluster frequency (Ws)

E=trichome number per leaf (col-0)

F= % cluster frequency (Col-0)

G= trichome number per leaf (vps28-1)

H= % cluster frequency (vps28-1)

I= trichome number per leaf (elch)

J= % cluster frequency (elch)

K= trichome number per leaf (elch vps28-1)

L= % cluster frequency (elch vps28-1)

M= % cluster frequency(average)

*= crosstab test against elch

E 5. Genetic analysis of the triple knock-out *elch vps28-2 vps37-1*

	A	B	C	D	E	F	G	H	I	J	K	L	M	N
	1	3	108	0	128	0	98	1	125	4	101	3,9	120	11,6
		4	104	0	123	0	103	1,9	118	4,2	100	4	110	12,7
	2	3	138	0	123	0	104	1,9	130	4,6	108	3,7	100	12
		4	136	0	124	0	103	1,9	129	3,9	94	4,2	100	14
	3	3	130	0	126	0	100	2	112	4,5	112	4,4	90	16,6
		4	132	0	123	0	102	2,1	110	3,6	110	3,6	80	20
	4	3	109	0	114	0	98	2	94	4,2	94	4,2	110	10,9
		4	106	0	116	0	96	1	93	4,3	84	4,7	110	14,5
	5	3	119	0	109	0	101	2	105	4,8	105	3,8	90	11,1
		4	118	0	106	0	107	2,8	104	3,8	104	3,8	120	12,5
	6	3	126	0	113	0	98	1,1	114	4,4	114	4,3	115	9,5
		4	124	0	112	0	99	1	111	4,5	111	3,6	125	9,6
	7	3	132	0	117	0	116	2,5	121	4,1	121	3,3	118	10,1
		4	134	0	112	0	114	1,7	122	4,1	122	3,2	125	10,4
	8	3	130	0	129	0	113	1,7	104	3,8	104	3,8	140	9,2
		4	131	0	123	0	112	1,8	101	3,9	101	3,9	150	10
	9	3	119	0	134	0	124	2,4	108	3,7	108	3,7	120	10
		4	116	0	130	0	120	1,6	103	3,9	103	2,9	118	11,1
	10	3	112	0	139	0	116	1,7	118	4,2	118	4,2	120	11,6
		4	114	0	132	0	104	1,9	116	3,4	116	3,4	123	10,5
	11	3	109	0	136	0	100	2	116	3,4	116	3,4	140	10
		4	106	0	138	0	102	2,1	114	4,4	114	3,5	130	9,2
	12	3	112	0	129	0	112	1,7	119	5	119	4,2	90	8,8
		4	113	0	123	0	113	2,6	113	3,5	113	3,5	85	14,1
	13	3	123	0	119	0	99	1	112	3,6	112	4,4	120	10,3
		4	129	0	118	0	94	2,1	107	3,7	107	3,7	140	9,2
	14	3	128	0	104	0	100	2	111	4,5	111	3,6	125	10,4
		4	125	0	107	0	102	2,1	112	3,6	112	3,5	120	10
	15	3	120	0	112	0	104	2,2	109	3,7	109	3,6	135	9,9
		4	119	0	119	0	103	2,1	104	3,9	104	2,8	110	9,8
	16	3	123	0	123	0	90	1,1	108	4,6	108	3,7	95	12,6
		4	126	0	125	0	94	2,1	103	3,9	103	3,8	98	11,1
	17	3	138	0	129	0	118	1,8	111	4,5	111	4,5	100	12
		4	131	0	121	0	114	1,7	114	4,4	114	3,5	110	11,8
	18	3	116	0	116	0	103	2,1	102	3,9	102	3,9	105	10,5
		4	114	0	111	0	102	2,1	98	3	98	3	110	9
	19	3	113	0	117	0	112	1,8	100	4	100	4	120	9,1
		4	118	0	113	0	113	1,8	94	3,2	94	3,1	125	9,6
	20	3	102	0	120	0	100	2	101	4	101	3,9	110	10
		4	101	0	121	0	104	2,1	96	4,2	96	3,1	112	8,9
N			5910		6052		4207		5410		5351		5761	
O								1,8		4,01		3,8		10,91
P														<0,001*

A= plant number

B= leaf number

C= trichome number per leaf (Ws)

D= % cluster frequency (Ws)

E=trichome number per leaf (col-0)

F= % cluster frequency (Col-0)

G= trichome number per leaf (*elch*)H= % cluster frequency (*elch*)I= trichome number per leaf (*elch vps37-1*)J= % cluster frequency (*elch vps37-1*)K= trichome number per leaf (*elch vps28-2*)L= cluster trichomes/ leaf (*elch vps28-2*)M= cluster trichomes/ leaf (*elch vps28-2 vps37-1*)N= % cluster frequency (*elch vps28-2 vps37-1*)*= crosstab test against *elch vps28-2* and *elch vps37-1*

E 6. Statistics of promoter rescue analysis of the *ELCH* under the *ELCH* promoter

line number	leaf number	trichome number / leaf	number of WT trichomes	number of <i>elch</i> trichomes
1	3	84	84	0
	4	84	84	0
2	3	89	89	0
	4	88	88	0
3	3	79	79	0
	4	78	78	0
4	3	106	106	0
	4	104	104	0
5	3	88	88	0
	4	87	87	0
6	3	88	88	0
	4	86	86	0
7	3	84	84	0
	4	81	81	0
8	3	90	90	0
	4	92	92	0
9	3	94	94	0
	4	92	92	0
10	3	90	90	0
	4	92	92	0
11	3	87	87	0
	4	82	82	0
12	3	95	95	0
	4	90	90	0
13	3	102	102	0
	4	104	104	0
14	3	100	100	0
	4	104	104	0
15	3	80	80	0
	4	84	84	0
16	3	78	78	0
	4	78	78	0
17	3	84	84	0
	4	83	83	0
18	3	81	81	0
	4	83	83	0
19	3	93	93	0
	4	95	95	0
20	3	90	90	0
	4	92	92	0
Total		3600	3600	
% <i>elch</i> trichomes				0%
rescue status				Rescued

E 7. Statistics of promoter rescue analysis of *VPS23-2* under the *ELCH* promoter

line number	leaf number	trichome number / leaf	number of WT Trichomes	number of <i>elch</i> trichomes
1	3	78	78	0
	4	74	74	0
2	3	82	82	0
	4	81	81	0
3	3	79	79	0
	4	78	78	0
4	3	87	87	0
	4	89	89	0
5	3	94	94	0
	4	92	92	0
6	3	95	95	0
	4	97	97	0
7	3	102	102	0
	4	104	104	0
8	3	90	90	0
	4	92	92	0
9	3	87	87	0
	4	84	84	0
10	3	79	79	0
	4	79	79	0
11	3	84	84	0
	4	82	82	0
12	3	90	90	0
	4	92	92	0
13	3	93	93	0
	4	94	94	0
14	3	88	88	0
	4	89	89	0
15	3	79	79	0
	4	79	79	0
16	3	84	84	0
	4	86	86	0
17	3	87	87	0
	4	89	89	0
18	3	102	102	0
	4	101	101	0
19	3	100	100	0
	4	102	102	0
20	3	74	74	0
	4	72	72	0
Total		3560	3560	
% <i>elch</i> trichomes				0%
rescue status				Rescued

E 8. Statistics of promoter rescue analysis of VPS23-3 under the *ELCH* promoter

line number	leaf number	trichome number/ leaf	number of WT trichomes	number of <i>elch</i> trichomes
1	3	82	80	2
	4	83	81	2
2	3	90	88	2
	4	92	90	2
3	3	97	95	2
	4	98	96	2
4	3	91	89	2
	4	90	89	1
5	3	84	83	1
	4	80	79	1
6	3	97	95	2
	4	92	90	2
7	3	99	97	2
	4	90	88	2
8	3	80	79	1
	4	84	82	2
9	3	100	98	2
	4	102	100	2
10	3	97	95	2
	4	94	92	2
11	3	78	78	0
	4	79	79	0
12	3	80	79	1
	4	82	80	2
13	3	84	82	2
	4	80	79	1
14	3	90	89	1
	4	92	90	2
15	3	94	92	2
	4	90	89	1
16	3	110	108	2
	4	108	106	2
17	3	79	78	1
	4	74	74	0
18	3	80	79	1
	4	82	81	1
19	3	87	85	2
	4	84	82	2
20	3	90	88	2
	4	92	90	2
Total		3557	3494	63
% <i>elch</i> trichomes				1,80%
rescue status				No rescue

References

- Albertson, R., B. Riggs and W. Sullivan (2005).** "Membrane traffic: a driving force in cytokinesis." Trends Cell Biol **15**(2): 92-101.
- Amerik, A. Y., J. Nowak, S. Swaminathan and M. Hochstrasser (2000).** "The Doa4 deubiquitinating enzyme is functionally linked to the vacuolar protein-sorting and endocytic pathways." Mol Biol Cell **11**(10): 3365-80.
- Audhya, A., I. X. McLeod, J. R. Yates and K. Oegema (2007).** "MVB-12, a fourth subunit of metazoan ESCRT-I, functions in receptor downregulation." PLoS ONE **2**(9): e956.
- Babst, M. (2005).** "A protein's final ESCRT." Traffic **6**(1): 2-9.
- Babst, M., D. J. Katzmann, W. B. Snyder, B. Wendland and S. D. Emr (2002).** "Endosome-associated complex, ESCRT-II, recruits transport machinery for protein sorting at the multivesicular body." Dev Cell **3**(2): 283-9.
- Babst, M., G. Odorizzi, E. J. Estepa and S. D. Emr (2000).** "Mammalian tumor susceptibility gene 101 (TSG101) and the yeast homologue, Vps23p, both function in late endosomal trafficking." Traffic **1**(3): 248-58.
- Babst, M., T. K. Sato, L. M. Banta and S. D. Emr (1997).** "Endosomal transport function in yeast requires a novel AAA-type ATPase, Vps4p." Embo J **16**(8): 1820-31.
- Babst, M., B. Wendland, E. J. Estepa and S. D. Emr (1998).** "The Vps4p AAA ATPase regulates membrane association of a Vps protein complex required for normal endosome function." Embo J **17**(11): 2982-93.
- Bache, K. G., T. Slagsvold, A. Cabezas, K. R. Rosendal, C. Raiborg and H. Stenmark (2004).** "The growth-regulatory protein HCRP1/hVps37A is a subunit of mammalian ESCRT-I and mediates receptor down-regulation." Mol Biol Cell **15**(9): 4337-46.
- Baluska, F., A. Hlavacka, J. Samaj, K. Palme, D. G. Robinson, T. Matoh, D. W. McCurdy, D. Menzel and D. Volkmann (2002).** "F-actin-dependent endocytosis of cell wall pectins in meristematic root cells. Insights from brefeldin A-induced compartments." Plant Physiol **130**(1): 422-31.
- Baluska, F., F. Liners, A. Hlavacka, M. Schlicht, P. Van Cutsem, D. W. McCurdy and D. Menzel (2005).** "Cell wall pectins and xyloglucans are internalized into dividing root cells and accumulate within cell plates during cytokinesis." Protoplasma **225**(3-4): 141-55.
- Bhat, R. A., T. Lahaye and R. Panstruga (2006).** "The visible touch: in planta visualization of protein-protein interactions by fluorophore-based methods." Plant Methods **2**: 12.

- Bilodeau, P. S., J. L. Urbanowski, S. C. Winistorfer and R. C. Piper (2002).** "The Vps27p Hse1p complex binds ubiquitin and mediates endosomal protein sorting." Nat Cell Biol **4**(7): 534-9.
- Bilodeau, P. S., S. C. Winistorfer, W. R. Kearney, A. D. Robertson and R. C. Piper (2003).** "Vps27-Hse1 and ESCRT-I complexes cooperate to increase efficiency of sorting ubiquitinated proteins at the endosome." J Cell Biol **163**(2): 237-43.
- Bishop, N. and P. Woodman (2001).** "TSG101/mammalian VPS23 and mammalian VPS28 interact directly and are recruited to VPS4-induced endosomes." J Biol Chem **276**(15): 11735-42.
- Bowers, K. and T. H. Stevens (2005).** "Protein transport from the late Golgi to the vacuole in the yeast *Saccharomyces cerevisiae*." Biochim Biophys Acta **1744**(3): 438-54.
- Carlton, J. G., M. Agromayor and J. Martin-Serrano (2008).** "Differential requirements for Alix and ESCRT-III in cytokinesis and HIV-1 release." Proc Natl Acad Sci U S A **105**(30): 10541-6.
- Carlton, J. G. and J. Martin-Serrano (2007).** "Parallels between cytokinesis and retroviral budding: a role for the ESCRT machinery." Science **316**(5833): 1908-12.
- Chu, T., J. Sun, S. Saksena and S. D. Emr (2006).** "New component of ESCRT-I regulates endosomal sorting complex assembly." J Cell Biol **175**(5): 815-23.
- Clough, S. J. and A. F. Bent (1998).** "Floral dip: a simplified method for *Agrobacterium*-mediated transformation of *Arabidopsis thaliana*." Plant J **16**(6): 735-43.
- Curtiss, M., C. Jones and M. Babst (2007).** "Efficient cargo sorting by ESCRT-I and the subsequent release of ESCRT-I from multivesicular bodies requires the subunit Mvb12." Mol Biol Cell **18**(2): 636-45.
- D'Avino, P. P., M. S. Savoian and D. M. Glover (2005).** "Cleavage furrow formation and ingression during animal cytokinesis: a microtubule legacy." J Cell Sci **118**(Pt 8): 1549-58.
- Dhonukshe, P., F. Baluska, M. Schlicht, A. Hlavacka, J. Samaj, J. Friml and T. W. Gadella, Jr. (2006).** "Endocytosis of cell surface material mediates cell plate formation during plant cytokinesis." Dev Cell **10**(1): 137-50.
- Dhonukshe, P., J. Samaj, F. Baluska and J. Friml (2007).** "A unifying new model of cytokinesis for the dividing plant and animal cells." Bioessays **29**(4): 371-81.
- Doyotte, A., M. R. Russell, C. R. Hopkins and P. G. Woodman (2005).** "Depletion of TSG101 forms a mammalian "Class E" compartment: a multicisternal early endosome with multiple sorting defects." J Cell Sci **118**(Pt 14): 3003-17.
- Dupre, S., C. Volland and R. Haguenauer-Tsapis (2001).** "Membrane transport: ubiquitylation in endosomal sorting." Curr Biol **11**(22): R932-4.

- Eastman, S. W., J. Martin-Serrano, W. Chung, T. Zang and P. D. Bieniasz (2005).** "Identification of human VPS37C, a component of endosomal sorting complex required for transport-I important for viral budding." J Biol Chem **280**(1): 628-36.
- Feng, G. H., C. J. Lih and S. N. Cohen (2000).** "TSG101 protein steady-state level is regulated posttranslationally by an evolutionarily conserved COOH-terminal sequence." Cancer Res **60**(6): 1736-41.
- Finken-Eigen, M., R. A. Rohricht and K. Kohrer (1997).** "The VPS4 gene is involved in protein transport out of a yeast pre-vacuolar endosome-like compartment." Curr Genet **31**(6): 469-80.
- Frigerio, F., M. Casimir, S. Carobbio and P. Maechler (2008).** "Tissue specificity of mitochondrial glutamate pathways and the control of metabolic homeostasis." Biochim Biophys Acta **1777**(7-8): 965-72.
- Geldner, N. and G. Jurgens (2006).** "Endocytosis in signalling and development." Curr Opin Plant Biol **9**(6): 589-94.
- Gigolashvili, T., B. Berger, H. P. Mock, C. Muller, B. Weisshaar and U. I. Flugge (2007).** "The transcription factor HIG1/MYB51 regulates indolic glucosinolate biosynthesis in *Arabidopsis thaliana*." Plant J **50**(5): 886-901.
- Goh, T., W. Uchida, S. Arakawa, E. Ito, T. Dainobu, K. Ebine, M. Takeuchi, K. Sato, T. Ueda and A. Nakano (2007).** "VPS9a, the common activator for two distinct types of Rab5 GTPases, is essential for the development of *Arabidopsis thaliana*." Plant Cell **19**(11): 3504-15.
- Grebe, M., J. Xu, W. Mobius, T. Ueda, A. Nakano, H. J. Geuze, M. B. Rook and B. Scheres (2003).** "Arabidopsis sterol endocytosis involves actin-mediated trafficking via ARA6-positive early endosomes." Curr Biol **13**(16): 1378-87.
- Gruenberg, J. and H. Stenmark (2004).** "The biogenesis of multivesicular endosomes." Nat Rev Mol Cell Biol **5**(4): 317-23.
- Guertin, D. A., S. Trautmann and D. McCollum (2002).** "Cytokinesis in eukaryotes." Microbiol Mol Biol Rev **66**(2): 155-78.
- Haglund, K., P. P. Di Fiore and I. Dikic (2003).** "Distinct monoubiquitin signals in receptor endocytosis." Trends Biochem Sci **28**(11): 598-603.
- Haupt, S., G. H. Cowan, A. Ziegler, A. G. Roberts, K. J. Oparka and L. Torrance (2005).** "Two plant-viral movement proteins traffic in the endocytic recycling pathway." Plant Cell **17**(1): 164-81.
- Hicke, L. and R. Dunn (2003).** "Regulation of membrane protein transport by ubiquitin and ubiquitin-binding proteins." Annu Rev Cell Dev Biol **19**: 141-72.

- Hugdahl, J. D., C. L. Bokros, V. R. Hanesworth, G. R. Aalund and L. C. Morejohn (1993).** "Unique functional characteristics of the polymerization and MAP binding regulatory domains of plant tubulin." *Plant Cell* **5**(9): 1063-80.
- Hurley, J. H. and S. D. Emr (2006).** "The ESCRT complexes: structure and mechanism of a membrane-trafficking network." *Annu Rev Biophys Biomol Struct* **35**: 277-98.
- Jaillais, Y., I. Fobis-Loisy, C. Miege and T. Gaude (2008).** "Evidence for a sorting endosome in Arabidopsis root cells." *Plant J* **53**(2): 237-47.
- Jaillais, Y. and T. Gaude (2007).** "[Internalizing to control , or how endocytosis regulates auxin flux in plants]." *Med Sci (Paris)* **23**(2): 117-9.
- Jin, Y., J. J. Mancuso, S. Uzawa, D. Cronembold and W. Z. Cande (2005).** "The fission yeast homolog of the human transcription factor EAP30 blocks meiotic spindle pole body amplification." *Dev Cell* **9**(1): 63-73.
- Jordan, M. A. and L. Wilson (1998).** "Use of drugs to study role of microtubule assembly dynamics in living cells." *Methods Enzymol* **298**: 252-76.
- Jurgens, G. (2005).** "Cytokinesis in higher plants." *Annu Rev Plant Biol* **56**: 281-99.
- Katzmann, D. J., M. Babst and S. D. Emr (2001).** "Ubiquitin-dependent sorting into the multivesicular body pathway requires the function of a conserved endosomal protein sorting complex, ESCRT-I." *Cell* **106**(2): 145-55.
- Katzmann, D. J., G. Odorizzi and S. D. Emr (2002).** "Receptor downregulation and multivesicular-body sorting." *Nat Rev Mol Cell Biol* **3**(12): 893-905.
- Katzmann, D. J., C. J. Stefan, M. Babst and S. D. Emr (2003).** "Vps27 recruits ESCRT machinery to endosomes during MVB sorting." *J Cell Biol* **162**(3): 413-23.
- Kirik, V., P. E. Grini, J. Mathur, I. Klinkhammer, K. Adler, N. Bechtold, M. Herzog, J. M. Bonneville and M. Hulskamp (2002).** "The Arabidopsis TUBULIN-FOLDING COFACTOR A gene is involved in the control of the alpha/beta-tubulin monomer balance." *Plant Cell* **14**(9): 2265-76.
- Kirik, V., J. Mathur, P. E. Grini, I. Klinkhammer, K. Adler, N. Bechtold, M. Herzog, J. M. Bonneville and M. Hulskamp (2002).** "Functional analysis of the tubulin-folding cofactor C in Arabidopsis thaliana." *Curr Biol* **12**(17): 1519-23.
- Kostelansky, M. S., J. Sun, S. Lee, J. Kim, R. Ghirlando, A. Hierro, S. D. Emr and J. H. Hurley (2006).** "Structural and functional organization of the ESCRT-I trafficking complex." *Cell* **125**(1): 113-26.

- Lalonde, S., D. W. Ehrhardt, D. Loque, J. Chen, S. Y. Rhee and W. B. Frommer (2008).** "Molecular and cellular approaches for the detection of protein-protein interactions: latest techniques and current limitations." Plant J **53**(4): 610-35.
- Luduena, R. F. and M. C. Roach (1991).** "Tubulin sulfhydryl groups as probes and targets for antimitotic and antimicrotubule agents." Pharmacol Ther **49**(1-2): 133-52.
- Lupas, A., M. Van Dyke and J. Stock (1991).** "Predicting coiled coils from protein sequences." Science **252**(5009): 1162-1164.
- Mathur, J. and C. Koncz (1998).** "Callus culture and regeneration." Methods Mol Biol **82**: 31-4.
- Mathur, J. and C. Koncz (1998).** "Establishment and maintenance of cell suspension cultures." Methods Mol Biol **82**: 27-30.
- Mathur, J. and C. Koncz (1998).** "PEG-mediated protoplast transformation with naked DNA." Methods Mol Biol **82**: 267-76.
- Mathur, J. and C. Koncz (1998).** "Protoplast isolation, culture, and regeneration." Methods Mol Biol **82**: 35-42.
- Maxfield, F. R. and T. E. McGraw (2004). Endocytic recycling. Nat Rev Mol Cell Biol. **5**: 121-32.
- Morita, E., V. Sandrin, S. L. Alam, D. M. Eckert, S. P. Gygi and W. I. Sundquist (2007).** "Identification of human MVB12 proteins as ESCRT-I subunits that function in HIV budding." Cell Host Microbe **2**(1): 41-53.
- Morita, E., V. Sandrin, H. Y. Chung, S. G. Morham, S. P. Gygi, C. K. Rodesch and W. I. Sundquist (2007).** "Human ESCRT and ALIX proteins interact with proteins of the midbody and function in cytokinesis." Embo J **26**(19): 4215-27.
- Morita, E. and W. I. Sundquist (2004).** "Retrovirus budding." Annu Rev Cell Dev Biol **20**: 395-425.
- Odorizzi, G., M. Babst and S. D. Emr (1998).** "Fab1p PtdIns(3)P 5-kinase function essential for protein sorting in the multivesicular body." Cell **95**(6): 847-58.
- Oestreich, A. J., B. A. Davies, J. A. Payne and D. J. Katzmann (2007).** "Mvb12 is a novel member of ESCRT-I involved in cargo selection by the multivesicular body pathway." Mol Biol Cell **18**(2): 646-57.
- Otegui, M. S. and C. Spitzer (2008).** "Endosomal functions in plants." Traffic.
- Paciorek, T., E. Zazimalova, N. Ruthardt, J. Petrasek, Y. D. Stierhof, J. Kleine-Vehn, D. A. Morris, N. Emans, G. Jurgens, N. Geldner and J. Friml (2005).** "Auxin inhibits endocytosis and promotes its own efflux from cells." Nature **435**(7046): 1251-6.

- Pickett-Heaps, J. D. and D. H. Northcote (1966).** "Organization of microtubules and endoplasmic reticulum during mitosis and cytokinesis in wheat meristems." J Cell Sci **1**(1): 109-20.
- Raiborg, C., T. E. Rusten and H. Stenmark (2003).** "Protein sorting into multivesicular endosomes." Curr Opin Cell Biol **15**(4): 446-55.
- Razi, M. and C. E. Futter (2006).** "Distinct roles for Tsg101 and Hrs in multivesicular body formation and inward vesiculation." Mol Biol Cell **17**(8): 3469-83.
- Robatzek, S., D. Chinchilla and T. Boller (2006).** "Ligand-induced endocytosis of the pattern recognition receptor FLS2 in Arabidopsis." Genes Dev **20**(5): 537-42.
- Saksena, S., J. Sun, T. Chu and S. D. Emr (2007).** "ESCRTing proteins in the endocytic pathway." Trends Biochem Sci **32**(12): 561-73.
- Samuels, A. L., T. H. Giddings, Jr. and L. A. Staehelin (1995).** "Cytokinesis in tobacco BY-2 and root tip cells: a new model of cell plate formation in higher plants." J Cell Biol **130**(6): 1345-57.
- Scheuring, S., O. Bodor, R. A. Rohricht, S. Muller, A. Beyer and K. Kohrer (1999).** "Cloning, characterisation, and functional expression of the *Mus musculus* SKD1 gene in yeast demonstrates that the mouse SKD1 and the yeast VPS4 genes are orthologues and involved in intracellular protein trafficking." Gene **234**(1): 149-59.
- Scheuring, S., R. A. Rohricht, B. Schoning-Burkhardt, A. Beyer, S. Muller, H. F. Abts and K. Kohrer (2001).** "Mammalian cells express two VPS4 proteins both of which are involved in intracellular protein trafficking." J Mol Biol **312**(3): 469-80.
- Schweitzer, J. K., E. E. Burke, H. V. Goodson and C. D'Souza-Schorey (2005).** "Endocytosis resumes during late mitosis and is required for cytokinesis." J Biol Chem **280**(50): 41628-35.
- Shi, A., S. Pant, Z. Balklava, C. C. Chen, V. Figueroa and B. D. Grant (2007).** "A novel requirement for *C. elegans* Alix/ALX-1 in RME-1-mediated membrane transport." Curr Biol **17**(22): 1913-24.
- Slagsvold, T., K. Pattni, L. Malerod and H. Stenmark (2006).** "Endosomal and non-endosomal functions of ESCRT proteins." Trends Cell Biol **16**(6): 317-26.
- Spitzer, C., S. Schellmann, A. Sabovljevic, M. Shahriari, C. Keshavaiah, N. Bechtold, M. Herzog, S. Muller, F. G. Hanisch and M. Hulskamp (2006).** "The Arabidopsis elc mutant reveals functions of an ESCRT component in cytokinesis." Development **133**(23): 4679-89.
- Staehelin, L. A. and P. K. Hepler (1996).** "Cytokinesis in higher plants." Cell **84**(6): 821-4.
- Steinborn, K., C. Maulbetsch, B. Priester, S. Trautmann, T. Pacher, B. Geiges, F. Kuttner, L. Lepiniec, Y. D. Stierhof, H. Schwarz, G. Jurgens and U. Mayer (2002).** "The Arabidopsis

PILZ group genes encode tubulin-folding cofactor orthologs required for cell division but not cell growth." *Genes Dev* **16**(8): 959-71.

Strickland, L. I. and D. R. Burgess (2004). "Pathways for membrane trafficking during cytokinesis." *Trends Cell Biol* **14**(3): 115-8.

Stuchell, M. D., J. E. Garrus, B. Muller, K. M. Stray, S. Ghaffarian, R. McKinnon, H. G. Krausslich, S. G. Morham and W. I. Sundquist (2004). "The human endosomal sorting complex required for transport (ESCRT-I) and its role in HIV-1 budding." *J Biol Chem* **279**(34): 36059-71.

Surpin, M. and N. Raikhel (2004). "Traffic jams affect plant development and signal transduction." *Nat Rev Mol Cell Biol* **5**(2): 100-9.

Sutter, J. U., P. Campanoni, M. Tyrrell and M. R. Blatt (2006). "Selective mobility and sensitivity to SNAREs is exhibited by the Arabidopsis KAT1 K⁺ channel at the plasma membrane." *Plant Cell* **18**(4): 935-54.

Swamy, M., G. M. Siegers, S. Minguet, B. Wollscheid and W. W. Schamel (2006). "Blue native polyacrylamide gel electrophoresis (BN-PAGE) for the identification and analysis of multiprotein complexes." *Sci STKE* **2006**(345): pl4.

Teo, H., D. J. Gill, J. Sun, O. Perisic, D. B. Veprintsev, Y. Vallis, S. D. Emr and R. L. Williams (2006). "ESCRT-I core and ESCRT-II GLUE domain structures reveal role for GLUE in linking to ESCRT-I and membranes." *Cell* **125**(1): 99-111.

Teo, H., O. Perisic, B. Gonzalez and R. L. Williams (2004). "ESCRT-II, an endosome-associated complex required for protein sorting: crystal structure and interactions with ESCRT-III and membranes." *Dev Cell* **7**(4): 559-69.

Tian, Q., L. Olsen, B. Sun, S. E. Lid, R. C. Brown, B. E. Lemmon, K. Fosnes, D. F. Gruis, H. G. Opsahl-Sorteberg, M. S. Otegui and O. A. Olsen (2007). "Subcellular localization and functional domain studies of DEFECTIVE KERNEL1 in maize and Arabidopsis suggest a model for aleurone cell fate specification involving CRINKLY4 and SUPERNUMERARY ALEURONE LAYER1." *Plant Cell* **19**(10): 3127-45.

Twell, D., S. K. Park, T. J. Hawkins, D. Schubert, R. Schmidt, A. Smertenko and P. J. Hussey (2002). "MOR1/GEM1 has an essential role in the plant-specific cytokinetic phragmoplast." *Nat Cell Biol* **4**(9): 711-4.

Ueda, T., M. Yamaguchi, H. Uchimiya and A. Nakano (2001). "Ara6, a plant-unique novel type Rab GTPase, functions in the endocytic pathway of Arabidopsis thaliana." *Embo J* **20**(17): 4730-41.

- Volker, A., Y. D. Stierhof and G. Jurgens (2001).** "Cell cycle-independent expression of the Arabidopsis cytokinesis-specific syntaxin KNOLLE results in mistargeting to the plasma membrane and is not sufficient for cytokinesis." J Cell Sci **114**(Pt 16): 3001-12.
- Walter, M., C. Chaban, K. Schutze, O. Batistic, K. Weckermann, C. Nake, D. Blazevic, C. Grefen, K. Schumacher, C. Oecking, K. Harter and J. Kudla (2004).** "Visualization of protein interactions in living plant cells using bimolecular fluorescence complementation." Plant J **40**(3): 428-38.
- Williams, R. L. and S. Urbe (2007).** "The emerging shape of the ESCRT machinery." Nat Rev Mol Cell Biol **8**(5): 355-68.
- Winter, V. and M. T. Hauser (2006).** "Exploring the ESCRTing machinery in eukaryotes." Trends Plant Sci **11**(3): 115-23.
- Xie, W., L. Li and S. N. Cohen (1998).** "Cell cycle-dependent subcellular localization of the TSG101 protein and mitotic and nuclear abnormalities associated with TSG101 deficiency." Proc Natl Acad Sci U S A **95**(4): 1595-600.
- Yoshimori, T., F. Yamagata, A. Yamamoto, N. Mizushima, Y. Kabeya, A. Nara, I. Miwako, M. Ohashi, M. Ohsumi and Y. Ohsumi (2000).** "The mouse SKD1, a homologue of yeast Vps4p, is required for normal endosomal trafficking and morphology in mammalian cells." Mol Biol Cell **11**(2): 747-63.

Zusammenfassung

Kürzlich wurde das *Arabidopsis* ELCH Gen, ein Homolog des Vps23 / TSG101 und Schlüsselkomponente des pflanzlichen ESCRT Komplexes, funktionell charakterisiert (Spitzer et al, Development, 2006). Die *elch* Mutante zeigt multiple Nuklei in verschiedenen Zelltypen was eine Rolle in der Zytokinese indiziert. VPS28 und VPS37 sind weitere bekannte Komponenten des ESCRT Komplexes, die bei Doppel- und Dreifach-Knock Outs in Kombination mit ELCH einen synergistischen Phänotyp zeigen. Dies weist auf ihre Beteiligung an der ELCH-abhängigen Regulation der Zytokinese hin. Die Regulation der Zytokinese ist demnach die Funktion des gesamten ESCRT Komplexes und nicht eine ESCRT unabhängige Funktion von ELCH. Die Rolle des ESCRT Komplex während der Zytokinese in Hefe ist unklar, jedoch weisen Mutationen in einem oder mehreren ESCRT Komponenten bei Säugern und *Arabidopsis* auf einen Zytokinesedefekt hin, was vermuten lässt, dass die Rolle der ESCRT-Maschinerie in der Zytokinese in multizellulären Organismen konserviert sein könnte.

Ein zweites Homolog des VPS23, VPS23-2 (At5g13860), zeigt hohe Sequenähnlichkeit zu ELCH (72%). Ein dominant-negatives VPS23-2-Konstrukt zeigt den gleichen Phänotyp wie die *elch* Mutante und im Rescue-Experiment kann die Expression von VPS23-2 unter ELCH-Promoter die *elch* Mutante retten. VPS23-2 ist demnach funktionell redundant zu ELCH.

Zusätzlich zu ELCH und VPS23-2 wurde ein Drittes VPS23 Homolog, VPS23-3 (At2g38830), identifiziert, das es nur bei Dicotyledonen gibt. Es zeigt einen geringeren Homologiegrad zum *Arabidopsis* ELCH (47%) verglichen mit ELCH zu *Oryza sativa* ELCH (66%) und VPS23-2 (72%). Genau wie ELCH wird VPS23-3 ubiquitär exprimiert, lokalisiert an den Endosomen, bindet mit seiner N-terminalen UEV-Domäne Ubiquitin und zeigt sich in Gelfiltrationen / Größenausschluss-chromatographien als Teil eines „High Molecular Weight Complex“, was darauf hindeutet, dass VPS23-3 eine Komponente des pflanzlichen ESCRT Systems ist. Überraschenderweise zeigte sich im Rescue-Experiment, dass VPS23-3 unter Kontrolle des ELCH-Promotors den *elch*-Phänotyp nicht retten konnte, was darauf hinweist, dass es eine andere zelluläre Funktion als die zwei anderen Vps23-Gene hat. Der Knock-Out von VPS23-3 zeigte eine Veränderung im Molekulargewicht des Komplexes in der „blue-native PAGE“, sowie unterschiedliche Interaktionen bei BiFC (bi-molecular fluorescence complementation) und in *in vitro* Transkriptions / Translations Experimenten. Dies lässt vermuten, dass VPS23-3 eine zusätzliche, vierte Komponente des *Arabidopsis* ESCRT-I Komplex darstellen könnte.

Erklärung

Ich versichere, dass ich die von mir vorgelegte Dissertation selbständig angefertigt, die benutzten Quellen und Hilfsmittel vollständig angegeben und die Stellen der Arbeit einschließlich Tabellen, Karten und Abbildungen -, die anderen Werken im Wortlaut oder dem Sinn nach entnommen sind, in jedem Einzelfall als Entlehnung kenntlich gemacht habe; dass diese Dissertation noch keiner anderen Fakultät oder Universität zur Prüfung vorgelegen hat; dass sie – abgesehen von unten angegebenen Teilpublikationen – noch nicht veröffentlicht worden ist sowie, daß ich eine solche Veröffentlichung vor Abschluß des Promotionsverfahrens nicht vornehmen werde. Die von mir vorgelegte Dissertation ist von Prof. Dr. Martin Hülskamp betreut worden.

Channakeshavaiah K. Chikkaputtaiah

Veröffentlichungen

The *Arabidopsis elch* mutant reveals functions of an ESCRT component in cytokinesis

Christoph Spitzer, Swen Schellmann, Aneta Sabovljevic, Mojgan Shahriari, Channa Keshavaiah, Nicole Bechtold, Michel Herzog, Stefan Müller, Franz-Georg Hanisch, and Martin Hülskamp. *Development* 2006 **133**: 4679-4689.

Lebenslauf

Persönliche Angaben:

Name: Channakeshavaiah Kolagondanahally Chikkaputtaiah
Geburtsdatum: 10. 04. 1979
Geburtsort: Bengaluru, Indien
Eltern: Vater : Chikkaputtaiah
Mutter: Muthamma
Staatsangehörigkeit: Indien
Familienstand: Ledig
Anschrift: Rothgerberbach 3, D-50676, Köln
E-mail: ckeshava@uni-koeln.de oder chinnatal@gmail.com
Phone: 017624333190
Ständigen Anschrift Kolagondanahally (post), Kanakapura (Taluk), Bengaluru Rural
(District), Karnataka (state), India, 562119

Schulbildung:

2005- Jan 09: Doktorarbeit in der dem AG Hülskamp, gefördert durch International Graduate School in Genetics and Functional Genomics, Universität Zu Köln, Deutschland

2003-2004: Junior Research Fellow, Central Food Technological Research Institute, Mysore, Indien

2001-2003: MSc (Agri.) Plant Biotechnology, University of Agricultural Sciences, Bengaluru, Indien

1997-2001: BSc (Agriculture), University of Agricultural Sciences, Bengaluru, Indien

Konferenzen besucht

2008: Vortrag mit dem Titel: Molekulare und funktionelle Charakterisierung von dem *Arabidopsis* ESCRT-I-Komplex in der Europäischen Netzwerk für Plant Research Endomembran Konferenz, Lecce, Italien

2008: Poster Anspruch: Dar *Arabidopsis* ELCH homolog VPS23-3 ist eine Komponente der anlage ESCRT System in Agricultural Biotechnology International Conference, Cork, Irland

2007: Poster Anspruch: Molekulare und funktionelle Charakterisierung von VPS23-3 in *Arabidopsis* in International Conference auf *Arabidopsis* Research, Beijing, China

Mit freundlichen Grüßen

(Channakeshavaiah K. Chikkaputtaiah)